Dynamics of Naturally Acquired Antibody Against Haemophilus influenzae Serotype *'a'* and the Impact of Vaccination

ANGJELINA KONINI

A DISSERTATION SUBMITTED TO THE FACULTY OF GRADUATE STUDIES IN PARTIAL FULFILLMENT OF THE REQUIREMENTS FOR THE DEGREE OF DOCTOR OF PHILOSOPHY

Graduate Program in Mathematics and Statistics

York University

Toronto, Ontario

May 2016

Abstract

Haemophilus (H.) influenzae is a human-restricted bacterial pathogen that can cause severe invasive disease. During the past two decades, the incidence of infections caused by *H. influenzae* serotype 'a' (Hia) has increased in several parts of the world, particularly in Aboriginal populations of North America. Currently, there is no vaccine available to prevent Hia infection. While efforts continue to develop an anti-Hia vaccine candidate, a number of key questions must be addressed to ensure that vaccination is effective in curtailing and possibly eliminating Hia from affected populations.

In this thesis, we develop mathematical models of Hia transmission and control dynamics and analyze them to address important practical questions. By simulating an in-host antibody boosting model, we predict the timelines and frequency of natural boosting of immunity in order to prevent invasive Hia disease. Using laboratory data collected in a Canadian population, this model indicates that frequent boosting of natural immunity is required to maintain anti-Hia antibodies at levels required to prevent Hia invasive disease. We also develop a stochastic in-host model of immune dynamics to evaluate the immune responses to a bivalent glycoconjugate vaccine against the two serotypes 'a' and 'b' of *H. influenzae*. In particular, we investigate the effect of such a vaccine on the generation of anti-Hia immune response in the presence of pre-existing immunity to one serotype elicited by prior vaccination or natural infection. Our results suggest that the protection conferred by

a bivalent combined vaccine may be affected by the use of carrier protein previously used in *H. influenzae* serotype 'b' conjugate vaccines.

At the population level, we develop the first stochastic model of Hia transmission dynamics to evaluate vaccination strategies and the effect of booster doses. Our results highlight the importance of primary vaccination and timely booster doses of the individual immunity not only for infants, but also for a sizeable portion of susceptible individuals to maintain a high level of herd immunity in the population. Since age plays an important role in transmission of Hia, we also develop an age-structured model to evaluate vaccination strategies and determine the effect of age-specific vaccination coverages. We discuss the implications of our findings for population health.

Acknowledgments

I would like to express my special appreciation and thanks to my advisor Professor Seyed Moghadas, for supporting and encouraging my research all the way from when I first started the PhD program in the Department of Mathematics and Statistics, to the completion of this thesis. I am thankful for his excellent expertise and guidance provided throughout the past four years.

I also would like to thank my committee members, Professor Marina Ulanova and Professor Xin Gao for their collaboration, suggestions and insightful comments. Special thanks go to Dr. Eli Nix, member of Professor Ulanova's research team, for the help provided with laboratory data collection used in our antibody boosting model.

Most importantly, I would like to express my gratitude to my family for their constant help and support and particularly to the little one, Angelo, to whom this dissertation is dedicated.

Contents

List of Tables

List of Figures

List of Abbreviations

Abbreviation	Description
AICD	Activation-Induced Cell Death
APC	Antigen Presenting Cell
CIES	Carrier-Induced Epitopic Suppression
CRF	Chronic Renal Failure
DTap	Diphteria Tetanus accelular Pertussis
DTaP-HB-IPV-Hib	Diphtheria, Tetanus, Pertussis, Hepatitis B, Polio, and *Haemophilus influenzae* serotype 'b'
GMC	Geometric Mean Concentration
HBOC	*Haemophilus influenzae* serotype 'b' Conjugate Vaccine
Hia	*Haemophilus influenzae* serotype 'a'
Hib	*Haemophilus influenzae* serotype 'b'
Hib-CP-Hia	Bivalent unimolecular vaccine against *Haemophilus influenzae* serotypes 'a' and 'b'
Hib-CP/Hia-CP	Bivalent combined vaccine against *Haemophilus influenzae* serotypes 'a' and 'b'
LHS	Latin Hypercube Sampling
MHC II	Major Histocompatibility Complex Class II
OMP	Outer Membrane Protein
PCV	Pneumococcal Vaccine
PRCC	Partial Rank Correlation Coefficient
PRP	Polyribosylribitol Phosphate Polysaccharide

Chapter 1

Introduction

Haemophilus (*H.*) *influenzae* is a bacterial pathogen isolated exclusively from humans. *H. influenzae* serotype 'a' (Hia) is one of the 6 known encapsulated serotypes of this bacterial pathogen, classified based on their distinct capsular antigens [1]. The past decade has witnessed the emergence of severe community-acquired acute infections caused by Hia among Canadian Aboriginal peoples and several other populations worldwide [2, 3]. The rate of invasive Hia disease in northern communities, especially in the pediatric populations, has reached alarming rates, with potential for the spread in the general Canadian population. This underscores the urgent need for the development of preventive measures such as vaccination. Experience with *H. influenzae* serotype 'b' (Hib) vaccine over the past two decades suggests that immunization could be an effective measure in curtailing Hia.

Despite marked decrease in the incidence of Hib following the start of vaccination in the late 1980s, elimination of Hib colonization has not yet been achieved in several affected populations [4, 5]. Resurgence of Hib in some North American populations has been re-

ported, causing concerns for the spread of disease to unvaccinated populations [4, 6]. Several factors may have contributed to this resurgence, including the decline of protective Hib antibody concentrations after primary immunization [4, 7–10] and deferral of the booster dose vaccination [5, 12]. Given these observations, and ongoing efforts for vaccine development against Hia, there is a clear need for evaluation of immunization strategies to identify those that are most effective in the prevention and possible elimination of Hia disease.

Because both vaccine-induced immunity and naturally acquired immunity wane over time, individuals may be at risk of becoming sub-clinically infected, and contribute to the spread of disease without clinical manifestations. Furthermore, since vaccination limits the circulation of Hia strains in the population, it directly interferes with the natural boosting of immunity conferred by re-exposure. It is therefore imperative to investigate the long-term epidemiological impact of vaccination, and determine the timelines for booster vaccination to prevent Hia infection. For this investigation, we will develop mathematical models that encapsulate biological and epidemiological mechanisms of disease transmission pertaining to Hia infection dynamics, and address several important topics. These include:

- Frequency of Hia recurrent infections and timelines of humoral immune responses;
- Impact of vaccination and herd immunity on curtailing Hia;
- Vaccine formulation and the potential immune interferences.

We develop and simulate a boosting model of antibody concentrations, and use data collected for anti-Hia antibodies in serum samples of healthy and immunocompromised adults in a population of Northwestern Ontario, Canada. We investigate both the duration

of immunity without boosting and the average time interval between subsequent exposures to Hia. The study of the boosting model includes parametrization, simulations, and sensitivity analysis of evaluation of changes in the model outputs with respect to variations in input parameters.

We present the first stochastic model of Hia transmission dynamics, and evaluate vaccination strategies in a population with the assumption of well-mixed (homogeneous) interactions. Since estimates published in the literature suggest that most infections occur amongst children and older adults with underlying medical conditions, we extend this model to incorporate age-structure and matrix of contact patterns. We use the age structure model to identify key parameters that affect the long-term epidemiological outcomes of immunization.

Model outcomes using stochastic simulations naturally depend on the choice of parameters. We therefore need to measure the variations in model outcomes due to parameter changes. This quantification is inferred through sensitivity analyses using the Latin Hypercube Sampling techniques. We perform multiple regression analyses to investigate and rank the relative importance of parameters in model outputs for disease dynamics. Through these analyses, we determine key parameters that affect the long-term epidemiological outcomes of vaccination strategies.

To understand the effect of vaccine formulation on the elicitation of optimal immune responses against both Hia and Hib, we develop an in-host model of immune dynamics to simulate immune interferences in the presence of a bivalent *H. influenzae* glycoconjugate vaccine against Hia. For these simulations, we consider several scenarios of naïve and

primed immune systems due to previous exposure or vaccination. We use continuous time Markov-Chain Monte-Carlo simulations based on available parameter estimates in the published literature. We place our findings in the context of vaccine development against Hia, and discuss their implications for vaccination policies.

The findings of research presented in this thesis generate new knowledge necessary for the development of vaccination policies to protect against Hia, and can therefore directly contribute towards reducing the rates of incidence, hospitalization, death, and severe outcomes associated with this infection. Considering significant cost-savings that can be achieved through immunization (prevention) rather than primary care (treatment), this research has enormous potential to bring significant health and economic benefits, via reducing healthcare costs nationwide. Although invasive Hia disease is more confined to Aboriginal communities at this stage, the risk of its spread to the wider Canadian population cannot be discounted, especially amongst the elderly and immunocompromised individuals. Hence, this research is highly relevant and applicable to a broader population setting than solely considering Aboriginal populations.

The research conducted here is novel in several aspects. It provides the first stochastic model for the transmission dynamics of Hia. Second, the proposed vaccination model, for the first time, evaluates the outcomes of a potential vaccine candidate, and provides information on plausible strategies for curtailing Hia infection. Third, in the context of ongoing efforts to develop a new anti-Hia vaccine, it provides important information on comparative evaluation of bivalent vaccine formulations, which could be used to maximize population-wide benefits of vaccination.

Chapter 2

Haemophilus influenzae

H. influenzae is an important bacterial pathogen that can cause severe invasive disease. The invasive disease affects mainly young children, adults with some underlying conditions, and immunocompromised individuals [2, 3]. *H. influenzae* infection can manifest as meningitis, epiglottitis, otitis media, bacteremia, pneumonia, septic arthritis, cellulitis and septicemia [13]. It was first found in a group of patients during an influenza outbreak in 1892 and it was mistakenly considered to be the causative agent of the viral influenza infection, until the discovery of the influenza virus in 1933 [11]. However, its name was kept as a result of its initial mischaracterization in relation to viral influenza.

H. influenzae is a human-restricted bacterial pathogen that is transmitted via direct contact with an infectious individual by airborne droplets through coughing and sneezing [14]. It enhabits the upper respiratory tract and is part of normal bacterial flora of oropharynx and nasopharynx in a large proportion of the population [15, 16]. Most infections caused by *H. influenzae* bacteria are carriage (without manifestation of any clinical symptoms) and

may never develop into disease [17]. These bacteria are opportunistic pathogens that usually live in the host without causing any harm or disease, while waiting for an opportunity such as the presence of a viral infection, reduced immunity, or weakened immune system.

H. influenzae is characterized by extensive antigenic diversity in their polysaccharide capsules. The organism may be unencapsulated (nontypeable), or typeable and classified into 1 of 6 serotypes (namely: a, b, c, d, e, and f) [1]. Nontypeable *H. influenzae* is highly variable and counts for the majority of localized respiratory tract infections that are caused by these bacteria. Nontypeable strains are antigenically divergent and individuals can be colonized with different strains in different times during their childhood [18, 19]. Nontypeable *H. influenzae* infections are responsible for causing otitis media in children and bronchitis in adults, but may also cause invasive disease, such as bacteremia and pneumonia [20]. Among the encapsulated strains, serotypes 'a' and 'b' are the most virulent [21].

Hib was the major cause of bacterial meningitis in young children worldwide before the introduction of the conjugated Hib vaccine in the late 1980s [22]. Routine infant vaccination against Hib dramatically decreased the incidence of invasive Hib disease and carriage in countries where vaccination programs were implemented [22]. Prior to the implementation of Hib vaccination, about 20,000 children younger than 5 years of age developed severe invasive disease and about 1000 died in the United States alone each year. By 2006, the number of reported Hib cases was down to only 29 per year [23].

Since protection conferred by Hib vaccines is specific to serotype 'b' polysaccharide capsule, widespread vaccination against Hib may have unmasked disease caused by other

serotypes [24]. During the preceding decade, the incidence of infections caused by Hia has increased by differentiated rates of morbidity in different populations worldwide, particularly in Aboriginal communities of North America [25–27]. Currently there is no vaccine available against Hia infections, and significant efforts continue for the development of a conjugated anti-Hia vaccine.

2.1 Epidemiology of *H. influenzae*

Hib was the most common cause of invasive disease among children two decades ago [28]. World Health Organization estimated that prior to the introduction of conjugated vaccine, Hib caused around 3 million cases of invasive disease and 386,000 deaths each year in children under 5 years of age [30]. Disease incidence was higher in children 4-18 months and rare in older children and adults. The prevalence of carriage at birth was low, but gradually increased in early childhood and thereafter declined gradually with age. The peak incidence of Hib disease was estimated between 6 and 12 months of age, and thereafter declined markedly, with a rare presence in adults [17]. There are studies that show that 20% of children are colonized in the first year and up to 50% colonized by age 5 years [29]. Before the start of vaccination era, the epidemiology of Hib varied in different populations [31]. In the industrialized world, the peak incidence of Hib disease occurred around 12 months of age with pneumonia as the most common clinical manifestation. In developing countries, the disease typically occurred in infants younger than 1 year old, with meningitis and epiglottits as the most frequent clinical symptom [28]. Universal pediatric

immunization against Hib dramatically decreased the Hib invasive disease rates.

The preceding decade has witnessed the emergence of Hia as the dominant encapsulated strain of *H. influenzae* in several specific geographic locations and populations [25, 32]. Severe infections caused by Hia have reached alarming rates in terms of morbidity in Canadian Aboriginal communities [25]. The case-fatality rate of invasive Hia disease among pediatric cases reported by Canadian IMPACT centers in 1996-2001 reached 16% [33]. From 2000 to 2010, 56% of identified cases with serotype information were caused by Hia in Canadian northern populations, with an average Hia incidence of 4.6 cases per 100,000 population per year over 11 years [25]. Specific reasons behind an increased incidence of invasive Hia disease among some Indigenous populations remain unknown. Explicators may include genetic and environmental factors, especially considering that the same populations experienced the highest incidence rates of invasive Hib disease prior to Hib vaccine [2].

Current rates of Hia colonization in general North American population is unknown. Early studies show the presence of Hia in North American Arctic, including Alaska and Northern Canada, Western Canadian provinces, southwestern parts of the USA, especially among Indigenous populations living in these areas, as well as some areas of South America (Brazil) [2]. However, due to the lack of comprehensive surveillance programs in many countries, the epidemiological data of Hia-associated disease are not complete, potentially underestimating the impact of Hia infections worldwide [3].

Emergence of nontypeable *H. influenzae* as the most prevalent *H. influenzae* that caused invasive disease was reported in studies worldwide [34]. In several populations, the inci-

dence of other serotypes has increased. In England and Wales, estimates during 2001-2010 indicated an 11.0% year-on-year increase in Hif and a 7.4% increase in Hie [35].

2.2 Biological Characteristics of *H. influenzae*

H. influenzae is a small, gram-negative bacterium, which belongs to the *Pasteurellaceae* family. Encapsulated strains of *H. influenzae* isolated from cerebrospinal fluid are coccobacilli. Non-encapsulated organisms isolated from sputum are pleomorphic and often exhibit long threads and filaments. *H. influenzae* bacteria are immobile since they lack the presence of flagella. The organism is generally aerobic but can grow as a facultative anaerobe. The bacteria grow best around 35-37 degrees Celsius with a pH level of 7.6 and specific growth factors that can be found in the blood stream. The organism is characterized by the presence of a capsular polysaccharide in all encapsulated strains, which plays a major role in the virulence of the pathogen. The capsule is a well-organized polysaccharide layer that lies outside the cell envelope of bacteria. Serotypes 'a' and 'b' are the most virulent strains and their capsules are composed of a neutral sugar, an alcohol (ribitol), and a phosphodiester [36].

The pathogenesis of *H. influenzae* infections is not completely understood, although the presence of the capsule in the encapsulated strains is known to be a major factor in virulence. The accepted pathogenesis begins with pharynx as the portal of entry [37]. When the bacteria breach the epithelial barriers, and enters sites which are normally free of the germs such as blood or cerebrospinal fluid, they are able to cause invasive disease [11, 40].

Their capsule allows them to resist phagocytosis and complement-mediated lysis in the non-immune host. Therefore, the bacteria invade the blood or cerebrospinal fluid without aggravating an inflammatory response and attracting phagocytes [38, 39]. Encapsulation facilitates the spread of bacteria from one host to another by enhancing the bacteria ability to survive the dehydration stress that occurs during transfer between hosts [40].

H. influenzae was the first free-living organism to have its entire genome sequenced [38]. There are several main virulence factors in *H. influenzae* such as: capsule (present only in encapsulated strains), fimbrial adhesin, IgA protease, lipooligosaccharide and protein D. The main virulence factors in nonencapsuated strains are the adhesin proteins, which mediate the adherence of microorganism to epithelial cell surfaces facilitating invasion, colonization and other subsequent pathogenesis of the microorganism [41]. Lipooligosaccharide lipid A, which is present in Gram-negative bacteria only, has endotoxic activities. IgA protease inactivates human immunoglubolin A present in the mucosal surfaces. Protein D is a highly conserved surface lipoprotein present in all encapsulated and unencapsulated strains [42]. The main role of this protein is damaging the ciliary function in human nasopharyngeal tissue and is, therefore, involved in the pathogenesis of upper respiratory tract infections [43]. Some of the virulence factors present in *H. influenzae* are immunogenic and can be used in designing vaccine candidates against infection caused by *H. influenzae*.

2.3 Clinical and Subclinical Manifestations

Clinical diagnosis of *H. influenzae* is typically confirmed by bacterial culture. Diagnosis is considered confirmed when the organism is isolated from a sterile body site. In this respect, *H. influenzae* cultured from the nasopharyngeal cavity or sputum would not indicate invasive *H. influenzae* disease, because these sites are colonized in disease-free individuals [22]. Most surveys agree that nasopharyngeal or throat culture recover Hib in 3% to 5% of young children [44]. However, *H. influenzae* isolated from cerebrospinal fluid or blood would indicate invasive *H. influenzae* infection. Hospitalization is generally required for invasive *H. influenzae* infections and the antimicrobial treatment is necessary. However, treatment depends on where the infection is located at, severity of the infection, the age of the patient, and the patients medical history. The pathogen is susceptible to chloramphenicol and third generation cephalosporins (e.g. cefotaxime, ceftriaxone, and cefuroxime) [45]. Many cases who are diagnosed after presenting chest infections caused by nontypeable *H. influenzae* do not respond to penicillins or first-generation cephalosporins. Without treatment, infection due to *H. influenzae* can be rapidly fatal, particularly by meningitis and epiglottitis. In case of survival, *H. influenzae* infections can cause lifelong disability. Up to 20% of patients who survive Hib meningitis have permanent hearing loss or other long-term neurological sequelae [46–48].

H. influenzae frequently colonizes the nasopharynx in healthy individuals and can cause local infections, such as otitis media, sinusitis or pneumonia. Most *H. influenzae* infections are carriage which means the individual harbors the pathogen in the absence of clinical

manifestation of the illness [49]. Both carriage and the cases with invasive disease play an important role in transmission. Colonization is defined as the presence of viable *H. influenzae* organisms in the human pharyngeal mucosa. *H. influenzae* carriage rates are low in the first 6 months of life, reach a maximum between the ages of 3 and 5 years, and gradually decline in adulthood [17]. Children will have a strain for weeks to months, which will then be cleared and the acquisition of a new strain may occur [50]. The carriage rates might be higher under crowding circumstances or presence of Hib disease within a closed population [51]. Most strains of *H. influenzae* live in their host without causing disease, but can cause infection only when other factors create an opportunity. Different factors impact the development of invasive disease. Some of these factors include the presence of a viral infection, reduced immune function or chronically inflamed tissues. Clinical features of invasive *H. influenzae* disease may include initial symptoms of an upper respiratory tract infection mimicking a viral infection, usually associated with a low-grade fever. This may progress to the lower respiratory tract within a few days, with features often resembling those of a wheezy bronchitis. The cough may persist for weeks without appropriate treatment. More serious manifestations of *H. influenzae* include meningitis, epiglottitis, pneumonia, arthritis, bacterimia, sepsis and cellulitis, which are usually caused by encapsulated strains. Those infections affect many organ systems and depending on it, specific clinical symptoms are associated with them. Hallmarks of Hib meningitis are fever, decreased mental status, and stiff neck (these symptoms also occur with meningitis caused by other bacteria) [14]. Epiglottitis is an infection and swelling of the epiglottis, the tissue in the throat that covers and protects the larynx during swallowing. Epiglottitis may

cause life-threatening airway obstruction. Septic arthritis (joint infection), cellulitis (rapidly progressing skin infection which usually involves face, head, or neck), and pneumonia (which can be mild or severe) are common manifestations of invasive disease [14]. Otitis media and acute bronchitis due to *H. influenzae* are generally caused by non-typeable strains [20].

2.4 Prevention

Vaccination against Hib targets the capsular polysaccharide antigen that is specific to Hib and is effective for Hib but not other serotypes [52]. Vaccine is usually given between two months and five years of age. Currently there is no vaccine available against Hia or other serotypes. The experience with Hib vaccines over the past 20 years has demonstrated that even highly vulnerable populations can be successfully protected using immunization with protein-polysaccharide conjugated vaccine [53, 54]. Therefore, immunization of vulnerable populations against Hia may curtail Hia incidence in affected communities. Serum anti-capsular antibodies are the principle protective factors against *H. influenzae* infections since polysaccharide antigens do not stimulate T lymphocytes required for the development of immunological memory and cell-mediated immunity [14]. Immunoglobulin G (IgG) is the main type of antibodies produced against *H. influenzae* infections. IgG is found in all body fluids. It is the smallest but most common antibody (75% to 80% of all the antibodies). Immunoglobulin M (IgM) is the largest antibody in the human circulatory system that appears first in response to the initial exposure to an antigen [55]. At birth, infants are

protected through maternal, transplacentally acquired anti-capsular IgG. Over time, the level of maternally acquired antibodies declines. As children approach 2 years of age, their own antibodies to the capsular polysaccharide (established only for Hib) begin to appear. The precise level of antibody required for protection against invasive disease is not clearly established. However, a titer of 1 $\mu g/ml$ is suggested to provide long-term protection against invasive disease in the vaccinated population [56]. It is considered a protective response after vaccination required to assure a minimal level of 0.15 $\mu g/ml$ (protective level) during the course of a year [56].

Natural immunity against *H. influenzae* infections is based on antibodies that develop as a result of subclinical infections (carriage) or contacts with other cross-reactive bacteria [7]. Rates of carriage in the population affect the duration of protective immunity against invasive *H. influenzae* disease. It is challenging to determine the rates of carriage since many cases of subclinical infections may not seek clinical attention, and are therefore not included in the true prevalence of the infection in the population. High levels of carriage are usually associated with high serum anti-capsular antibody concentrations [57]. The impact of carriage on disease incidence is complex. On one hand, encountering the pathogen increases the risk of invasive disease. On the other hand, it contributes to the rise of protective immune responses by increasing the level of antibody concentration [7]. The level of boosting and the risk of developing invasive disease depend on the level of pre-existing antibody concentration at the time of exposure to the pathogen. Several studies have provided data suggesting that unvaccinated individuals are protected against invasive Hib disease if the concentration of serum antibodies is above 0.15 $\mu g/ml$ [56, 58, 59]. A

much higher antibody level (10 $\mu g/ml$), was assumed to be required for protection against acquisition of carriage [7].

Based on the experience with Hib vaccination, a vaccine against Hia composed of purified capsular polysaccharide has low immunogenicity and cannot stimulate T-cell responses, which are essential for long lasting effects of adaptive immunity. In young ages, the antibody response to T-cell independent antigens (such as *H. influenzae*) is low, consists of a high proportion of IgM antibody, and there is no booster response to subsequent doses of antigens [37]. Thus producing a conjugate vaccine through covalent linkage to protein molecules is important to converting polysaccharides into T-cell dependent antigens. Given the chemical similarities between Hia and Hib capsular polysaccharides, it has been suggested that a bivalent Hib-Hia glycoconjugate vaccine formulation with a similar carrier protein previously used for Hib vaccine could be utilized to induce effective immune protection against both Hia and Hib infections [2, 3]. In this context, the formulation of a bivalent vaccine should be carefully evaluated since pre-existing immunity against Hib may interfere with the generation and boosting of the anti-Hia antibodies.

2.5 Anti-Hia Vaccine and Vaccination

Currently, there is no vaccine available for preventing Hia infection, and the herd immunity in the population is potentially generated through natural infections. Because the incidence of Hib has been dramatically reduced over the past 20 years following the introduction of vaccine, an anti-Hia vaccine may also be a successful measure in curtailing Hia infection.

While efforts continue for the development of a new anti-Hia vaccine, a number of key questions must be addressed in order to maximize the population-wide benefits of vaccination in Hia prevention, and raise the herd immunity to levels required for pathogen elimination. Here, we outline these questions that are addressed in this thesis through modelling, simulations, and data and statistical analysis.

In the absence of vaccination, exposure to the pathogen will lead to the development of adaptive immune responses. As antibody titres decline over time, the pre-existing immune responses wane, which increases the susceptibility of individuals to Hia infection, and severe outcomes. Recurrent exposure to Hia can help boost the level of antibody titres for Hia prevention. When a vaccine is introduced, the circulation of Hia bacteria in the population is reduced, and therefore the individual exposure to this pathogen will be decreased. This will in turn reduce the chance of boosting immune responses. Therefore, the interplay between vaccination dynamics and the immune dynamics at both the individual and population levels has important consequence for the use of Hia vaccine. We will explore these dynamics to determine the rates at which pre-existing immunity declines, and how frequently the immune responses should be boosted. The objectives here are to address the following questions:

- What are the timelines for decline of antibody responses following exposure to Hia in the absence of vaccination?
- How frequently should the protective antibodies against Hia be boosted in order to eliminate the risk of Hia infection?

When an anti-Hia vaccine becomes available, vaccination strategies will need to be informed by the vaccine coverage, booster coverage, timelines for booster vaccination, and target age groups in the population for vaccination. Our questions here are formulated as follows:

- Can vaccination of only infants prevent the spread of the disease in the population? Since Hib vaccine has been implemented in the universal infant immunization programs, it has been suggested that anti-Hia vaccine will be targeted for immunization of infants.
- If needed (determined by the outcomes of infant immunization), what are the primary rates of vaccination for older susceptible individuals?
- Under what conditions, a booster vaccination is required for individuals who have received the primary dose?

As reported in the incidence of Hia and Hib, age can play a significant role in the transmission of infection. The incidence of these infections could also be affected by contact patterns between individuals. Estimates published in the literature suggest that most infections occur amongst children and older adults with underlying medical conditions [2, 3]. Therefore age may be a factor to be considered in transmission dynamics of Hia and vaccination. Considering age in vaccination dynamics could therefore reveal more information on the target groups and their vaccination coverage. We will address the following question:

- What is the age-specific vaccination coverage for curtailing Hia disease?

Considering the similarities of capsular polysaccharide antigens between Hib and Hia, possible vaccine candidates include a bivalent Hia-Hib vaccine with a carrier protein to immunize individuals against both Hia and Hib. In naïve populations with no prior exposure to these pathogens, or vaccination against Hib, the choice of vaccine formulation may not interfere with the immune response at the host level. However, considering that several populations worldwide have been exposed to Hib or Hia and the protective vaccine against Hib was implemented in many countries (affected by Hib) as part of their infant immunization programs, the vaccine formulation may play a significant role in protective levels of the vaccine-induced immunity. In the context of pre-existing immunity, our aim is to simulate the immune interferences and vaccine dynamics to address the following question:

- What are the implications of pre-existing immune responses to Hib in the design of a new bivalent anti-Hia vaccine?

To address the above questions, we will employ mathematical and computational methodologies as well as data and statistical analysis. In the context of ongoing efforts to develop a new anti-Hia vaccine candidate, the work presented in this thesis is important in addressing several key public health questions, which include the effectiveness of immunization strategies, optimal scenarios for long-lasting protection in the population, and the most effective vaccine formulations to provide protection against Hia infections. Since our methodology relies on the development of mathematical and computational models, we will first present an overview of the existing models of *H. influenzae* in the literature.

Chapter 3

Review of Existing *H. influenzae* Modeling

Mathematical models have been used to gain new knowledge of the mechanisms of *H. influenzae* disease pathogenesis, transmission, and control programs. During the preceding two decades, a number of models have been developed to study various aspects of Hib, including the epidemiology of disease before and after the introduction of anti-Hib vaccines [5, 7, 8, 17, 28, 49, 62, 63]. Most models have taken a computational approach, and divided the population into compartments based on the clinical and epidemiological statuses of individuals (e.g., susceptible, clinically infectious, and subclinically infectious), and defined rates at which individuals move between the compartments. These models can be classified as deterministic or stochastic, and individual or population based. Deterministic models approximate the average behavior of the system and may be used when the population size under study is large. In a stochastic model, state variables are not described by

unique values, but rather by probability distributions, incorporating the possibilities and the probability of events occurring. These models may require a larger set of parameters compared to deterministic models, and can be used even when the populations size is relatively small, accounting for large variations and stochasticity. Some of the Hib models published in the literature deal with large groups (population-based models) [5, 62], while others trace individuals through time (individual-based models) [49]. Individual-based models can be used to study complex interventions, but they require significant amount of information and may present computational challenges in parameterization [64]. Nevertheless, individual-based models account for stochasticity, and are capable of representing more realistic scenarios in disease transmission dynamics [65].

One of the earliest models of Hib (Auranen et al., 1996) described Hib infection in a family with small children. The aim of this individual-based Markov-process model was to estimate transmission rates of Hib infection and quantify the effect of the family size and age structure on the prevalence of Hib carriage. This model was fitted to data collected in the United Kingdom from 1991 to 1992, and Finland from 1985 to 1986 prior to the introduction of Hib vaccination into the immunization programs of these countries. The authors observed an age-dependence in carriage prevalence, which led to decline in transmission rates by age. Their results showed an increase in the prevalence of carriage as the family size increases.

Before the introduction of vaccines against Hib, herd immunity in the population was mainly generated as a result of carriage and cross-reactive bacteria with similar or identical antigens to Hib, which circulated in the population and boosted the immunity against

Hib. Several studies have discussed the role of carriage and cross-reactive antigens in the development of immunity against Hib. Coen et. al. (1998) developed a compartmental model to explore the relationship between Hib carriage and disease within populations by reviewing empirical studies for the pattern of Hib. They used maximum likelihood methods to estimate parameters of the model by comparing existing age-structured, deterministic models to the observed epidemiological patterns. Their results suggested that Hib carriage may act as an immunizing process, leading to the development of natural immunity against disease. Hib carriers have higher antibody titers than non-carriers regardless of the vaccination status. From the analysis of the data sets, their study concluded that a susceptible-infected-susceptible (SIS) model fits the data better than a susceptible-infected-recovered (SIR) model, since immunity against the disease is not permanent and human hosts who clear Hib pharyngeal carriage can become recolonized in a relatively short time period. Based on the estimated force of infection, the authors suggested that all ages are capable of acquiring the organism, although there might be a small decline for the older age groups, which might come as a result of behavioral or immunological factors. Considering the relatively low force of infection of Hib carriage, their results support the theory that carriage is not the only determinant of the immunity to disease. The observed dramatic decrease in Hib disease incidence could best be explained if the majority of the naturally-acquired immunity were attributed to cross-reactive bacteria.

In 2002 Leino et al., studied the effect of cross-reactive antigens in Hib infection dynamics. They applied a statistical model to estimate the total rate of immunizing infections of Hib and cross-reactive bacteria in Finland and the United Kingdom prior to wide-scale

vaccinations. Their results supported earlier findings that cross-reactive bacteria may play an important role in the epidemiology of Hib and generation of immunity. They suggested that the rate of cross-reactive pathogens varies between populations and that the geographical variation in Hib epidemiology can be explained by different exposure rates to such bacteria.

After the introduction of vaccines against Hib, mathematical models were more widely used to study the effectiveness of Hib vaccination [8]. These models have attempted to address questions regarding optimal schedule and dosage of vaccination. Furthermore, a number of studies have investigated how vaccination alters the age distribution of the disease and waning of natural immunity in individuals and the population, which would indicate the need for boosting vaccination [7, 17].

The vaccine against Hib has been shown to have important consequences for the epidemiology of disease. Naturally, vaccination can reduce the occurrence of carriage due to limitation in pathogen circulation, and this could lead to the waning of the individual immunity and its effects extend well beyond self-protection and impact the population level of immunity (known as herd immunity). This indirect effect was documented in a model of Hib dynamics and natural immunity studied by Leino et al. in 2000. The model was used to study the duration of natural immunity to Hib under different forces of infection. This statistical model was built on the assumption that the magnitude of the initial antibody response, the rate of decline of antibody concentrations, and the force of infection together determine the antibody concentration level after an initial antigenic stimulus. The model examined how antibody concentrations can vary in different populations depending on

the force of infection. If the force of infection is relatively low, vaccinating young children would result in a decrease in the circulation of Hib bacteria as well as a decrease in the number of invasive infections in the unvaccinated cohort. When the force of infection is high, the effect of vaccination is more complicated. Following vaccination, there is a possibility that the incidence of invasive disease in the unvaccinated cohort could increase. The limitation in pathogen circulation could result in a decline of antibody concentrations, and therefore protective immunity in adults might disappear. The study suggested that the end result could be a higher incidence of disease in older age groups than before the vaccination programs were applied. These estimates serve to predict possible changes in the herd immunity.

In a follow-up study, Leino et al., (2004) incorporated the waning of natural immunity in a structured population model. They built an individual-based stochastic simulation model and considered different contact structures where transmission of infection occurs (i.e., families, daycare units and school classes) to study the protective immunity in the unvaccinated population obtained by Hib vaccination. The model showed that when the circulation of the bacteria is diminished, the immunity conferred by natural infection will wane over time, and those who are not vaccinated may experience a higher risk of infection. According to the study, even a fairly small effect on carriage can result in a considerable reduction in the incidence of invasive Hib disease. The model was also used to explore the effects of different conjugate Hib vaccines and vaccination schedules on achieving sufficiently high antibody concentrations.

The effect of Hib vaccination on the pathogen transmission was further studied by Au-

ranen et al. (2004). The authors developed an individual-based stochastic simulation model and embedded the demographics of Finland population in the mid-1990s. Different network contacts such as family, day-care groups, and school classes were defined to represent typical sites of Hib transmission. Age dependence was incorporated in the model through age distribution of attending different contact sites and activities. Immunity against invasive disease was stimulated by the total rate of acquisition of Hib carriage and cross-reactive bacterial encounters. Findings of the model analysis showed that the prevalence of Hib carriage exhibits an age-dependent pattern. Transmission occurs between children and adults in families, and pre-school and school-aged children played an important role in maintaining Hib circulation. Furthermore, through simulation experiments, the number of secondary infections generated by a single infectious case ($\mathcal{R}_0$) was estimated at 1.04 in the age range between 4 and 16 years, which was higher than $\mathcal{R}_0$ of 0.83 for the rest of the population. The study showed that considering the small number of secondary infections for a single carrier, even moderate levels of vaccination might impact Hib transmission. This suggests that for obtaining sufficiently high level of herd immunity in the population, the effect of vaccination on carriage should carry over to older children.

After the introduction of vaccines against Hib in the routine infant immunization programs, a decline in the vaccine effectiveness was noticed in different populations. The decline may have been due to a lower immunogenic version of the vaccine being used, decline of protective Hib antibody concentrations after primary immunization, or deferral of the booster dose vaccination. McVernon et al. (2007), studied the causes of decline in the vaccine effectiveness in the United Kingdom. The authors developed an age-structured

deterministic susceptible-infected-recovered-susceptible (SIRS) mathematical model to investigate the impact of vaccine on herd immunity. Their model predicted that the shortage of vaccine would have no effect on the incidence of Hib disease for the first three years. The study results highlighted the importance of maintaining high levels of antibody concentrations among age groups at higher risk of invasive disease after wide scale immunization. This conclusion was consistent with a previously published work. Similarly, Leino et al., (2004) suggested that vaccine and vaccination schedules should result in high antibody concentrations, in addition to immunological memory.

Mathematical models have also been used to study different epidemiological patterns of Hib that were observed after the introduction of vaccines. Jackson et al. (2012), developed an age-structured mathematical model of Hib transmission that can be applied in multiple contexts. The model was useful to study the initial rapid decline in the Hib incidence after the introduction of vaccines. Their model accounts for the rises in the Hib incidence that were noted in the United Kingdom 7 years after the catch-up campaign and in the Alaska Natives populations after the switch of vaccine types from individual conjugated Hib vaccine to acellular DTap-IPV-Hib. This model was originally developed in response to the 2007-2009 Hib vaccine shortage in the United States, but it could also be useful for optimizing the introduction of Hib vaccines in populations with no prior exposure to the pathogen or vaccine against Hib. The model was implemented for the United States, England and Wales, and the Alaska Native populations. It classifies populations in a number of states on the basis of age, Hib antibody levels (high, low, and none) and disease status (susceptible, colonized, diseased and immune infants). The study suggested several important insights

into the epidemiology of Hib and the design of Hib vaccination programs. First, the model illustrated that in the United States, and England and Wales, Hib transmission is driven by children 2-4 years of age, which is in contrast with previous models that suggested the transmission of carriage occurs mostly between individuals of approximately the same age, known as assortative mixing [8, 17, 62]. Second, the model indicated that Hib transmission dynamics differ across distinct populations, and in the Alaska Native populations is mainly driven by children 5-9 years of age. The difference in the transmission dynamics may have important consequences for the design of Hib vaccination programs. There may be populations for which a policy of a single dose at 12-15 months would reduce invasive Hib nearly as much as a 3-dose primary series plus a booster would (for example, the United States and England and Wales). In contrast, offering only a single dose at 12-15 months of age would be considerably less effective for the Alaska Native populations. In these settings, the force of infection is high even for young infants, which has important implications for the choice of vaccine. The model predicts that both PRP-T (polyribosylribitol phosphate polysaccharide (PRP) conjugated to tetanus toxoid (T)) and HBOC (PRP conjugated to a nontoxic mutant of diphtheria toxin) vaccines are much less effective than the PRP-OMP (PRP conjugated to Neisseria meningitides outer membrane protein, OMP) vaccine, since PRP-OMP stimulates protective antibodies after the first dose at 2 months of age, which is not the case for the other two vaccine formulations. Furthermore, in some populations, a single dose at 12-15 months may lead to a higher reduction of Hib disease compared to a 3-dose primary without a booster. These findings highlighted the importance of evaluating Hib transmission dynamics for optimizing vaccination.

The mathematical models developed in this thesis are the first ones to describe the dynamics of Hia infection and disease. There are no other models of Hia transmission and control dynamics published in the literature. The antibody-boosting model developed here is used to investigate the dynamics of naturally acquired antibodies against Hia. We used data collected for anti-Hia antibodies in serum samples of healthy and immunocompromised adults in a population of Northwestern Ontario, Canada. The input data were provided by our collaborators at Northern Ontario School of Medicine (Dr. Ulanova's research team). The analysis of the boosting model includes parameterization, simulations, and the Latin Hypercube Sampling technique for sensitivity of the outputs with respect to variations in input parameters. The vaccination model presented in this thesis will, for the first time, evaluate the outcomes of a potential vaccine candidate, and provide important information on plausible strategies for curtailing Hia infection. Since the prevalence of Hia carriage exhibits an age-dependent pattern, an age structure model is constructed and used to reveal more information on the target groups and their vaccination coverage. In the context of ongoing efforts to develop an anti-Hia vaccine candidate, the stochastic in-host model of immune dynamics also provides information on the effective vaccine formulation that maximizes the population-wide benefits of vaccination, considering the historical precedence in terms of exposure to Hia or Hib. We use continuous time Markov-Chain Monte-Carlo simulations based on available parameter estimates in the published literature. Further details of the computational methods used in simulations are provided in Appendix A. The findings will have important implications for current efforts towards vaccine development against Hia, as well as vaccination policies.

Chapter 4

Dynamics of Naturally Acquired Antibody against Hia

The preceding decade has witnessed the emergence of Hia as the dominant encapsulated strain of *H. influenzae* in several specific geographic locations and populations, including Aboriginal populations in North America [2, 3]. Clinical and epidemiological studies of Hia indicate that Aboriginal children (younger than 5 years of age) and adults with predisposing medical conditions are most affected by invasive Hia disease [2]. Understanding of the immunological and epidemiological characteristics of this pathogen is imperative to develop preventive measures with long-lasting effects. Of particular importance is the duration of protective immunity against Hia invasive disease, which is primarily affected by rates of carriage in the population.

Similar to Hib, since vaccination with a conjugate vaccine specific to Hia could reduce the circulation of Hia bacteria, and therefore the incidence of Hia carriage, determining

timelines for boosting of protective immunity will be essential for the maintenance of a high level of herd immunity. In case of Hib, new infections were estimated to occur once in 4 years to maintain serum antibody concentrations ≥ 1.0 μg/ml prior to the introduction of conjugated Hib vaccine [7]. Currently, there are no estimates of Hia recurrent infections and timelines for boosting of antibody concentration.

In this study, we develop a model of secondary antigenic response using data for anti-Hia antibody concentrations in serum samples of participants in a population of Northwestern Ontario, Canada. Our aim is to estimate timelines for boosting antibody concentrations following priming for different populations' characteristics. We consider age, sex, ethnicity (i.e., Aboriginal and non-Aboriginal), and health status (including those presenting chronic renal failure) of individuals in stratifying collected data. Since rates of antibody decay against Hia are still unknown, we parameterized the model using available estimates from the published studies for Hib. We base this assumption on the similarities between Hia and Hib capsular polysaccharide antigens [66, 67].

4.1 Methodology

Our methodology includes several steps described below, including sample collection and laboratory assays (see Appendix B for details), data analysis, model development, simulation experiments and sensitivity analyses of the model outcomes. Data collection and analysis for this part of the research were approved by the Thunder Bay Regional Health Sciences and Lakehead University Research Ethics Board.

Table 4.1: Summary of the data collected based on the analysis of Hia seroprevalence in a population of Northwestern Ontario, Canada. CRF: chronic renal failure; F: female; M: Male.

	Aboriginal				**Non Aboriginal**			
	Healthy		CRF		Healthy		CRF	
Age/Sex	F	M	F	M	F	M	F	M
19–34	29	5	2	4	10	7	2	0
35–59	23	5	14	7	13	7	4	4
≥ 60	3	1	8	2	5	6	6	19
All	55	11	24	13	28	20	12	23

4.1.1 Study area

The analysis is based on Hia seroprevalence data collected during September 2010–August 2012, in a population of Northwestern Ontario, Canada, which is characterized by a presence of a significant proportion of Indigenous peoples, i.e., 19.6% of the total population in this area. In comparison, according to the 2006 Canadian Census, Indigenous peoples comprise 3.8% of the Canadian population. Healthy adults aged 19–80 years who self-identified as either Aboriginal or non-Aboriginal were recruited from the Thunder Bay area. Individuals with chronic renal failure (CRF) aged 24–91 years were recruited from the Renal Services, Thunder Bay Regional Health Sciences Centre. Characteristics of the participant groups are presented in a previously published study [68]. We summarize the demographic and health status of participating subjects in Table 1.

4.1.2 Stratification with antibody concentration

On the basis of previous findings on immunological correlates of protection against Hib disease, we hypothesized that anti-Hia polysaccharide antibody concentrations of 1 μg/ml or above provide long-term protection against invasive Hia disease and concentrations of 5 μg/ml or above prevent colonization of the upper airways. For the purpose of simulations, we stratified the collected data for the level of antibody concentrations and the corresponding average ages of individuals in Figure 4.1. In all categories of healthy and CRF participants, the level of antibody concentration < 1 μg/ml corresponds to the lowest fraction of individuals, with an average age older than 50 years.

We used logistic regression to investigate the effect of age and sex on the concentration of anti-Hia capsular polysaccharide antibody in serum samples of study participants. The statistical significance of adding the interaction term for age and sex was assessed by using a likelihood ratio test. We performed this analysis for both Aboriginal and non-Aboriginal participants. All tests were at a two-sided significance level of 0.05. The results of this analysis showed that variables of sex and age were not significant on the level of antibody concentration, suggesting that the antibody-boosting model could be developed independently of these variables.

4.1.3 Antibody Boosting Model

To develop the model, we assumed that in the absence of any boosting, the initial antibody level decays in the exponential form $c(t) = c_0 e^{-k(t-t_0)^a}$, where $c(t)$ is the antibody concen-

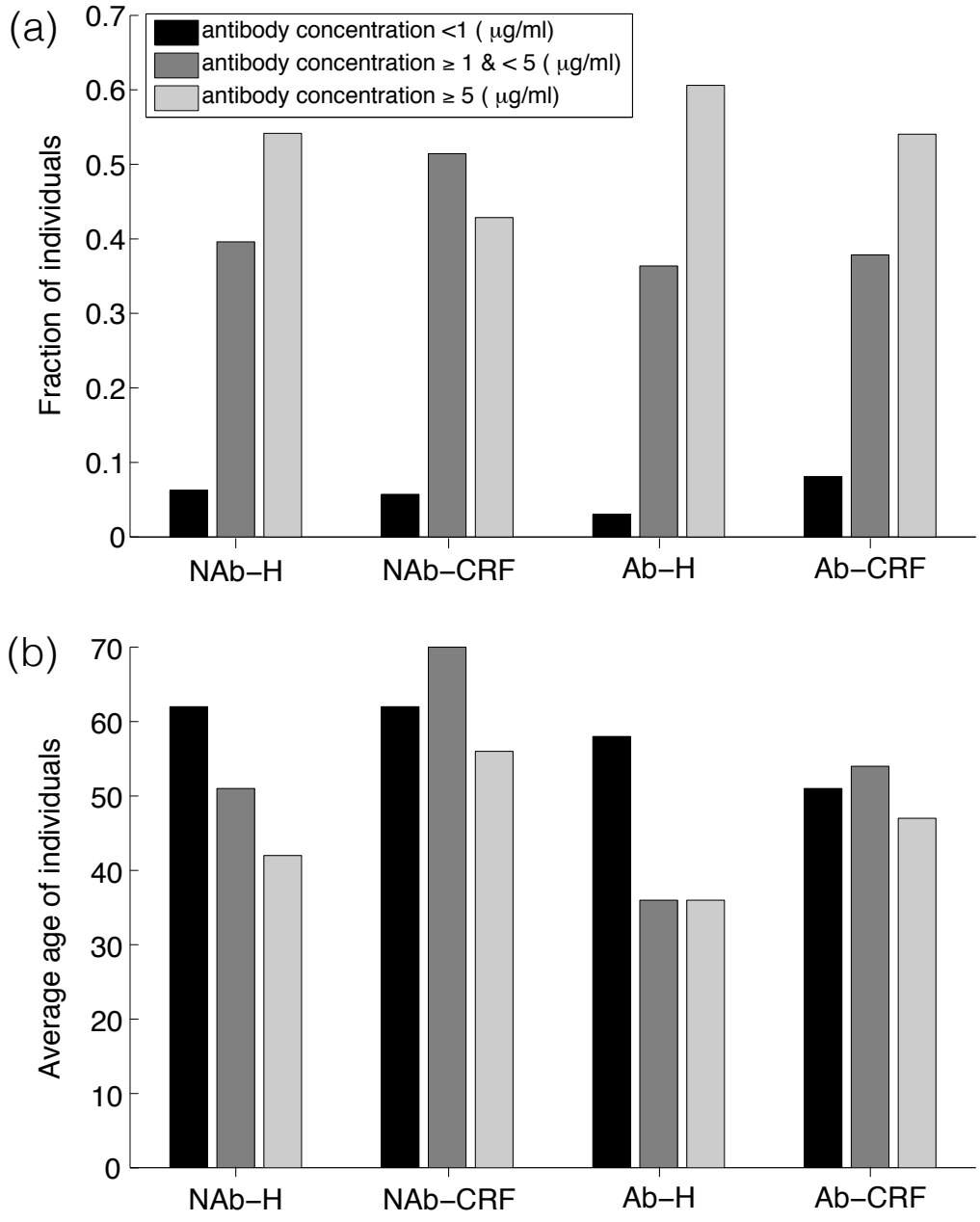

Figure 4.1: (a) The fraction of individuals at low risk of infection (AC $\geq$ 5 μg/ml; light grey), low risk of invasive disease (1 μg/ml $\leq$ AC $<$ 5 μg/ml; dark grey); and high risk of invasive disease (AC $<$ 1 μg/ml; black). (b) The corresponding average ages of individuals identified as healthy Non-Aboriginal (NAb-H); Non-Aboriginal with chronic renal failure (NAb-CRF); healthy Aboriginals (Ab-H); and Aboriginals with chronic renal failure (Ab-CRF). AC: total IgG and IgM antibody concentration.

tration at time t; c_0 is the initial concentration, k is the decay rate; and a is the parameter in the range $0-1$ regulating the antibody decline. If $a = 1$, the boosting model has an exponential decline of the absolute antibody concentration, whereas for $a < 1$, the rate of decline is attenuated in comparison with the exponential model [69].

When stimulating challenge occurs after time t_0, the antibody concentration is increased in the process of boosting immune responses. The level of boosting, however, depends on $c(t)$ at the time of antigenic challenge. Consistent with previous work, we considered two threshold levels of antibody concentrations:

i) Subclinical threshold (L_1): concentration above this level prevents the development of subclinical disease following exposure, and a minimal stimulation of the immune system may occur.

ii) Invasive threshold (L_2): concentration above this level, but below L_1 is not adequate for infection protection. However, this level of antibody concentration will mitigate infection if occurs, and prevent severe form of invasive disease. Exposure to infection during the period in which antibody $L_2 < c(t) < L_1$ leads to a moderate boosting of the immune response and a measurable increase in the antibody concentration.

The maximum level of boosting occurs when $c(t) < L_2$, especially when the individual is naïve. Due to possibility of boosting immunity following priming, we enhanced the exponential decay model to include the increase in the level of antibody concentration. We considered $c'(t) = -kc(t) + b(t)$ where $b(t)$ is the boosting rate at the time of antigenic challenge. This rate depends on several key parameters, and we used the Heaviside step

function to describe the increase in $c(t)$ [70]. We defined:

$$\theta(t) = \frac{\beta[H(L_1 - c(t)) + H(L_2 - c(t))]}{1 + H(L_1 - c(t))} \tag{4.1}$$

where β is the the maximum boosting rate in the absence of pre-exiting immunity. Denoting the average time for a secondary antigenic challenge following priming by τ, we defined $b(t) = \theta(t)\delta(t - n\tau)$ for $n = 1, 2, \cdots$, where Kronecker δ is defined by:

$$\delta(t - n\tau) = \begin{cases} 1 & \text{if } t = n\tau \\ \\ 0 & \text{if } t \neq n\tau \end{cases} \tag{4.2}$$

This functional form of boosting allows for the increase in the antibody concentration based on the amount of $c(t)$ at the time of antigenic challenge.

For antibody concentrations below L_2, the magnitude of simulated boosting response was full at the time of exposure (that is similar to the case where there is no pre-existing immunity). This magnitude reduced by 50% (as defined by $\theta(t)$) for antibody concentrations between L_2 and L_1 at the time of exposure.

4.2 Parameterization and Simulations

We parameterized the model using available estimates from the published studies for *H. Influenzae* type 'b'. In the absence of vaccination, the duration and the rate of antibody decline depend on the incidence of infection in the population [7]. We assumed a decay rate in

the range $0.08 - 0.16$ (converted to a rate per month) [7], and used antibody concentration levels of $L_1 = 5$ and $L_2 = 1$ (μg/ml) for preventing subclinical infection (carriage) and invasive disease, respectively. Previous work pertinent to Hib indicates that individuals with antibody concentrations above 1 μg/ml were protected against invasive disease despite the occurrence of infection [7, 71]. We estimated the rate of boosting $\beta = c_m$ as a result of new antigenic challenge following priming, where c_m is the geometric mean concentration (GMC) of the measurements of antibody concentrations.

To determine the timelines for decline of antibody concentration, we used the Latin Hypercube Sampling (LHS) technique to evaluate the effect of simultaneous variation of model parameters on the outcomes. We ran simulations for a 10-year period following priming, when k and a are given by LHS. To allow for the simultaneous variations of these parameters, samples of size $n = 1000$ were generated in which each parameter was treated as a random variable and assigned a probability function. These parameters were uniformly distributed and sampled within their respective ranges. Each parameter set was simulated using the antibody concentration measured for each individual in the collected samples as the initial condition at time t_0. For each scenario, corresponding to the average number of years for a new antigenic challenge, we ran 1000 independent simulations, and determined the geometric mean concentration (GMC) and 95% confidence intervals of the antibody concentration within 10 years.

4.3 Results

4.3.1 Duration of immunity without secondary antigenic response

For scenarios in which there is no new antigenic challenge, we observed that the level of antibody concentration in healthy Aboriginal individuals would be expected to fall below the level (1 μg/ml) assumed for protection against invasive disease 3 years after priming (Figure 4.2(a), black curve). The period of protection against invasive disease is shorter (2 years) for immunocompromised Aboriginal individuals suffering from CRF (Figure 4.2(a), red curve). The corresponding protection periods for non-Aboriginals against invasive disease are 2 years (for healthy individuals) and 1 year (for individuals with CRF condition), as shown in Figure 4.2(b).

4.3.2 Average time between exposures

We simulated the model to estimate the average time within which an antigenic challenge will need to occur in order to maintain the population level of antibody concentration above 1 $\mu g/ml$. For Aboriginal individuals, we estimated that a new antigenic challenge will need to occur once in 5 and 2 years for healthy and CRF subjects, respectively (Figures 4.2(c-d)). For healthy non-Aboriginals, a new antigenic challenge was estimated to occur once in 2 years. This challenge was estimated to occur more often (once every year) to prevent the risk of invasive disease in non-Aboriginals with CRF condition.

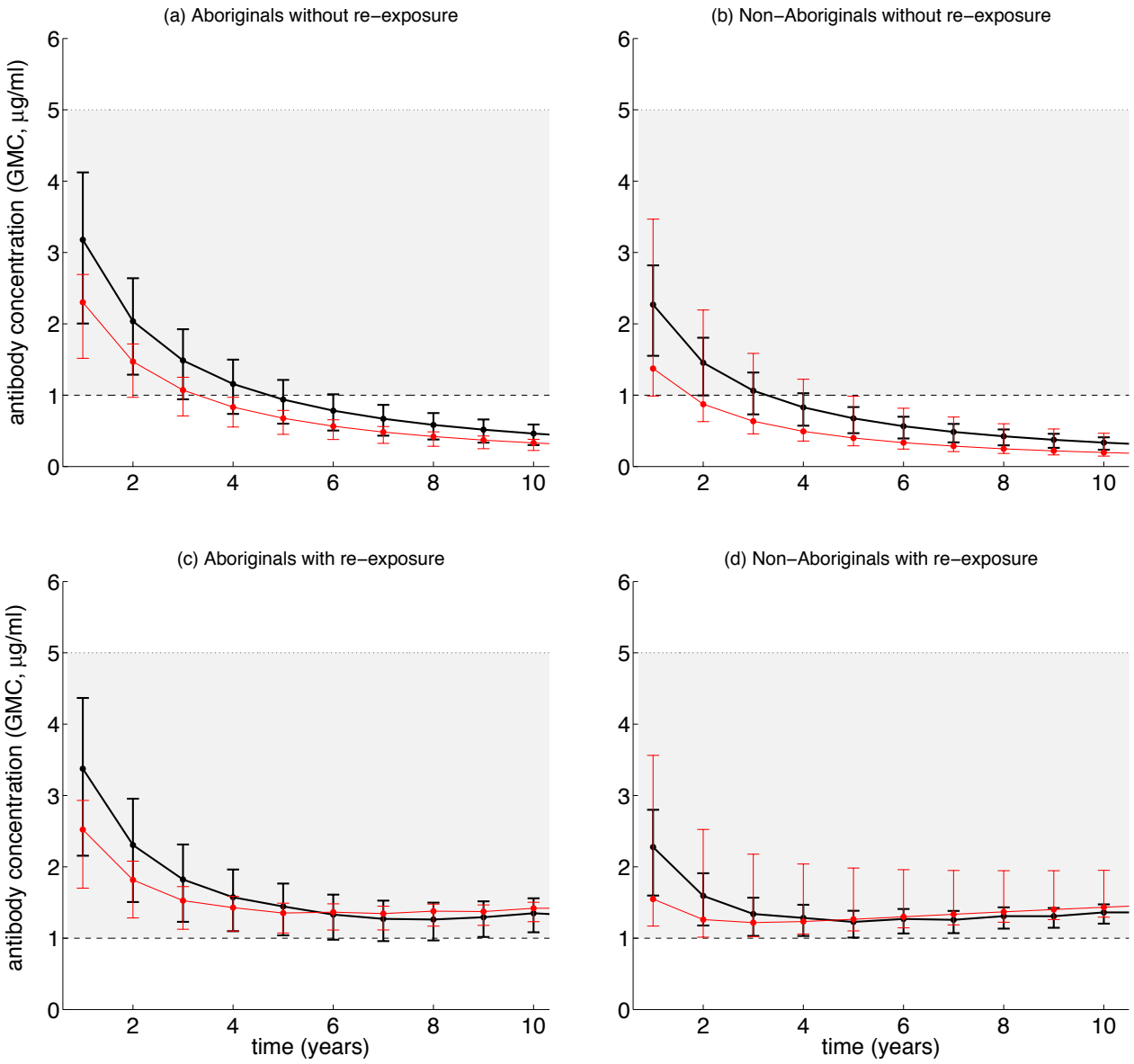

Figure 4.2: The median GMC antibody levels with their predictive 95% confidence intervals over a 10-year time period following priming, without (a-b) and with a new antigenic challenge (c-d). The risk of carriage is shown in grey area. Black and red curves correspond to healthy and CRF subjects, respectively. For Aboriginals (panel c), new antigenic challenge occurred once in 5 years for healthy individuals (black curve) and once in 2 years for individuals with CRF condition (red curve). For non-Aboriginals (panel d), new exposure occurred once in 2 years for healthy individuals (black curve) and once every year for individuals with CRF condition (red curve).

4.4 Interpretation

Our results, based on parameter estimates for Hib, indicate that Hia colonization (possibly in the form of carriage) may be occurring more frequently in some populations, such as North American Indigenous people, compared to previous estimates for Hib [7]. Indeed, recent studies indicate that Aboriginal adults have significantly higher serum bactericidal activity against Hia compared to non-Aboriginal individuals living in the same geographic area, suggesting an increased exposure to the pathogen in the former population [68]. Although current rates of Hia colonization in the North American population or immunological correlates of protection against this pathogen are unknown, our data suggest that adult serum antibody concentrations are above the threshold required for prevention of Hia invasive disease in Aboriginal populations of Northwestern Ontario (Canada). Our model indicates that frequent boosting is required to maintain the anti-Hia capsular polysaccharide antibody levels against Hia invasive disease, particularly in individuals with chronic renal failure who are immunocompromised as a result of profound metabolic consequences of uremia, underlying medical conditions (e.g., type 2 diabetes mellitus), and hemodialysis procedure [72].

We should mention the limitations that highlight the need for further investigations and data collection in specific population settings. First and foremost is the fact that we parameterized our model with the range of antibody decay previously estimated for Hib. However, to estimate Hia-specific decay rates of antibody concentrations in the absence of vaccination, subsequent measurements of serum samples should be collected for several

years. While such data can provide better estimates of timelines for boosting concentrations, we note that antigens from several organisms other than Hia can also induce cross-reactive antibodies to Hia capsular polysaccharide [73, 74], and may therefore increase the antibody concentration. Since the relative importance of antibodies arising in response to encounters with cross-reactive bacteria is unknown, the measurements of the serum Hia antibody concentration may not be reliable in detecting carriage.

Also, considering that the majority of invasive Hia disease cases occur among young children, it is important to mention that the demographics of our study group, comprised of adults only, do not fully reflect the immunoepidemiology of this infection. Studying the natural immunity against Hia in paediatric populations should be subject of future work.

4.4.1 Conclusions

Measurements of antibody concentration in a sample of population in an area with high incidence of invasive disease, show that a significant fraction of participants have anti-Hia antibody levels above 1 μg/ml. The model developed here suggests that frequent boosting of immunity through natural infection (possibly in the form of carriage) is required to maintain protective antibody levels above 1 μg/ml observed in data. Amongst factors that could affect the incidence rate of Hia carriage and disease, and therefore herd immunity in the population, are socio-economic and environmental conditions, particularly in Canadian northern communities with predominantly Aboriginal populations. These factors warrant further investigation for understanding biological and epidemiological mechanisms responsible for high prevalence of Hia circulation in these population settings. This

understanding is also important for implementing immunization and booster strategies with long-lasting effects when a new Hia vaccine candidate becomes available.

Chapter 5

A Vaccination Model for Hia

Currently, there is no vaccine available for prevention of Hia, and the disease is treated with antibiotics upon diagnosis. As efforts continue for the development of an anti-Hia protein-polysaccharide conjugated vaccine, it is important to understand the effect of such a vaccine on the incidence of infection in the population. Our goal here is to provide this understanding using a modelling framework, and thereby identify immunization strategies for achieving the best short-term and long-term outcomes. This framework is represented as a stochastic model of Hia transmission and control dynamics in a well-mixed population, where interactions are assumed to be homogeneous and age-independent. We will relax this assumption and enhance our model to an age-structured in Chapter 6.

The effectiveness of immunization strategies and optimal scenarios for long-lasting protection are affected by the interplay between the dynamics of vaccine-induced immunity at the individual level, and herd immunity at the population level [75–77]. Previous dynamical models of Hib conjugate vaccine have greatly enhanced our understanding of the

effect of vaccine-induced and natural immunity on the incidence of invasive Hib disease, and on the role of boosting the humoral immune response upon re-exposure to antigenic challenge [5, 7–10]. Although vaccination can induce indirect protection through herd immunity, reduction in pathogen transmission can have a profound impact on the long-term maintenance of immunity in the population. As carriage of *H. influenzae* organisms is largely impeded following the implementation of vaccination, protective antibody titres decline over time due to decreased boosting of immunity, which will in turn affect the levels of herd immunity. These factors will guide the development of our modelling framework.

5.1 Deterministic Model

To develop the model, we make some realistic assumptions as validated in biological studies [5, 14, 36]. The population is divided into classes of susceptible individuals (S) with no prior exposure to Hia; exposed individuals who are infected but not yet infectious (L); infectious individuals who are subclinical (C) referred to as carriage, and transmit the disease without developing clinical manifestations; infectious individuals who are currently subclinical (A), but will develop Hia disease; and infectious individuals with Hia disease (I). We also considered two classes of individuals following recovery from Hia infection. The first class (V_b) includes those who have recovered from Hia carriage and disease, and are fully protected against re-infection for a certain period of time. The second class (V_p) includes individuals whose full protection has waned over time, currently having partial immunity, and may experience carriage if exposed to Hia and infection occurs. We as-

sumed that the level of immunity following recovery from Hia infection declines from full to partial (thereby moving individuals from V_b to V_p), and ultimately to low levels considered as fully susceptible (i.e., moving individuals from V_p to S). We introduced the class L_v for individuals who are exposed to Hia during the period of partial protection and become infected. The schematic representation of movements between these classes is presented in Figure 5.1.

Based on the assumption of homogeneously mixing population the model can be expressed by the following system of differential equations using a proportional incidence of infection:

$$\begin{aligned}
\frac{dS}{dt} &= \mu N + \sigma_p V_p - \frac{\beta S}{N}[I + \delta(C + A)] - \mu S \\
\frac{dL}{dt} &= \frac{\beta S}{N}[I + \delta(C + A)] - \theta L - \mu L \\
\frac{dC}{dt} &= q\theta L + \theta L_v - \gamma_1 C - \mu C \\
\frac{dA}{dt} &= (1 - q)\theta L - \alpha A - \mu A \\
\frac{dI}{dt} &= \alpha A - \gamma_2 I - \mu I \\
\frac{dV_b}{dt} &= \gamma_1 C + \gamma_2 I - \sigma V_b - \mu V_b \\
\frac{dV_p}{dt} &= \sigma V_b - \frac{\eta\beta V_p}{N}[I + \delta(C + A)] - \sigma_p V_p - \mu V_p \\
\frac{dL_v}{dt} &= \frac{\eta\beta V_p}{N}[I + \delta(C + A)] - \theta L_v - \mu L_v,
\end{aligned} \tag{5.1}$$

where N is the total population size. Parameters of this model are defined in Table 5.1.

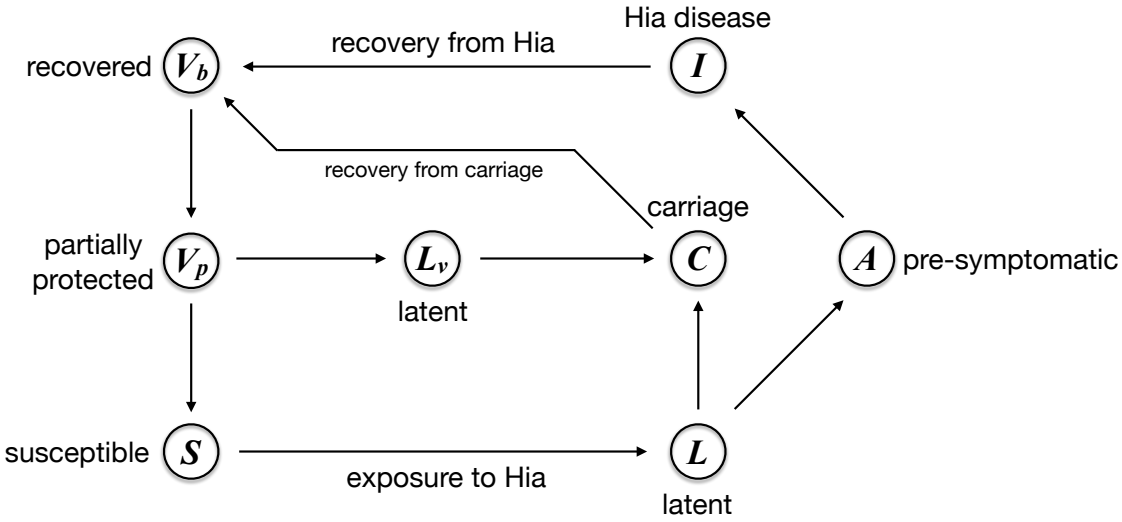

Figure 5.1: Schematic model structure in the absence of vaccination.

5.1.1 Reproduction number

A key parameter in the study of communicable disease is the basic reproduction number, denoted by $\mathcal{R}_0$, which is defined as the expected number of secondary cases produced by a typical infectious individual in a completely susceptible population during the infectious period [78]. If $\mathcal{R}_0 < 1$, then on average an infected individual produces less than one new infection over the course of his or her infectious period, and therefore the number of infections can not grow. On the other hand, if $R_0 > 1$, then each infected individual produces, on average, more than one new infection, and the disease can invade the population.

For the model proposed in 5.1, the basic reproduction number ($\mathcal{R}_0$) can be calculated using the method of next generation [78, 79] or individual tracing [80, 81]. Let $\mathcal{F}(x)$ represent the generation rate of new infections, and $\mathcal{V}(x)$ be the transfer rate, by all other means, of individuals between model compartments. Then we have

$$\mathcal{F}(x) = \begin{pmatrix} \frac{\beta S}{N}[I + \delta(C + A)] \\ 0 \\ 0 \\ 0 \end{pmatrix} \qquad \mathcal{V}(x) = \begin{pmatrix} \theta L + \mu L \\ -q\theta L - \theta L_v + \gamma_1 C + \mu C \\ -(1-q)\theta L + \alpha A + \mu A \\ -\alpha A + \gamma_2 I + \mu I \end{pmatrix}.$$

The next generation method calculates $\mathcal{R}_0$ as the dominant eigenvalue of the matrix FV^{-1}, where F and V are components of the Jacobian matrices of $\mathcal{F}(x)$ and $\mathcal{V}(x)$ at the disease-free state of the model. In our model, the disease-free state is given by $(N, 0, 0, 0, 0, 0, 0, 0)$, and therefore

$$FV^{-1} = \begin{pmatrix} 0 & \delta\beta & \delta\beta & \beta \\ 0 & 0 & 0 & 0 \\ 0 & 0 & 0 & 0 \\ 0 & 0 & 0 & 0 \end{pmatrix} \begin{pmatrix} \frac{1}{\mu+\theta} & 0 & 0 & 0 \\ \frac{q\theta}{(\mu+\gamma_1)(\mu+\theta)} & \frac{1}{\mu+\gamma_1} & 0 & 0 \\ \frac{(1-q)\theta}{(\mu+\alpha)(\mu+\theta)} & 0 & \frac{1}{\mu+\alpha} & 0 \\ \frac{(1-q)\theta\alpha}{(\mu+\alpha)(\mu+\theta)(\mu+\gamma_2)} & 0 & \frac{\alpha}{(\mu+\alpha)(\mu+\gamma_2)} & \frac{1}{\mu+\alpha} \end{pmatrix}.$$

The dominant eigenvalue of FV^{-1} is

$$\mathcal{R}_0 = \frac{q\delta\beta\theta}{(\mu+\theta)(\mu+\gamma_1)} \longleftarrow \text{total number of secondary infections generated during Hia carriage}$$

$$+ \frac{(1-q)\delta\beta\theta}{(\mu+\theta)(\mu+\alpha)} \longleftarrow \text{total number of secondary infections generated during pre-symptomatic infection}$$

$$+ \frac{(1-q)\alpha\beta\theta}{(\mu+\theta)(\mu+\alpha)(\mu+\gamma_2)} \longleftarrow \text{total number of secondary infections generated during Hia disease}$$

No previous study has estimated $\mathcal{R}_0$ for Hia, and we therefore assumed $\mathcal{R}_0$ in the range 1.2–1.4 estimated in studies of Hib [82] and other pathogens that cause bacterial meningitis, such as *N. meningitidis* serotype C [83]. The epidemiological data on Hia incidence do not provide sufficient information on the rate of disease transmission. We therefore calculated the transmission parameter β based on a given reproduction number, while fixing other parameters of the model.

5.1.2 Vaccination dynamics

We now extend the basic model 5.1 to include vaccination. For a new vaccine candidate, the population level of immunity against Hia infection can be elevated by vaccinating infants (V_n) or other susceptible individuals (S_v). We assume that vaccine induces full protection for a period of time, and this protection gradually wanes (V_p) to levels that prevent the

development of Hia disease, but Hia carriage may still occur if transmission takes place [5]. The complete loss of vaccine-induced protection transfers the individuals from V_p to the susceptible state (S_n) [5, 8]. Individuals who receive a booster dose during the period of partial protection move from V_p to V_b (and in case of vaccination for susceptibles, move from S_p to S_b) and acquire a transient full protection again. Protection of booster vaccination wanes over time, moving individuals from V_b and S_b to V_{bp} (Figure 5.2). In our model, it is assumed that the level of vaccine-induced protection for infants and susceptible individuals is the same as that acquired by natural infection [5]. We revisit this assumption when we develop the age-structure model in Chapter 6. Booster dose is assumed to be administered for those who have been vaccinated with the first dose [30].

5.2 Stochastic Model

5.2.1 Stochastic structure

We develop a stochastic structure of the model by assuming that the occurrence of events depends on the rates of movement between different compartments in the deterministic model. We consider time t as a continuous variable, and define the following random vector for $t \in [0, \infty)$

$$\vec{X}(t) = (S(t), V_n(t), V_p(t), V_b(t), L(t), L_v(t), C(t), A(t), I(t), V_{bp}(t), S_v(t), S_p(t), S_n(t)),$$

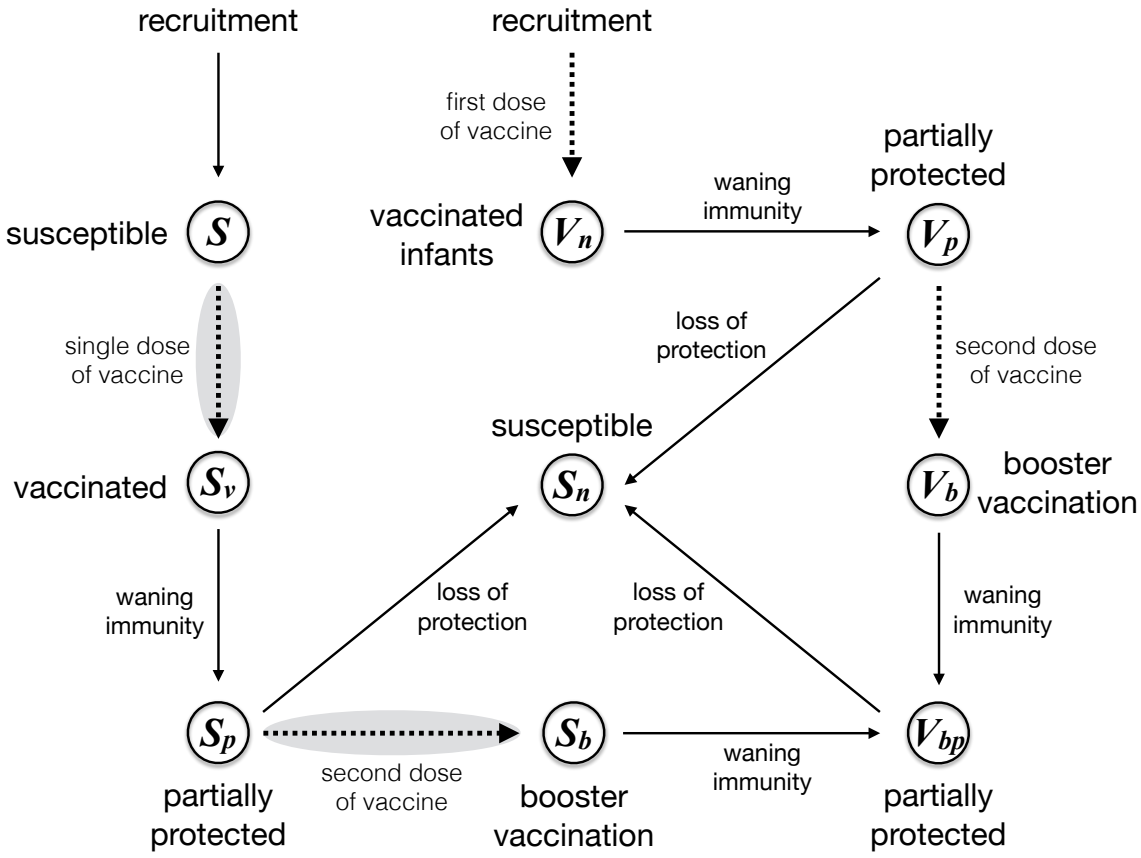

Figure 5.2: Schematic diagram for vaccination dynamics.

with $\Delta\vec{X}(t) = \vec{X}(t+\Delta t) - \vec{X}(t)$, which represents changes that occur to the random vector at Δt units of time. We also define the transition probability as

$$\begin{aligned}\Pr(\Delta\vec{X}(t)) = &\big(\Theta(S), \Theta(V_n), \Theta(V_p), \Theta(V_b), \Theta(L), \Theta(L_v), \\ &\Theta(C), \Theta(A), \Theta(I), \Theta(V_{bp}), \Theta(S_v), \Theta(S_p), \Theta(S_n) \mid \Delta\vec{X}(t)\big),\end{aligned}$$

where

$$\Theta(\cdot) = \begin{cases} -1 & \text{decrease in the class } (\cdot) \\ 0 & \text{no change in the class } (\cdot) \\ 1 & \text{increase in the class } (\cdot) \end{cases}$$

The function $\Theta(\cdot)$ describes the change in a class (i.e., $\Theta(\cdot) = -1$: an individual leaves the class; $\Theta(\cdot) = 0$: no changes occur in the class; $\Theta(\cdot) = 1$: an individual enters the class). We assume that Δt is sufficiently small, so that at most one change of status can occur during the time interval Δt, which can be viewed as a Markov chain process. The resulting stochastic model can be described as a continuous time Markov model, with the transition matrix for random events for all subpopulations given in Matrix 1. During simulations, the number of individuals in each subpopulation is updated on each transition time from the associated event.

5.2.2 Parameterization

For a new vaccine candidate, we assign the parameter p to represent the coverage of vaccination for infants, with the baseline value of $p = 0$ in the absence of vaccination. Previous work on the dynamics of natural immunity caused by Hib estimated that, prior to the introduction of conjugated Hib vaccines, new Hib infections occurred once in 4 years to prevent infection from progressing to invasive Hib disease [7]. In our study on the naturally acquired immunity against Hia in a Canadian Aboriginal population presented in Chapter 4, we estimated that the incidence of carriage may be occurring more frequently than that estimated for Hib. Using these estimates, we assume the ranges 2-4 years for protection against Hia carriage, and 6-10 years for protection against Hia disease following natural infection or vaccination. Similar to previous estimates for Hib [7], we consider the probability of carriage following primary infection with Hia in the range 0.6-0.9. It is assumed that Hia in the form of carriage or pre-symptomatic is 50% less infectious than Hia

disease. Furthermore, susceptibility to encounter new Hia infection during partial protection is assumed to be reduced by 50%. The incubation period for Hia is estimated between 2 and 4 days [84]. We consider a latent period of 2 days for colonization during which no transmission can occur, and an average period of 1 day for pre-symptomatic infection before developing Hia disease. The duration of carriage is unknown, but may range from several days to several weeks [5, 7], and the risk of infection transmission persists as long as bacteria are present whether or not there is nasal discharge [84]. We assume an average infectious period of 50 days for Hia carriage. The variation in these parameters and their effect on the model outcomes will be addressed through sensitivity analyses. Hia disease is considered non-communicable within 24-48 hours after starting effective treatment [84]. Since individuals with clinical manifestation of Hia disease are likely to receive antibiotic treatment, and considering the delay of one day in start of the treatment, we assume an average infectious period of 2 days for Hia disease. Model parameters and their values are listed in Table 5.1.

To evaluate the effect of vaccination, we consider several parameters including the coverage of primary vaccination for infants (p); the coverage of booster vaccination (p_v) for those who have received primary vaccination during infancy; the rate of primary vaccination (ξ) for susceptible individuals; and the coverage of booster vaccination (p_s) for susceptible individuals who have received primary vaccination. These parameters will be varied within their respective ranges in simulation scenarios.

Matrix 1. Transition matrix for the stochastic simulations.

	S	V_n	V_p	V_b	L	L_v	C	A	I	V_{bp}	S_v	S_p	S_n	
recruitment to S	$+1$	0	0	0	0	0	0	0	0	0	0	0	0	$(1-p)\mu N$
vaccination of infants	0	$+1$	0	0	0	0	0	0	0	0	0	0	0	$p\mu N$
infection of S	-1	0	0	0	$+1$	0	0	0	0	0	0	0	0	$\frac{\beta S[I+\delta(C+A)]}{N}$
waning protection in V_n	0	-1	$+1$	0	0	0	0	0	0	0	0	0	0	σV_n
booster vaccination for V_p	0	0	-1	$+1$	0	0	0	0	0	0	0	0	0	$p_v\sigma_p V_p$
loss of protection in V_p	0	0	-1	0	0	0	0	0	0	0	0	0	$+1$	$(1-p_v)\sigma_p V_p$
infection of V_p	0	0	-1	0	0	$+1$	0	0	0	0	0	0	0	$\frac{\eta\beta V_p[I+\delta(C+A)]}{N}$
waning protection in V_b	0	0	0	-1	0	0	0	0	0	$+1$	0	0	0	σV_b
infection of V_{bp}	0	0	0	0	0	$+1$	0	0	0	-1	0	0	0	$\frac{\eta\beta V_{bp}[I+\delta(C+A)]}{N}$
loss of protection in V_{bp}	0	0	0	0	0	0	0	0	0	-1	0	0	$+1$	$\sigma_p V_{bp}$
vaccination of susceptibles	-1	0	0	0	0	0	0	0	0	0	$+1$	0	0	ξS
waining protrction in S_v	0	0	0	0	0	0	0	0	0	0	-1	$+1$	0	σS_v
infection of S_p	0	0	0	0	0	$+1$	0	0	0	0	0	-1	0	$\frac{\eta\beta S_p[I+\delta(C+A)]}{N}$
booster vaccination for S_p	0	0	0	$+1$	0	0	0	0	0	0	0	-1	0	$p_s\sigma_p S_p$
loss of protection in S_p	0	0	0	0	0	0	0	0	0	0	0	-1	$+1$	$(1-p_s)\sigma_p S_p$
infection of S_n	0	0	0	0	$+1$	0	0	0	0	0	0	0	-1	$\frac{\beta S_n[I+\delta(C+A)]}{N}$
carriage from L	0	0	0	0	-1	0	$+1$	0	0	0	0	0	0	$q\theta L$
pre-symptomatic from L	0	0	0	0	-1	0	0	$+1$	0	0	0	0	0	$(1-q)\theta L$
carriage from L_v	0	0	0	0	0	-1	$+1$	0	0	0	0	0	0	θL_v
Hia disease from A	0	0	0	0	0	0	0	-1	$+1$	0	0	0	0	αA
recovery from Hia carriage	0	0	0	$+1$	0	0	-1	0	0	0	0	0	0	$\gamma_1 C$
recovery from Hia disease	0	0	0	$+1$	0	0	0	0	-1	0	0	0	0	$\gamma_2 I$
natural death for S	-1	0	0	0	0	0	0	0	0	0	0	0	0	μS
natural death for V_n	0	-1	0	0	0	0	0	0	0	0	0	0	0	μV_n
natural death for V_p	0	0	-1	0	0	0	0	0	0	0	0	0	0	μV_p
natural death for V_b	0	0	0	-1	0	0	0	0	0	0	0	0	0	μV_b
natural death for L	0	0	0	0	-1	0	0	0	0	0	0	0	0	μL
natural death for L_v	0	0	0	0	0	-1	0	0	0	0	0	0	0	μL_v
natural death for C	0	0	0	0	0	0	-1	0	0	0	0	0	0	μC
natural death for A	0	0	0	0	0	0	0	-1	0	0	0	0	0	μA
natural death for I	0	0	0	0	0	0	0	0	-1	0	0	0	0	μI
natural death for V_{bp}	0	0	0	0	0	0	0	0	0	-1	0	0	0	μV_{bp}
natural death for S_v	0	0	0	0	0	0	0	0	0	0	-1	0	0	μS_v
natural death for S_p	0	0	0	0	0	0	0	0	0	0	0	-1	0	μS_p
natural death for S_n	0	0	0	0	0	0	0	0	0	0	0	0	-1	μS_n

5.2.3 Model implementation

We use a Markov Chain Monte Carlo method to simulate the stochastic model. In simple stochastic SIR models, the basic reproduction number can be used to assess the likelihood of an outbreak taking place, which is determined by the probability [85]:

$$1 - (1/\mathcal{R}_0)^{\text{initial number of infections}}$$

For the range 1.2–1.4 of $\mathcal{R}_0$, the probability of an epidemic taking place is greater than 0.17 with a single initial infection. For the purpose of simulations, we choose the initial number of infections $C(0) = 10$ and $I(0) = 1$ in a total population of size $N = 100,000$. To estimate the transition time (i.e., step-size in stochastic simulations) to the next event, we let $\Delta t = U_1/\Phi$, where U_1 is a random variate drawn from the uniform distribution on the unit interval $(0, 1)$, and Φ is equal to the sum of the rates for all possible events. We then order the events as an increasing fraction of Φ and generate another uniform deviate ($U_2 \in [0, 1]$) to determine the nature of the next event (see the transition matrix 1). Simulations are run for a large number of samples ($n = 1000$) to calculate the average of sample realizations of the stochastic process in each scenario. For each simulation, the durations of vaccine-induced protection against Hia carriage and disease were randomly sampled from their ranges. For scenarios presented here, we fix $\mathcal{R}_0 = 1.3$, and simulate the model with parameter values given in Table 5.1 for various rates of vaccination.

Table 5.1: Description of model parameters with their values (ranges) used for stochastic simulations.

Parameter	Description	Value or Range
$\mathcal{R}_0$	basic reproduction number	1.2–1.4
η	reduced susceptibility during partial protection	0.5
δ	reduced transmissibility during carriage or pre-symptomatic infection	0.5
$1/\sigma$	average duration of protection against subclinical infection	2–4 years
$1/\sigma_p$	average duration of protection against Hia disease	6–10 years
$1/\theta$	average duration of latency	2 days
q	fraction of Hia exposed individuals who undergo carriage	0.6–0.9
$1/\alpha$	average duration of pre-symptomatic infection	1 day
$1/\gamma_1$	duration of carriage infection	2–10 weeks
$1/\gamma_2$	duration of communicable Hia disease (under treatment)	1–2 days
$1/\mu$	average lifetime	70 years

5.3 Results

In the absence of vaccination, Figure 5.3a shows the prevalence of Hia carriage that peaks within 3-4 years, creating a high level of herd immunity in the population that results in the decline of carriage up to year 10. After a transient period of protection following recovery from carriage, individuals may encounter a new infection, which leads to the second peak with a significantly smaller magnitude over 20 years of simulations. As shown in Figure

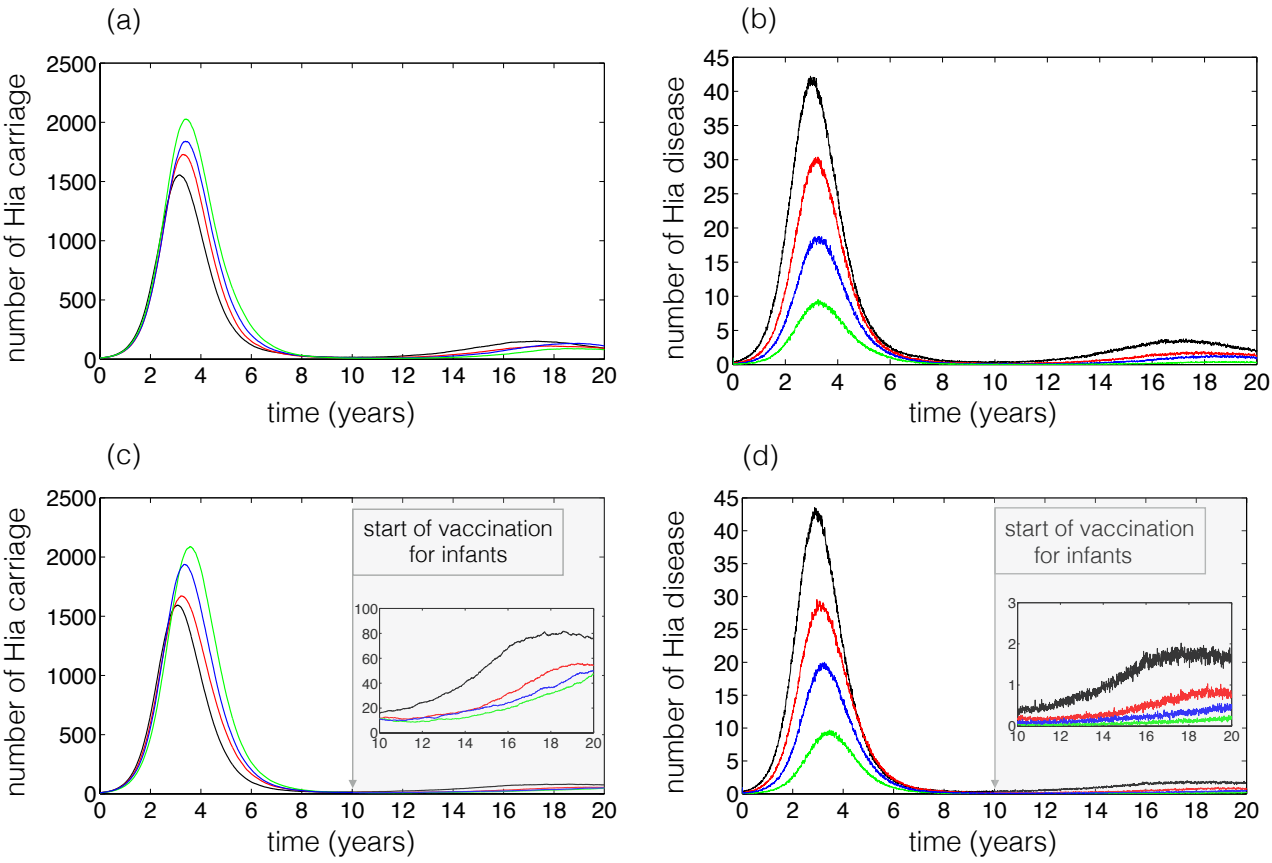

Figure 5.3: Time profiles of Hia carriage and disease without vaccination (a,b) and with vaccination of infants (c,d) starting at year 10. Vaccine coverage of first dose for infants was fixed at 95%, with a booster dose (second dose) of 95% coverage (c,d). Simulations were run with $\rho = 1.3$ for $q = 0.6$ (black curves); $q = 0.7$ (red curves); $q = 0.8$ (blue curves); and $q = 0.9$ (green curves). Shaded area illustrates the vaccine era.

5.3a. The qualitative pattern of infection spread is independent of the fraction of individuals who experience Hia carriage (q) during primary infection. We observe qualitatively similar patterns for the incidence of Hia disease (Figure 5.3b).

Not surprisingly, vaccination reduces the incidence of infection for both Hia carriage and disease. If vaccination is offered only to infants, with a booster dose within 6-10 years after the primary dose, then the rate of infection spread is decelerated in the population

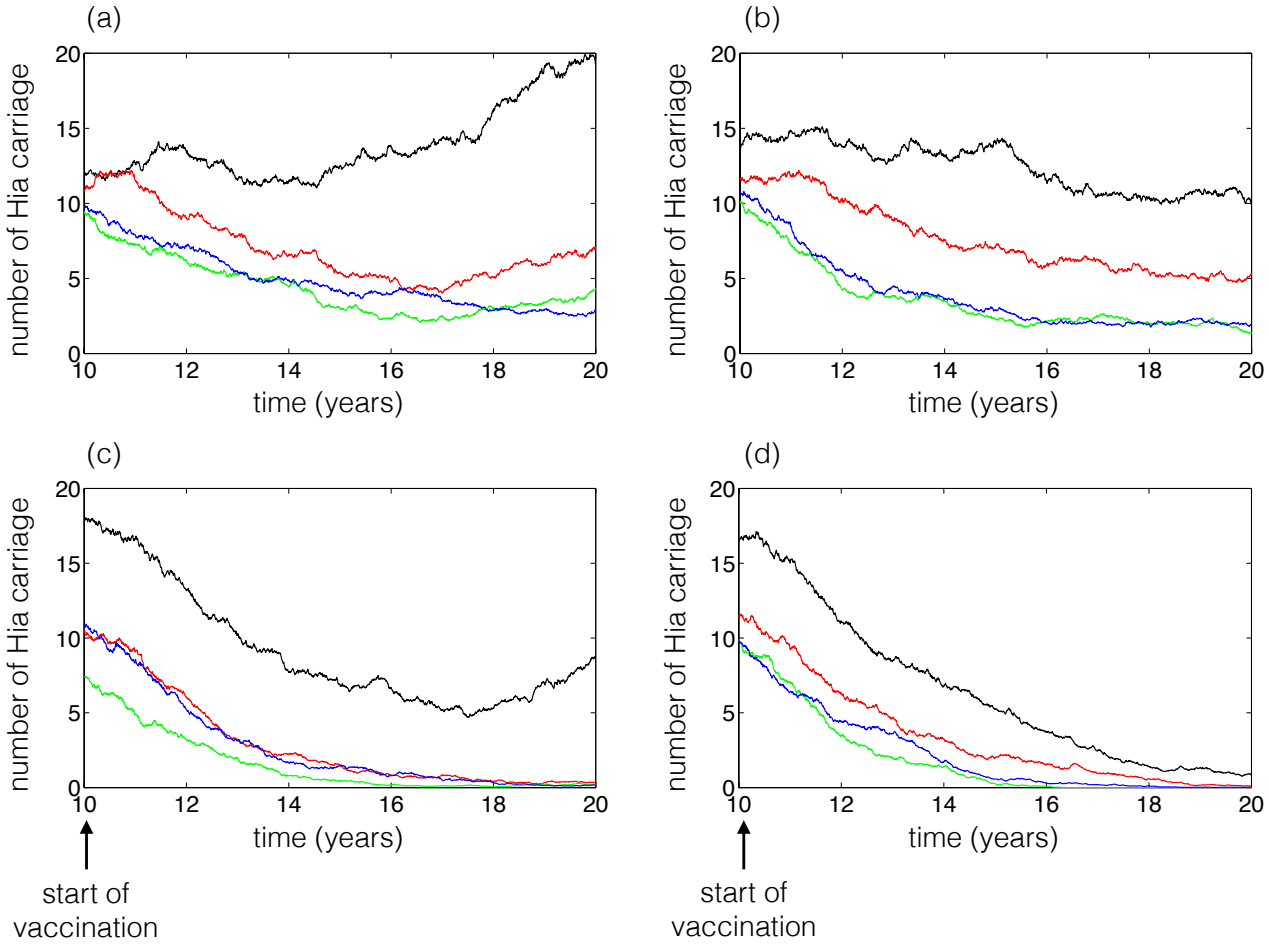

Figure 5.4: Time profiles of Hia carriage and disease with vaccination of infants and other susceptibles starting at year 10. In all scenarios, vaccine coverage of first dose for infants was fixed at 95%, with a booster dose (second dose) of 95% coverage. The rate of primary vaccination for susceptible individuals is $\xi = 10^{-4}$ per day (a,b) and $\xi = 2 \times 10^{-4}$ per day (c,d). The coverage of booster vaccination for susceptible individuals who received primary vaccination is 0 (a,c) and 100% (b,d). Simulations were run with $\mathcal{R}_0 = 1.3$ for $q = 0.6$ (black curves); $q = 0.7$ (red curves); $q = 0.8$ (blue curves); and $q = 0.9$ (green curves).

with lower magnitude compared to the scenario without vaccination (Figure 5.3c,d). However, the number of infections is still growing over a 10-year period following the start of vaccination.

5.3.1 Vaccination of susceptibles

We first implemented a single-dose vaccination of susceptible individuals (those who did no receive the primary vaccination) in combination with vaccination of infants. For the vaccination rate $\xi = 10^{-4}$ per day of susceptibles, corresponding to the probability 0.036 of receiving vaccine in a year, the increase in the number of Hia carriage can be prevented for several years, and even slightly decreased when q is sufficiently high (Figure 5.4a). With gradual decrease in the protection level of vaccinated individuals, the incidence of infection starts to increase. For these levels of vaccination for infants and susceptible individuals, we observe that the corresponding average number of cases with Hia disease remains below 1 over 10 years of simulations following the start of vaccination. When the rate of vaccination for susceptible individuals is increased to $\xi = 2 \times 10^{-4}$ per day (corresponding to the probability 0.07 of receiving vaccine in a year), the incidence of infection decreases, and the average number of Hia carriage may decline below 1 within 4-6 years for sufficiently high q (Figure 5.4c). As the immune protection of individuals wanes, the number of Hia carriage starts to rise again.

We then included a booster vaccination coverage and ran simulations for the rate $\xi = 10^{-4}$ per day of primary vaccination for susceptible individuals (Figure 5.4b). For a booster coverage of 100%, the incidence of infection declines over 10 years following the start of vaccination, but the average number of Hia carriage still remains above 1 (Figure 5.4b). This suggests that Hia infection may persist in the population through carriage even when a booster vaccination is implemented. When the rate of primary vaccination of susceptible

individuals increased to 2×10^{-4} per day (Figure 5.4d), the average number of Hia carriage decreases below 1 within 6-10 years, with a faster rate of decline for higher q. These simulations indicate that a low vaccination rate of susceptible individuals may not eliminate the pathogen even with 100% booster coverage. Furthermore, since Hia carriage may not be easily identified, especially when Hia disease is absent, these simulations suggest that Hia can persist in the population and possibly resurge in the form of Hia disease as the herd immunity declines over time.

5.3.2 Effect of vaccination on herd immunity

The patterns of Hia carriage and disease can be explained by the rise and fall of herd immunity in the population. Figure 5.5 shows the population level of protection against Hia carriage prior to, and after the start of, vaccination. Without vaccination, the second epidemic observed in Figures 5.3a,b results from the decline of herd immunity following the first epidemic peak (Figure 5.5a). With vaccination of only infants, the rate of decline of herd immunity is slightly reduced (Figure 5.5b). When primary and booster vaccination of susceptible individuals are implemented, the decline of herd immunity is halted, with possibly an increase in the population level of protection during 10 years of vaccination (Figure 5.5c,d). For a sufficiently high rate of vaccination for susceptible individuals, the herd immunity increases to levels required for elimination of Hia pathogen.

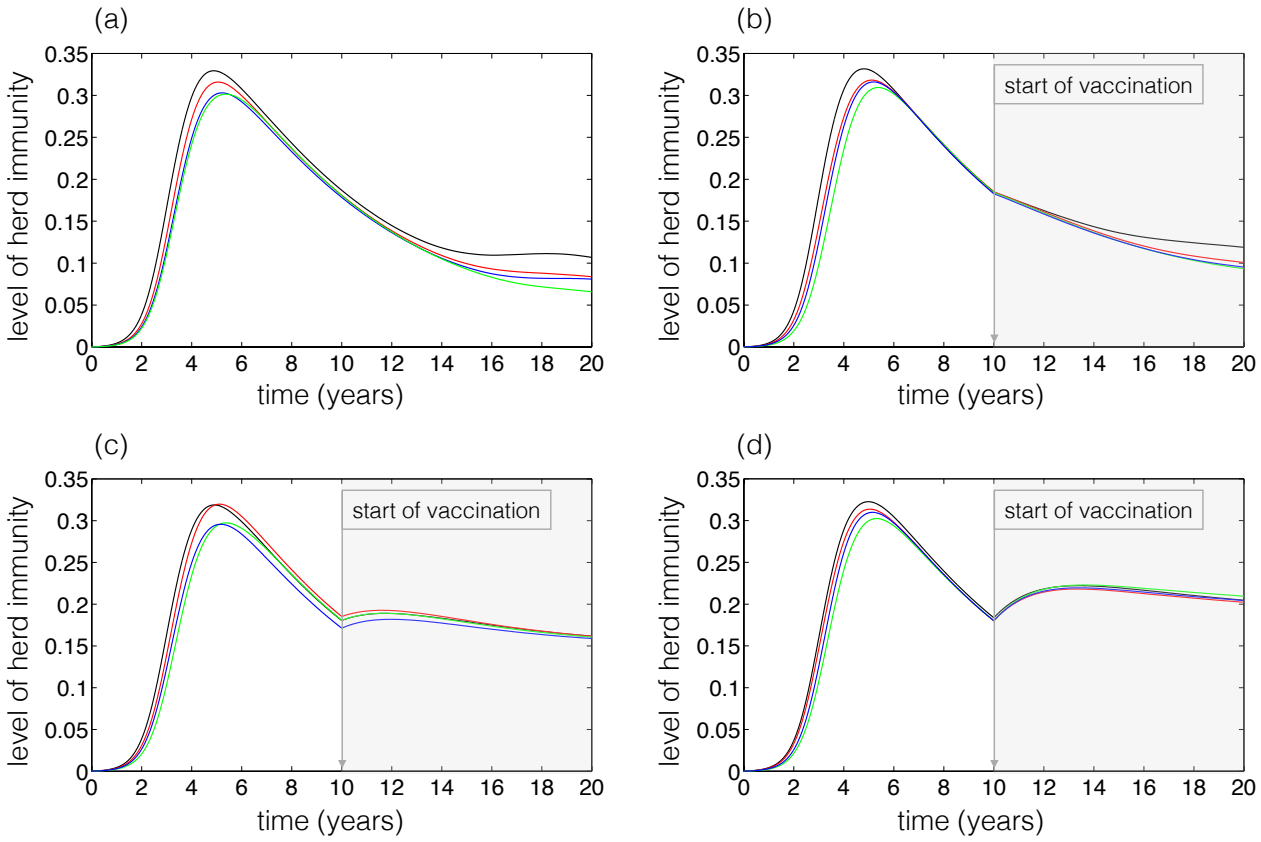

Figure 5.5: Level of herd immunity (fraction of population protected, conferred by fully protected individuals) against Hia carriage without vaccination (a); with vaccination of only infants at 95% coverage of both primary and booster vaccination (b); with primary vaccination of susceptible individuals at the rate $\xi = 10^{-4}$ per day and booster coverage of 100% (in addition to vaccination of newborns) (c); and with primary vaccination of susceptible individuals at the rate $\xi = 2 \times 10^{-4}$ per day and booster coverage of 100% (in addition to vaccination of infants). Simulations were run with $\mathcal{R}_0 = 1.3$ for $q = 0.6$ (black curves); and $q = 0.7$ (red curves); $q = 0.8$ (blue curves); $q = 0.9$ (green curves). Shaded area illustrates the vaccine era.

5.4 Sensitivity and Uncertainty Analyses

Due to similarities in the epidemiological characteristics of Hia and Hib, we parameterized the vaccination model using available estimates for Hib. However, we need to consider the variation in these parameters. To account for the uncertainty in the parameter space,

we carried out a sensitivity analysis using the Latin Hypercube Sampling (LHS) technique and calculated Partial Rank Correlation Coefficients (PRCC) to investigate the effect of parameter changes on the model outcomes, specifically on the number of Hia carriage and invasive disease. For this analysis, we considered six parameters and their associated ranges, including

$$\eta \in [0.3, 0.7], \qquad \delta \in [0.3, 0.7], \qquad q \in [0.6, 0.9],$$
$$\gamma_1 \in [0.0143, 0.071], \quad \sigma \in [0.00068, 0.00137], \quad \sigma_p \in [0.00027, 0.00046]$$

To allow for the simultaneous variations of these parameters, samples of size 1000 were generated in which each parameter was treated as a random variable and assigned a probability function. These parameters were uniformly distributed and sampled within their respective ranges. To calculate PRCC, we considered the equilibrium state of the deterministic model structure as the response (model output), assuming that there is no correlation between the input parameters [86]. The parameters with large PRCC values (close to 1 or -1) and their corresponding p-values smaller than the significance level (0.05) have the largest influence on the model outcomes [87]. In this analysis, the transmission rate was calculated based on the sampled parameter values with fixed $\mathcal{R}_0 = 1.3$. We examined scatter plots to verify the existence of monotonic relationships between the parameters used in LHS sampling and the equilibrium state as the response. The PRCC values and their associated t-statistics $p-$values are presented in Table 5.2. This analysis reveals that the rate of recovery from carriage (γ_1) is the most important parameter which has a negative effect on the response, as increasing γ_1 decreases the number of carriage at the equilibrium state

Table 5.2: Partial rank correlation coefficients and their associated p-values.

Parameter	γ_1	η	σ	σ_p	q	δ
PRCC	-0.9797	0.9099	0.7767	0.3953	0.1802	0.1900
$p-$value	< 0.001	< 0.001	< 0.001	< 0.001	0.0117	0.0078

of the system. The second most important parameter that strongly affects the response is the level of susceptibility to infection during partial protection period. In our model, we assumed that exposure to infection during this partial protection (if infection occurs) leads to carriage, but not to Hia disease.

Considering PRCC values in Table 5.2, we carried out simulations to calculate the average of independent realizations of the stochastic process using parameter samples generated by LHS. Figure 5.6 shows the results for different vaccination rates of susceptible individuals, while fixing the primary and booster coverage of infants at 95%. Similar to results presented in Figure 5.4, we observe that for a sufficiently low vaccination rate of susceptible individuals, Hia infection may persist in the population even when the primary vaccination of susceptibles is supplemented with 100% booster coverage.

5.5 Discussion

Here, we presented the first modelling framework of Hia infection using the natural history of the disease to investigate the effect of a new vaccine candidate on the incidence of

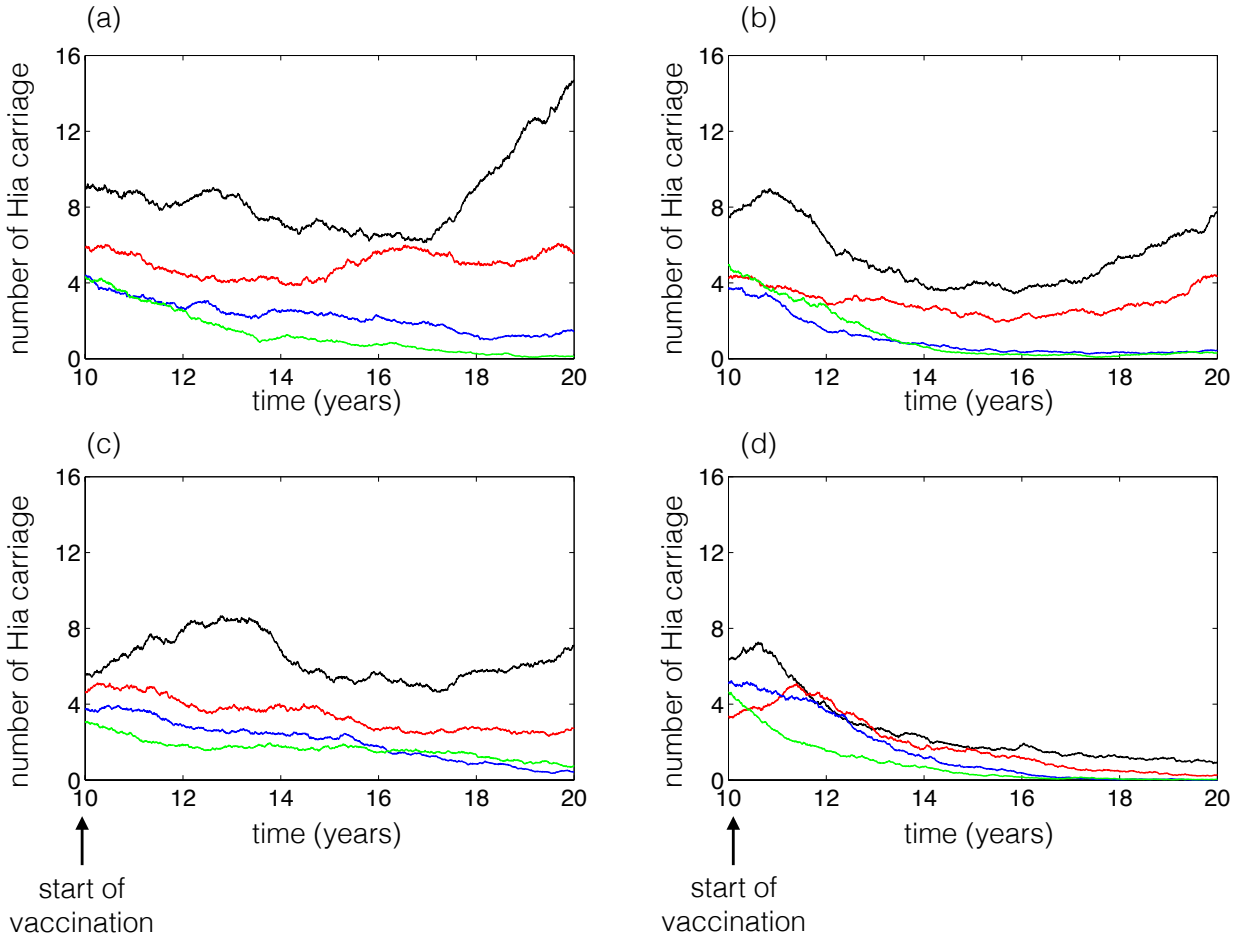

Figure 5.6: Time profiles of Hia carriage using the average realizations based on samples in parameter space generated by the LHS method. Vaccination of infants and susceptible individuals starts at year 10. In all scenarios, primary and booster vaccine coverages of infants were fixed at 95%. The rate of primary vaccination for susceptible individuals is $\xi = 10^{-4}$ per day (a,b) and $\xi = 2 \times 10^{-4}$ per day (c,d). The coverage of booster vaccination for susceptible individuals who received primary vaccination is 0 (a,c) and 100% (b,d). Simulations were run with $\mathcal{R}_0 = 1.3$ for $q = 0.6$ (black curves); $q = 0.7$ (red curves); $q = 0.8$ (blue curves); and $q = 0.9$ (green curves).

Hia carriage and disease. Given the similarities between Hia and Hib, we parameterize the stochastic model using available estimates for Hib prior to and after the introduction of universal infant immunization programs. Our simulations corroborate with observations of Hib incidence [5] in projecting that the maintenance of herd immunity through boosting

of individuals' protection is a key factor in reducing the incidence, and possibly elimination of Hia pathogen. We have shown that this goal cannot be achieved by vaccinating only infants even when a booster vaccination is implemented with a high coverage. Furthermore, while vaccinating susceptible individuals in addition to infants could significantly lower the incidence of Hia carriage and prevent the incidence of Hia disease, a high coverage of booster vaccination is required to prevent resurgence and wipe out Hia from the population.

Since most infections are transmitted through carriage, it is difficult to estimate transmissibility of Hia from available epidemiological data without collecting data associated with contact tracing. However, previous studies report a high prevalence of Hia as a cause of invasive community-acquired disease in some North American Indigenous populations, e.g., among Navajo and White Mountain Apache (incidence rate 20.2/100,000 persons for children < 5 years of age), Alaska Native (20.9/100,000 persons for children < 2 years of age), and northern Canada Indigenous peoples (101.9/100,000 persons for children < 2 years of age) [32, 33, 88]. A previous study in Alaska found a 43% rate of Hia carriage among close contacts of an infant presenting with invasive Hia disease [89]. The high incidence rates in these population settings could be related to genetic factors, environmental conditions, and prevalence of predisposing conditions [2, 3]. Data collected for anti-Hia antibodies in serum samples of participants in a population of Northwestern Ontario, Canada, used in our study presented in Chapter 4, suggest that the individuals with the condition of chronic renal failure have lower antibody concentrations compared to healthy individuals, and require more frequent boosting of immunity to prevent the risk of Hia disease

[61]. Crowding living condition with multigenerational households may also be a contributing factor to high incidence of Hia in these populations, as has been discussed for the spread of other infectious diseases such as influenza and tuberculosis [90–94]. These observations, combined with the results of our model, highlight the importance of vaccination and timely boosting of the individual's immunity within the expected duration of vaccine-induced protection against Hia.

In the absence of specific estimates of the parameters describing the natural history of Hia infection, and the effectiveness and duration of vaccine-induced protection against Hia carriage and disease, we have relied on available estimates for Hib infection. However, we considered a plausible range of parameter values in our simulations, and performed sensitivity and uncertainty analyses to verify the robustness of the findings. The results indicate that the rate of recovery from carriage and the reduced level of susceptibility during partial protection are the two most important parameters affecting the number of Hia carriage and disease at the model equilibrium. The recovery rate of Hia carriage is not certain, and clearly has a negative effect on the number of Hia carriage. This parameter, which also appears in the expression for the reproduction number $\mathcal{R}_0$, effectively relates to the infectious period of Hia carriage estimated to last from a few days to several weeks for *H. influenzae* infections, representing a key parameter in the persistence of Hia in the population. Other parameters that have significant to moderate effects on the equilibrium state of the system, and therefore Hia elimination, include the average durations of protection against Hia carriage and disease following vaccination or natural infection. We note that the reproduction number $\mathcal{R}_0$ is independent of the parameters η, σ, and σ_p, which can

greatly influence Hia elimination.

In the next Chapter, we will attempt to overcome some of the limitations related to the structure of the model proposed here. Specifically, we did not structure the model by age, but we understand that the incidence of Hia could be affected by age and the patterns of contacts between individuals [5, 8, 49]. We also note that antigens from several organisms other than Hia can induce cross-reactive antibodies to Hia capsular polysaccharide [73, 74], and may therefore increase the antibody concentrations. Although the relative importance of antibodies arising in response to encounters with cross-reactive bacteria is unknown [95], we consider this effect by the variation in the durations of naturally-acquired and vaccine-induced protection in our simulations to address the uncertainty in several immunologically-related parameters.

Chapter 6

An Age Structure Model of Hia

As reported in the incidence of Hia, age can play a significant role in transmission of infection. Estimates published in the literature suggest that most infections occur amongst children and older adults with underlying medical conditions [2, 3]. Therefore age may be an important factor to be considered in transmission dynamics of Hia and vaccination. The incidence of both carriage and symptomatic Hia infection could also be affected by contact patterns between individuals, which varies among different age groups. To incorporate the effect of these contact patterns, we develop an age-structured model to reveal more information on the target groups and their vaccination coverage. The model is used to evaluate vaccination strategies and their long-term epidemiological impact.

6.1 The Model

We develop an age-structured stochastic epidemic model, and consider four age groups in the population with the associated contact matrix. The age groups include: infants within the first year of birth; young children between 1 and 2 years of age; children between 2 and 10 years of age; and individuals older than 10 years of age. The population compartments in each age group represent different epidemiological and clinical statuses as susceptibles (S); exposed individuals who are not yet infectious (L); infectious individuals without symptoms referred to as carriage (C); infectious individuals who will develop symptomatic infection referred to as pre-symptomatic (A); infectious individuals with symptoms (I); vaccinated individuals (V); and recovered individuals (R). Susceptible individuals can become colonized with Hia bacteria through contacts with infectious cases.

In developing the model, we make some realistic assumptions as validated in biological studies, and used in our previous chapter. We assume that the level of immunity following recovery from Hia infection declines from full to partial (thereby moving individuals from R to P), and ultimately to low levels considered as fully susceptible (i.e., moving individuals from P to S). With partial immunity, we assume that individuals experience carriage if infected; however, susceptible individuals can also develop symptomatic Hia disease, and only a fraction of them may experience carriage. These assumptions that have been observed in clinical studies, have important implications for our modelling analysis. Since both vaccine-induced and naturally acquired immunity wane over time, individuals may enter the state of partial protection (V_p), and are therefore at risk of becoming infected. We

introduce the class (L_p) for individuals who are exposed to Hia and infected during partial protection conferred from a previous infection or vaccination.

The model includes two key aspects of the population over time-scales used for simulation dynamics: (i) average number of contacts between individuals in the same or different age groups; and (ii) movements of individuals from one compartment of an age group to the corresponding compartment of another age group due to changes in their age. Transitions between model compartments and different age groups are described in Figure 6.1.

The model is built using 4 sub-systems of ordinary differential equations. For infants less than 1 year of age (belonging to group 1 referred to as G_1), the following system of equations applies, where N_j is the total population size of age group j:

$$
\begin{aligned}
\frac{dS_1}{dt} &= bN + \sigma_p P_1 - S_1 \sum_{j=1}^{4} \beta_{1j} \frac{I_j + \delta(C_j + A_j)}{N_j} - \kappa_1 S_1 - \mu S_1 \\
\frac{dL_1}{dt} &= S_1 \sum_{j=1}^{4} \beta_{1j} \frac{I_j + \delta(C_j + A_j)}{N_j} - \theta L_1 - \mu L_1 \\
\frac{dC_1}{dt} &= q\theta L_1 + \theta L_{P1} - \gamma_1 C_1 - \mu C_1 \\
\frac{dA_1}{dt} &= (1-q)\theta L_1 - \alpha A_1 - \mu A_1 \\
\frac{dI_1}{dt} &= \alpha A_1 - \gamma_2 I_1 - \mu I_1 \\
\frac{dR_1}{dt} &= \gamma_1 C_1 + \gamma_2 I_1 - \sigma R_1 - \kappa_1 R_1 - \mu R_1 \\
\frac{dP_1}{dt} &= \sigma R_1 - \eta P_1 \sum_{j=1}^{4} \beta_{1j} \frac{I_j + \delta(C_j + A_j)}{N_j} - \sigma_p P_1 - \kappa_1 P_1 - \mu P_1 \\
\frac{dL_{P1}}{dt} &= \eta P_1 \sum_{j=1}^{4} \beta_{1j} \frac{I_j + \delta(C_j + A_j)}{N_j} - \theta L_{P1} - \mu L_{P1}
\end{aligned}
\tag{6.1}
$$

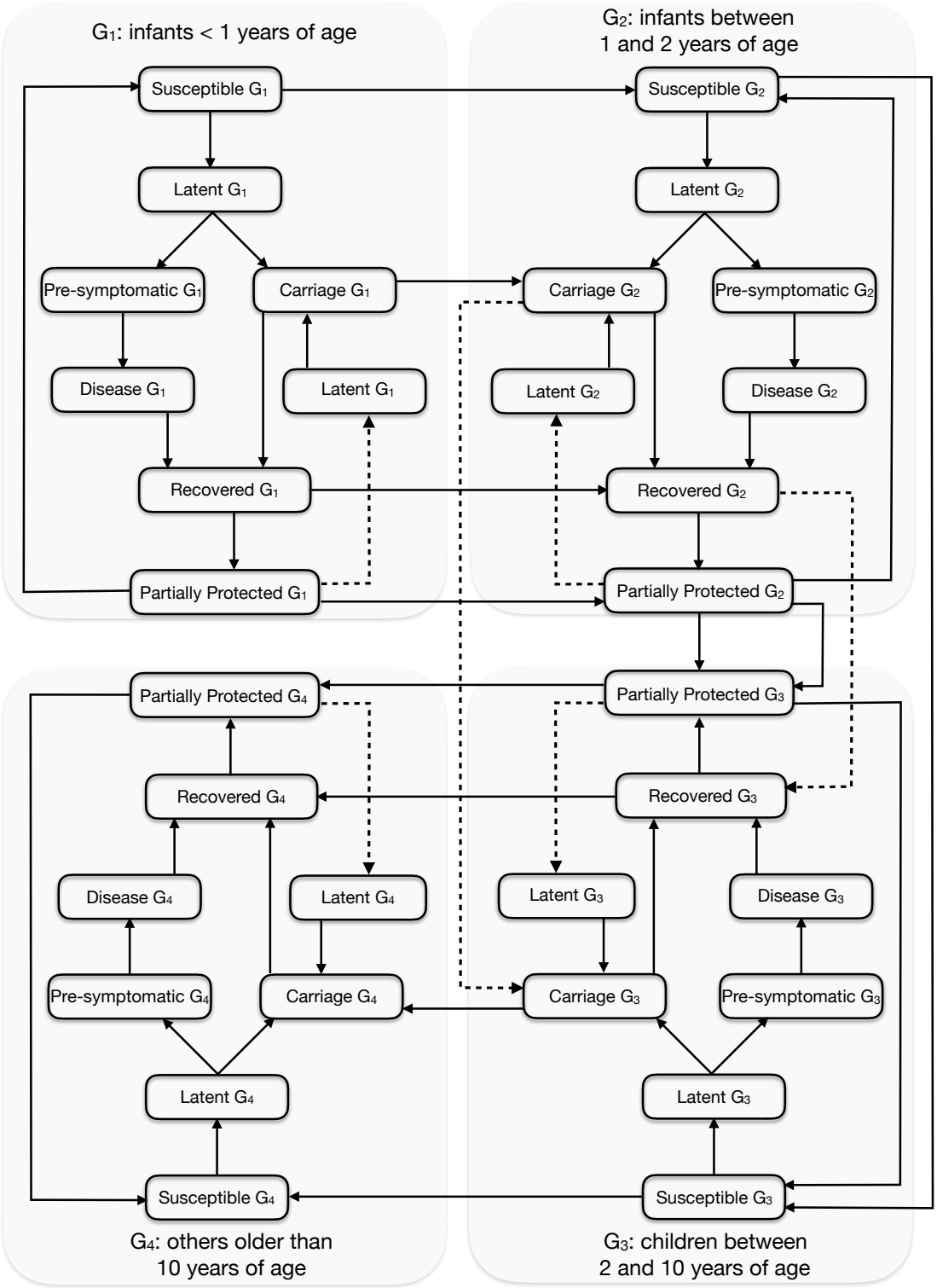

Figure 6.1: Leslie diagram for transitions between model compartments.

For the second and third age groups comprising young children between 1 and 2 years of age, and children between 2 and 10 years of age, the sub-systems are governed by the following equations for $i = 2, 3$:

$$
\begin{aligned}
\frac{dS_i}{dt} &= \kappa_{i-1}S_{i-1} + \sigma_p P_i - S_i \sum_{j=1}^{4} \beta_{ij} \frac{I_j + \delta(C_j + A_j)}{N_j} - \kappa_i S_i - \mu S_i \\
\frac{dL_i}{dt} &= S_i \sum_{j=1}^{4} \beta_{ij} \frac{I_j + \delta(C_j + A_j)}{N_j} - \theta L_i - \mu L_i \\
\frac{dC_i}{dt} &= q\theta L_i + \theta L_{Pi} - \gamma_1 C_i - \mu C_i \\
\frac{dA_i}{dt} &= (1-q)\theta L_i - \alpha A_i - \mu A_i \\
\frac{dI_i}{dt} &= \alpha A_i - \gamma_2 I_i - \mu I_i \\
\frac{dR_i}{dt} &= \gamma_1 C_i + \gamma_2 I_i + \kappa_{i-1} R_{i-1} - \sigma R_i - \kappa_i R_i - \mu R_i \\
\frac{dP_i}{dt} &= \kappa_{i-1} P_{i-1} + \sigma R_i - \eta P_i \sum_{j=1}^{4} \beta_{ij} \frac{I_j + \delta(C_j + A_j)}{N_j} - \sigma_p P_i - \kappa_i P_i - \mu P_i \\
\frac{dL_{pi}}{dt} &= \eta P_i \sum_{j=1}^{4} \beta_{ij} \frac{I_j + \delta(C_j + A_j)}{N_j} - \theta L_{Pi} - \mu L_{Pi}
\end{aligned}
\tag{6.2}
$$

In these sub-systems, κ_{i-1} ($i = 2, 3, 4$) represents the rate at which individuals in age group $i-1$ move to the corresponding compartments in age group i as a result of change in their ages. We also include the recruitment into the population through newborns in the first age group.

The system for the last age group (i.e., individuals older than 10 years of age) is described by the following differential equations:

$$
\begin{aligned}
\frac{dS_4}{dt} &= \kappa_3 S_3 + \sigma_p P_4 - S_4 \sum_{j=1}^{4} \beta_{4j} \frac{I_j + \delta(C_j + A_j)}{N_j} - \mu S_4 \\
\frac{dL_4}{dt} &= S_4 \sum_{j=1}^{4} \beta_{4j} \frac{I_j + \delta(C_j + A_j)}{N_j} - \theta L_4 - \mu L_4 \\
\frac{dC_4}{dt} &= q\theta L_4 + \theta L_{P4} - \gamma_1 C_4 - \mu C_4 \\
\frac{dA_4}{dt} &= (1-q)\theta L_4 - \alpha A_4 - \mu A_4 \\
\frac{dI_4}{dt} &= \alpha A_4 - \gamma_2 I_4 - \mu I_4 \\
\frac{dR_4}{dt} &= \gamma_1 C_4 + \gamma_2 I_4 + \kappa_3 R_3 - \sigma R_4 - \mu R_4 \\
\frac{dP_4}{dt} &= \kappa_3 P_3 + \sigma R_4 - \eta P_4 \sum_{j=1}^{4} \beta_{4j} \frac{I_j + \delta(C_j + A_j)}{N_j} - \sigma_p P_4 - \mu P_4 \\
\frac{dL_{P4}}{dt} &= \eta P_4 \sum_{j=1}^{4} \beta_{4j} \frac{I_j + \delta(C_j + A_j)}{N_j} - \theta L_{P4} - \mu L_{P4}
\end{aligned}
\tag{6.3}
$$

In these systems, the parameter β_{ij} is defined as βc_{ij}, where β is the baseline transmission of infection, and c_{ij} is the average number of contacts between an individual in group i and individuals in group j. The description of other parameters and their values are provided in Table 6.1.

6.1.1 Reproduction Number

For the model proposed here, the basic reproduction number ($\mathcal{R}_0$) can be calculated using the next generation method [78, 79]. Let $\mathcal{F}(x)$ represent the generation rate of new infections, and $\mathcal{V}(x)$ be the transfer rate, by all other means, of individuals between model compartments. Then we have

$$\mathcal{F}(x) = \begin{pmatrix} a_1[I_1 + \delta(C_1 + A_1)] + a_2[I_2 + \delta(C_2 + A_2)] + a_3[I_3 + \delta(C_3 + A_3)] + a_4[I_4 + \delta(C_4 + A_4)] \\ 0 \\ 0 \\ 0 \\ a_5[I_1 + \delta(C_1 + A_1)] + a_6[I_2 + \delta(C_2 + A_2)] + a_7[I_3 + \delta(C_3 + A_3)] + a_8[I_4 + \delta(C_4 + A_4)] \\ 0 \\ 0 \\ 0 \\ a_9[I_1 + \delta(C_1 + A_1)] + a_{10}[I_2 + \delta(C_2 + A_2)] + a_{11}[I_3 + \delta(C_3 + A_3)] + a_{12}[I_4 + \delta(C_4 + A_4)] \\ 0 \\ 0 \\ 0 \\ a_{13}[I_1 + \delta(C_1 + A_1)] + a_{14}[I_2 + \delta(C_2 + A_2)] + a_{15}[I_3 + \delta(C_3 + A_3)] + a_{16}[I_4 + \delta(C_4 + A_4)] \\ 0 \\ 0 \\ 0 \end{pmatrix}$$

where:

$$\begin{array}{cccc} a_1 = c_{11}\beta\frac{S_1}{N_1} & a_2 = c_{12}\beta\frac{S_1}{N_2} & a_3 = c_{13}\beta\frac{S_1}{N_3} & a_4 = c_{14}\beta\frac{S_1}{N_4} \\ a_5 = c_{21}\beta\frac{S_2}{N_1} & a_6 = c_{22}\beta\frac{S_2}{N_2} & a_7 = c_{23}\beta\frac{S_2}{N_3} & a_8 = c_{24}\beta\frac{S_2}{N_4} \\ a_9 = c_{31}\beta\frac{S_3}{N_1} & a_{10} = c_{32}\beta\frac{S_3}{N_2} & a_{11} = c_{33}\beta\frac{S_3}{N_3} & a_{12} = c_{34}\beta\frac{S_3}{N_4} \\ a_{13} = c_{41}\beta\frac{S_4}{N_1} & a_{14} = c_{42}\beta\frac{S_4}{N_2} & a_{15} = c_{43}\beta\frac{S_4}{N_3} & a_{16} = c_{44}\beta\frac{S_4}{N_4} \end{array}$$

and

$$\mathcal{V}(x) = \begin{pmatrix} \theta L_1 + \mu L_1 \\ -q\theta L_1 - \theta L_{P1} + \gamma_1 C_1 + \mu C_1 \\ -(1-q)\theta L_1 + \alpha A_1 + \mu A_1 \\ -\alpha A_1 + \gamma_2 I_1 + \mu I_1 \\ \theta L_2 + \mu L_2 \\ -q\theta L_2 - \theta L_{P2} + \gamma_1 C_2 + \mu C_2 \\ -(1-q)\theta L_2 + \alpha A_2 + \mu A_2 \\ -\alpha A_2 + \gamma_2 I_2 + \mu I_2 \\ \theta L_3 + \mu L_3 \\ -q\theta L_3 - \theta L_{P3} + \gamma_1 C_3 + \mu C_3 \\ -(1-q)\theta L_3 + \alpha A_3 + \mu A_3 \\ -\alpha A_3 + \gamma_2 I_3 + \mu I_3 \\ \theta L_4 + \mu L_4 \\ -q\theta L_4 - \theta L_{P4} + \gamma_1 C_4 + \mu C_4 \\ -(1-q)\theta L_4 + \alpha A_4 + \mu A_4 \\ -\alpha A_4 + \gamma_2 I_4 + \mu I_4 \end{pmatrix}.$$

According to the next generation method, $\mathcal{R}_0$ is the dominant eigenvalue of the matrix FV^{-1}, where F and V are components of the Jacobian matrices of $\mathcal{F}(x)$ and $\mathcal{V}(x)$ at the disease-free state of the model, given by $(S_1, 0, 0, 0, S_2, 0, 0, 0, S_3, 0, 0, 0, S_4, 0, 0, 0)$,

with

$$
\begin{aligned}
S_1 &= \frac{\beta N}{\mu + \kappa_1} \\
S_2 &= \Big(\frac{\kappa_1}{\mu + \kappa_2}\Big)\frac{\beta N}{\mu + \kappa_1} \\
S_3 &= \Big(\frac{\kappa_2}{\mu + \kappa_3}\Big)\Big(\frac{\kappa_1}{\mu + \kappa_2}\Big)\frac{\beta N}{\mu + \kappa_1} \\
S_4 &= \Big(\frac{\kappa_3}{\mu}\Big)\Big(\frac{\kappa_2}{\mu + \kappa_3}\Big)\Big(\frac{\kappa_1}{\mu + \kappa_2}\Big)\frac{\beta N}{\mu + \kappa_1}
\end{aligned}
$$

The Jacobian F and V are given by

$$
F = \begin{pmatrix}
0 & \delta a_1 & \delta a_1 & a_1 & 0 & \delta a_2 & \delta a_2 & a_2 & 0 & \delta a_3 & \delta a_3 & a_3 & 0 & \delta a_4 & \delta a_4 & a_4 \\
0 & 0 & 0 & 0 & 0 & 0 & 0 & 0 & 0 & 0 & 0 & 0 & 0 & 0 & 0 & 0 \\
0 & 0 & 0 & 0 & 0 & 0 & 0 & 0 & 0 & 0 & 0 & 0 & 0 & 0 & 0 & 0 \\
0 & 0 & 0 & 0 & 0 & 0 & 0 & 0 & 0 & 0 & 0 & 0 & 0 & 0 & 0 & 0 \\
0 & \delta a_5 & \delta a_5 & a_5 & 0 & \delta a_6 & \delta a_6 & a_6 & 0 & \delta a_7 & \delta a_7 & a_7 & 0 & \delta a_8 & \delta a_8 & a_8 \\
0 & 0 & 0 & 0 & 0 & 0 & 0 & 0 & 0 & 0 & 0 & 0 & 0 & 0 & 0 & 0 \\
0 & 0 & 0 & 0 & 0 & 0 & 0 & 0 & 0 & 0 & 0 & 0 & 0 & 0 & 0 & 0 \\
0 & 0 & 0 & 0 & 0 & 0 & 0 & 0 & 0 & 0 & 0 & 0 & 0 & 0 & 0 & 0 \\
0 & \delta a_9 & \delta a_9 & a_9 & 0 & \delta a_{10} & \delta a_{10} & a_{10} & 0 & \delta a_{11} & \delta a_{11} & a_{11} & 0 & \delta a_{12} & \delta a_{12} & a_{12} \\
0 & 0 & 0 & 0 & 0 & 0 & 0 & 0 & 0 & 0 & 0 & 0 & 0 & 0 & 0 & 0 \\
0 & 0 & 0 & 0 & 0 & 0 & 0 & 0 & 0 & 0 & 0 & 0 & 0 & 0 & 0 & 0 \\
0 & 0 & 0 & 0 & 0 & 0 & 0 & 0 & 0 & 0 & 0 & 0 & 0 & 0 & 0 & 0 \\
0 & \delta a_{13} & \delta a_{13} & a_{13} & 0 & \delta a_{14} & \delta a_{14} & a_{14} & 0 & \delta a_{15} & \delta a_{15} & a_{15} & 0 & \delta a_{16} & \delta a_{16} & a_{16} \\
0 & 0 & 0 & 0 & 0 & 0 & 0 & 0 & 0 & 0 & 0 & 0 & 0 & 0 & 0 & 0 \\
0 & 0 & 0 & 0 & 0 & 0 & 0 & 0 & 0 & 0 & 0 & 0 & 0 & 0 & 0 & 0 \\
0 & 0 & 0 & 0 & 0 & 0 & 0 & 0 & 0 & 0 & 0 & 0 & 0 & 0 & 0 & 0
\end{pmatrix}
$$

and

$$V = \begin{pmatrix} V_1 & 0 & 0 & 0 \\ 0 & V_2 & 0 & 0 \\ 0 & 0 & V_3 & 0 \\ 0 & 0 & 0 & V_4 \end{pmatrix}$$

with

$$V_1 = \begin{pmatrix} \theta+\mu & 0 & 0 & 0 \\ -q\theta & \gamma_1+\mu & 0 & 0 \\ -(1-q)\theta & 0 & \alpha+\mu & 0 \\ 0 & 0 & -\alpha & \gamma_2+\mu \end{pmatrix}, \quad V_2 = \begin{pmatrix} \theta+\mu & 0 & 0 & 0 \\ -q\theta & \gamma_1+\mu & 0 & 0 \\ -(1-q)\theta & 0 & \alpha+\mu & 0 \\ 0 & 0 & -\alpha & \gamma_2+\mu \end{pmatrix}$$

$$V_3 = \begin{pmatrix} \theta+\mu & 0 & 0 & 0 \\ -q\theta & \gamma_1+\mu & 0 & 0 \\ -(1-q)\theta & 0 & \alpha+\mu & 0 \\ 0 & 0 & -\alpha & \gamma_2+\mu \end{pmatrix}, \quad V_4 = \begin{pmatrix} \theta+\mu & 0 & 0 & 0 \\ -q\theta & \gamma_1+\mu & 0 & 0 \\ -(1-q)\theta & 0 & \alpha+\mu & 0 \\ 0 & 0 & -\alpha & \gamma_2+\mu \end{pmatrix}$$

Using Maple©, eigenvalues of matrix FV^{-1} are 0 and the product of $\frac{1}{(\gamma_1+\mu)(\gamma_2+\mu)(\theta+\mu)(\alpha+\mu)}$ with the roots of the quartic:

$$Z^4 - (a_1 + a_{11} + a_{16} + a_6)Z^3 + (a_1a_{11} + a_1a_{16} + a_1a_6 - a_{10}a_7 + a_{11}a_{16} + a_{11}a_6$$

$$- a_{12}a_{15} - a_{13}a_4 - a_{14}a_8 + a_{16}a_6 - a_2a_5 - a_3a_9)Z^2 + (a_1a_{10}a_7 - a_1a_{11}a_{16} - a_1a_{11}a_6$$

$$+ a_1a_{12}a_{15} + a_1a_{14}a_8 - a_1a_{16}a_6 - a_{10}a_{15}a_8 + a_{10}a_{16}a_7 - a_{10}a_3a_5 + a_{11}a_{13}a_4 + a_{11}a_{14}a_8$$

$$- a_{11}a_{16}a_6 + a_{11}a_2a_5 - a_{12}a_{13}a_3 - a_{12}a_{14}a_7 + a_{12}a_{15}a_6 - a_{13}a_2a_8 + a_{13}a_4a_6 - a_{14}a_4a_5$$

$$- a_{15}a_4a_9 + a_{16}a_2a_5 + a_{16}a_3a_9 - a_2a_7a_9 + a_3a_6a_9)Z - a_9a_8a_2a_{15} - a_5a_4a_{15}a_{10} - a_5a_3a_{14}a_{12}$$

$$+ a_5a_2a_{15}a_{12} + a_7a_4a_{13}a_{10} - a_8a_3a_{13}a_{10} - a_9a_7a_4a_{14} + a_9a_8a_3a_{14} - a_7a_2a_{13}a_{12} + a_{15}a_4a_6a_9$$

$$+ a_{16}a_2a_7a_9 - a_{16}a_3a_6a_9 + a_1a_{10}a_{15}a_8 - a_1a_{10}a_{16}a_7 - a_1a_{11}a_{14}a_8 + a_1a_{11}a_{16}a_6 + a_1a_{12}a_{14}a_7$$

$$- a_1a_{12}a_{15}a_6 + a_{10}a_{16}a_3a_5 + a_{11}a_{13}a_2a_8 - a_{11}a_{13}a_4a_6 + a_{11}a_{14}a_4a_5 - a_{11}a_{16}a_2a_5$$

$$+ a_{12}a_{13}a_3a_6 = 0$$

Since the solutions of this equation cannot be expressed explicitly in terms of parameters and the population sizes at the disease-free equilibrium, we obtained $\mathcal{R}_0 = 1.12$ numerically using parameters given in Table 5.1 as the largest eigenvalue of FV^{-1}.

6.1.2 Vaccination Dynamics

The population level of immunity against Hia infection can be increased by vaccinating different age-groups. We extended our age structure model to include age-specific vaccination. Individuals who receive the vaccine are fully protected against the disease for a period of time. We use previous estimates pertained to Hib for the duration of immune protection following primary vaccination in different age groups [7]. The immune protection induced by the vaccine wanes gradually over time and individuals will become partially protected. In the partially protected state, individuals are protected against the development of symptomatic disease, but carriage may still occur if transmission takes place. The complete loss

of immunity will lead to full susceptibility of individuals. In our model, it is assumed that the level of vaccine-induced protection for different age-groups is the same as that acquired by natural infection [5].

6.2 Stochastic Model

6.2.1 Stochastic Structure

To implement the model and simulate, we develop its stochastic structure by assuming that the occurrence of events depends on the rates of movement between different compartments in the deterministic model. We consider time t as a continuous variable, and define the following random vector for $t \in [0, \infty)$

$$\begin{aligned}\vec{X}(t) = (&S_1(t), V_1(t), V_{p1}(t), L_1(t), L_{p1}(t), C_1(t), A_1(t), I_1(t), R_1(t), P_1(t),\\ &S_2(t), V_2(t), V_{p2}(t), L_2(t), L_{p2}(t), C_2(t), A_2(t), I_2(t), R_2(t), P_2(t),\\ &S_3(t), V_3(t), V_{p3}(t), L_3(t), L_{p3}(t), C_3(t), A_3(t), I_3(t), R_3(t), P_3(t),\\ &S_4(t), V_4(t), V_{p4}(t), L_4(t), L_{p4}(t), C_4(t), A_4(t), I_4(t), R_4(t), P_4(t))\end{aligned}$$

where V_1, V_2, V_3 and V_4 represent respectively the states for vaccinated and fully protected individuals in difference age groups; V_{p1}, V_{p2}, V_{p3} and V_{p4} represent the corresponding states of partially protected individuals in different age groups.

Let $\Delta\vec{X}(t) = \vec{X}(t + \Delta t) - \vec{X}(t)$ represent changes that occur to the random vector at Δt

units of time. We define the transition probability as

$$\begin{aligned}\Pr(\Delta\vec{X}(t)) = &\big(\Theta(S_1),\Theta(V_1),\Theta(V_{p1}),\Theta(L_1),\Theta(L_{p1}),\Theta(C_1),\Theta(A_1),\Theta(I_1),\Theta(R_1),\Theta(P_1)\\ &\Theta(S_2),\Theta(V_2),\Theta(V_{p2}),\Theta(L_2),\Theta(L_{p2}),\Theta(C_2),\Theta(A_2),\Theta(I_2),\Theta(R_2),\Theta(P_2)\\ &\Theta(S_3),\Theta(V_3),\Theta(V_{p3}),\Theta(L_3),\Theta(L_{p3}),\Theta(C_3),\Theta(A_3),\Theta(I_3),\Theta(R_3),\Theta(P_3)\\ &\Theta(S_4),\Theta(V_4),\Theta(V_{p4}),\Theta(L_4),\Theta(L_{p4}),\Theta(C_4),\Theta(A_4),\Theta(I_4),\Theta(R_4),\Theta(P_4)\\ &\mid \Delta\vec{X}(t)\big),\end{aligned}$$

where

$$\Theta(\cdot) = \begin{cases} -1 & \text{decrease in the class } (\cdot) \\ 0 & \text{no change in the class } (\cdot) \\ 1 & \text{increase in the class } (\cdot) \end{cases}$$

The function $\Theta(\cdot)$ describes the change in a class (i.e., $\Theta(\cdot) = -1$: an individual leaves the class; $\Theta(\cdot) = 0$: no changes occur in the class; $\Theta(\cdot) = 1$: an individual enters the class). We assume that Δt is sufficiently small, so that at most one change of status can occur during the time interval Δt, which can be viewed as a Markov chain process. The resulting stochastic model can be described as a continuous time Markov model. During simulations, the number of individuals in each class is updated on each transition time based on the associated event and its outcomes.

6.2.2 Parameterization

Disease transmission can occur through contacts between susceptible and infectious individuals in the same or different age groups. We assign an age-specific transmission rate β_{ij} for a susceptible individual in age group i being infected as a result of contact with an infectious individual in age group j. These transmission rates are determined based on the contact matrix of age groups and the baseline transmission of infection determined by the reproduction number. We assume a homogeneous random mixing among members of each age group. To determine the transmission rates, we used contact matrix between different age groups to calculate $\beta_{ij} = \beta c_{ij}$, where c_{ij} is the number of proportional contacts between individuals in age group i and age group j, and β is the baseline transmission probability used in simulations (i.e., $\beta = 0.002$). The contact rates used in our simulations are previously described in published literature [96] and are given by the following matrix

$$\begin{pmatrix} c_{11} & c_{12} & c_{13} & c_{14} \\ c_{21} & c_{22} & c_{23} & c_{24} \\ c_{31} & c_{32} & c_{33} & c_{34} \\ c_{41} & c_{42} & c_{43} & c_{44} \end{pmatrix} = \begin{pmatrix} 3.8 & 3.8 & 0.9 & 0.8 \\ 3.8 & 3.8 & 0.9 & 0.8 \\ 1.6 & 1.6 & 12.9 & 1.2 \\ 2.9 & 2.9 & 3.9 & 3.7 \end{pmatrix}$$

The model includes an important aspect of the population dynamics over time-scales, which is the movement of individuals from one compartment to another due to changes in their age. In compartments 1,2 and 3, individuals transition from age group i to age group $i + 1$ by aging. In this context, κ_i is the rate at which individuals leave the i-th class (i.e.,

$1/\kappa_i$ is the life-span in class $i = 1, 2$ and 3). Individuals are only born in group 1 (at a rate b), but die at a rate μ of natural death.

For vaccination of each age group, we assigned the parameter p_i to represent the vaccine coverage in age group i, with the baseline value of $p_i = 0$ in the absence of vaccination. Using available parameters from previous literature, and our recent estimates for timelines of immunity following recovery from Hia infection presented in Chapter 4, we simulate the model for age-specific profiles of carriage over time. Consistent with [5, 7], we use different durations of protection following primary vaccination in different age groups. The model parameters and their values are listed in Table 6.1.

6.2.3 Model Implementation

We used a Markov Chain Monte Carlo method to simulate the stochastic model. Age groups considered in our model are: < 1 years of age; between 1 and 2 years of age; between 2 and 10 years of age; and older than 10 years of age. For the purpose of simulations, we chose the initial number of infections $C(0) = 5$ and $I(0) = 1$ introduced in the first age group. We considered a total population of size $N = 10,000$ with the following initial conditions for different age groups: $G_1 = 500$, $G_2 = 500$, $G_3 = 2000$ and $G_4 = 7000$.

To estimate the transition time (i.e., the step-size in stochastic simulations) to the next event, we let $\Delta t = U_1/\Phi$, where U_1 is a random variate drawn from the uniform distribution on the unit interval $(0, 1)$, and Φ is equal to the sum of the rates for all possible events. We then ordered the events as an increasing fraction of Φ and generated another uniform deviate ($U_2 \in [0, 1]$) to determine the nature of the next event. Simulations were run for

Table 6.1: Description of model parameters with their values (ranges) used for stochastic simulations.

Parameter	Description	Value or Range
$\mathcal{R}_0$	basic reproduction number	1.12
η	reduced susceptibility during partial protection	0.5
δ	reduced transmissibility during carriage	0.5
κ_1	average duration of stay in age group 1	1 year
κ_2	average duration of stay in age group 2	1 year
κ_3	average duration of stay in age group 3	8 years
$1/\sigma$	average duration of protection due to natural infection	4 years
$1/\sigma_p$	average duration of partial protection	6 years
$1/\xi_1$	average duration of protection following primary vaccine in age group 1 ($<$ 1 year of age)	1 year
$1/\xi_2$	average duration of protection following primary vaccine in age group 2 (1–2 years of age)	2 years
$1/\xi_3$	average duration of protection following primary vaccine in age group 3 (2–10 years of age)	4 years
$1/\xi_4$	average duration of protection following primary vaccine in age group 4 ($>$ 10 years of age)	4 years
$1/\theta$	average duration of latency	2 days
q	fraction of colonized individuals who undergo carriage	0.6–0.9
$1/\alpha$	average duration of pre-symptomatic infection	1 day
$1/\gamma_1$	duration of carriage infection	2–10 weeks
$1/\gamma_2$	duration of communicable disease (under treatment)	1–2 days
$1/\mu$	average lifetime	70 years

a large number of samples ($n = 500$) to calculate the average of sample realizations of the stochastic process in each scenario. For the purpose of illustrations, we consider the age-specific profile of carriage proportional to the total population size of the corresponding age group at any particular time during simulations.

6.3 Results

We ran the simulations for two scenarios of $q = 0.6$ and $q = 0.9$ for the fraction of exposed individuals who experience carriage without developing symptomatic infection. Figure 6.2 shows the curves of age-specific fraction of carriage in different age groups over a 20-year time period. In the absence of vaccination (Figure 6.2a), carriage curves increase over time, and saturate at their age-specific endemic states. For groups < 1 (blue curve) and older than 2 years of age (red and cyan curves), the persistence of infection (endemic state) follows a peak for the maximum incidence of carriage. This initial increase leads to a high level of herd immunity in the population that results in a significant decline of the carriage curves before approaching their endemic states. However, the incidence of carriage for those between 1 and 2 years of age (green curve) increases over time and stabilizes at its endemic state.

We then implemented vaccination at year 5 and ran the simulations. When only age group < 1 is vaccinated (with a coverage of 90%), a significant decline in the incidence of carriage in all age groups is observed over 20 years of simulation period (Figure 6.2b). While this leads to elimination of carriage in the group < 1 year of age (blue curve), elim-

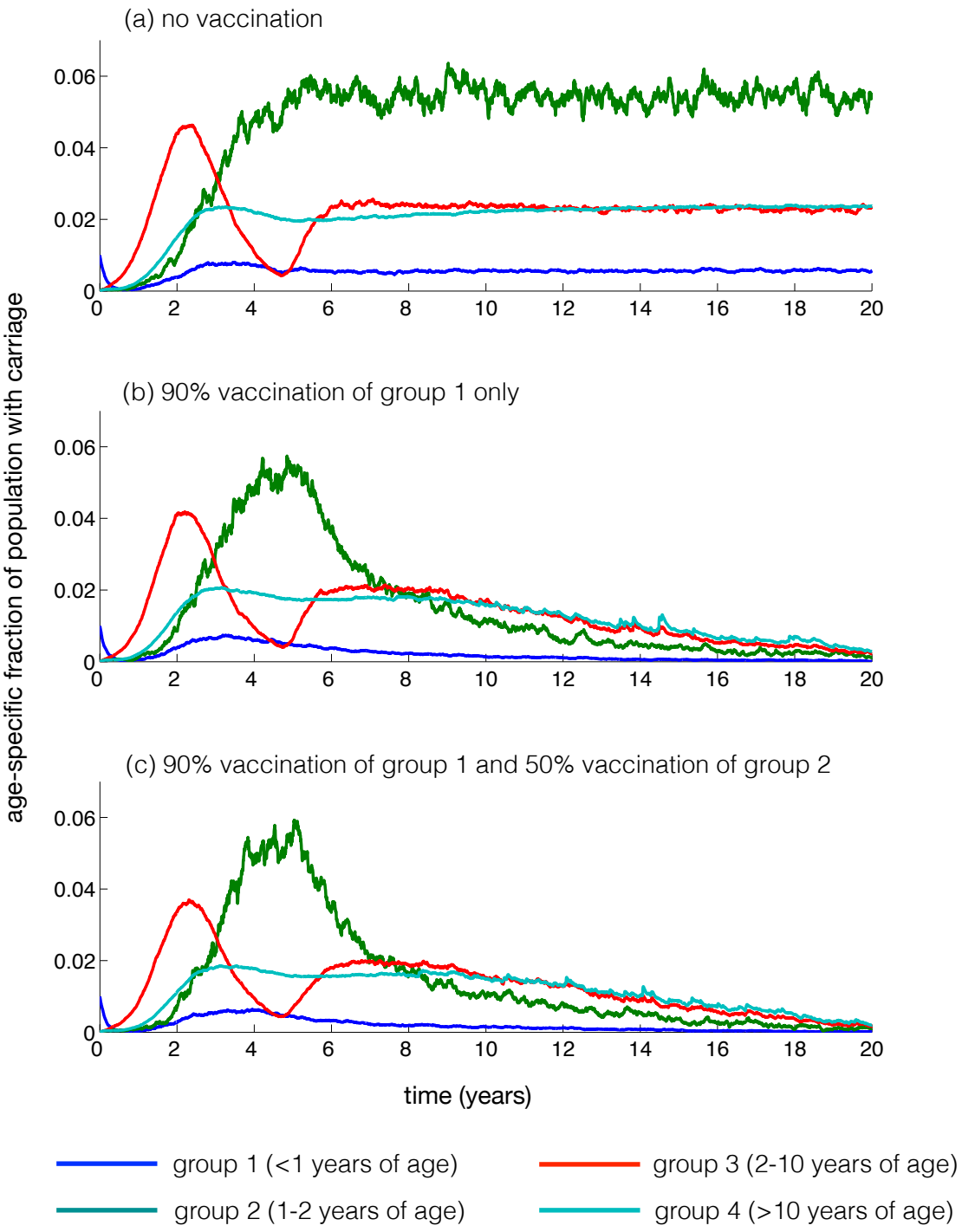

Figure 6.2: Time profiles of age-specific fraction of population with carriage: (a) no vaccination; (b) 90% vaccination of group 1 only; (c) 90% vaccination of group 1 and 50% vaccination of group 2. Simulations were run with $\beta = 0.002$ for $q = 0.6$.

ination of infection is still not achieved in other age groups within 15 years following the start of vaccination. Combining vaccination of age group 1 with 50% coverage of vaccination for age group 2 (between 1 and 2 years of age) leads to a faster decline of incidence in all age groups (Figure 6.2c), and possible elimination of carriage in the second age group (green curve). However, the level of herd immunity is still below the threshold required for elimination of infection in all age groups.

For the scenario of $q = 0.9$, and in the absence of vaccination, we observed similar results for saturation of age-specific carriage curves at their corresponding endemic states (Figure 6.3a). However, in contrast to the case of $q = 0.6$ (Figure 6.2a), all age groups show increasing incidence of carriage towards their endemic states. When vaccination is implemented, the incidence of carriage starts to decline for all age groups. We obtained similar results of declining trends for age-specific incidence of carriage corresponding to the scenarios of vaccinating age groups 1 and 2 within a 20-year simulation period. However, such decline was stabilizing towards the end of this period, and elimination was not achieved for age groups > 1 year of age (Figure 6.3b,c).

Overall our simulations show that vaccination of age groups 1 and 2 helps curtail the infection, but does not generate sufficient herd immunity in the population to eradicate the disease within 15 years of the start of the vaccination.

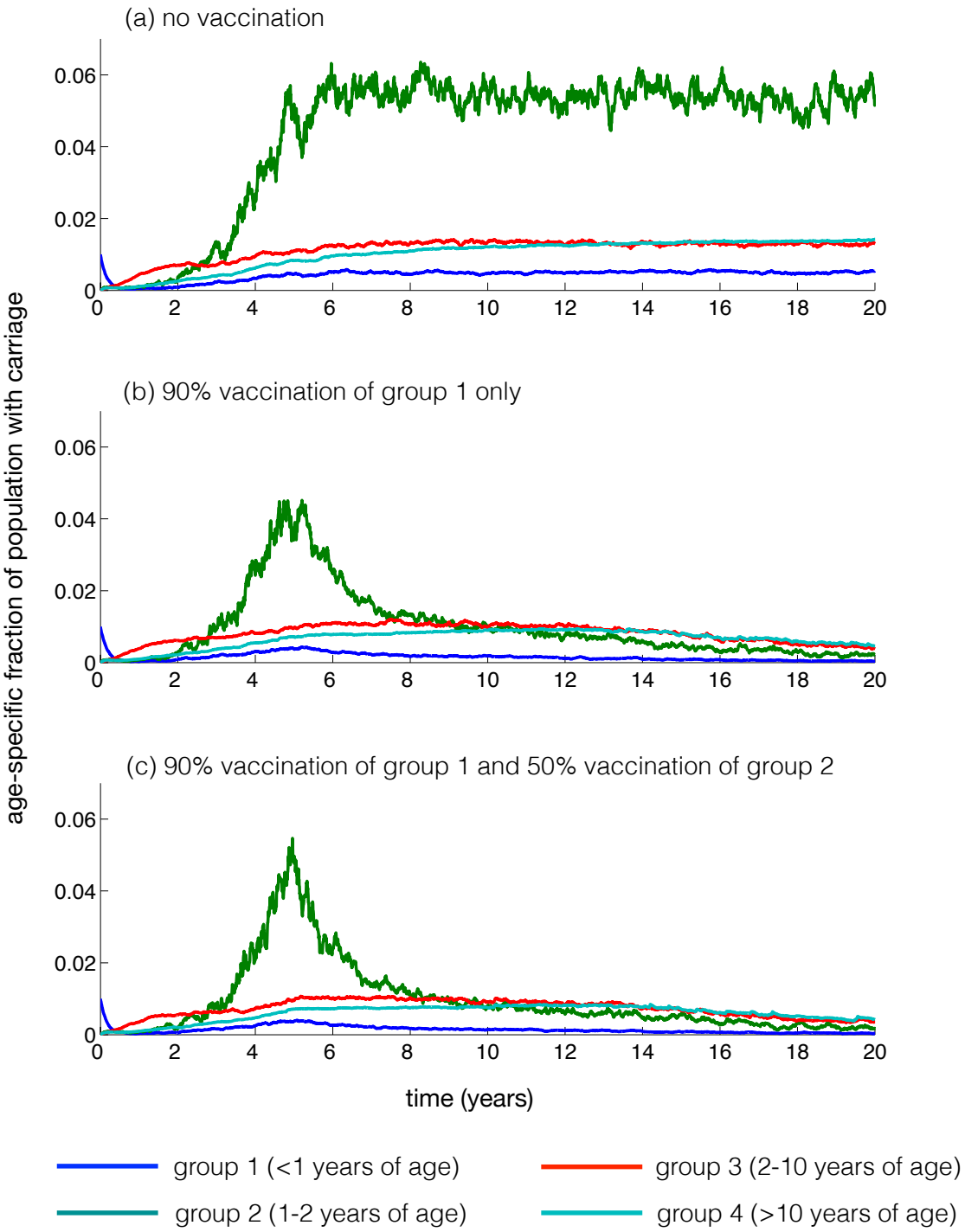

Figure 6.3: Time profiles of age-specific fraction of population with carriage: (a) no vaccination; (b) 90% vaccination of group 1 only; (c) 90% vaccination of group 1 and 50% vaccination of group 2. Simulations were run with $\beta = 0.002$ for $q = 0.9$.

6.4 Discussion

Considering that the incidence of *H. influenzae* infection could be affected by age and contact rates between individuals [5, 8, 49], we developed an age-structure stochastic epidemic model of Hia infection. We considered four age groups in the population and simulated the model for age-specific profiles of carriage over time. We studied the model dynamics, and used previous parameter estimates to evaluate the direct effects of vaccinating different age groups on the incidence of carriage over a 20-year time period.

In developing the model, we made some realistic assumptions as validated in biological studies [5, 14, 36], and used recent estimates for timelines of immunity following recovery from Hia infection derived from our previous work [97]. Our results show that several key model parameters should be carefully considered. These include the duration of vaccine-induced immunity, population size of each age group, and more importantly, the contact rates within and between different age groups that influence the incidence of infection. The average duration of protection against Hia carriage following vaccination or natural infection has a significant effect on the equilibrium state of the system, and therefore Hia elimination. Individuals who lose their full immune protection generated as a result of vaccination or natural infection will become partially protected. During the time of partial protection (which lasts on average longer than full protection period [7]), individuals are at risk of infection mainly led to carriage acquisition, which contributes to even higher incidence of carriage in the population. In this way, carriage will stabilize itself within the population (as observed by equilibrium state). High coverage of a vaccine which con-

fers long lasting immunity reduces the carriage incidence, but elimination depends on the aforementioned factors. A high incidence of carriage in the population may indicate the need for booster vaccination to raise the level of herd immunity. Implementation of booster vaccination in different age groups is expected to have a significant impact in the model outcomes. Investigating the effect of boosting immunity is subject of future work, which requires extension of the model to distinguish classes of primary and booster vaccination.

The results of this age-structured model remain consistent with those obtained in our previous study [98], indicating that vaccinating only infants may not sufficiently raise the level of herd immunity to eradicate the disease from the affected population. Our simulations are consistent with previous work pertaining to Hib [5], emphasizing the importance of maintaining a high level of herd immunity through boosting in order to reduce the incidence of carriage in different age groups.

Chapter 7

The effect of vaccine formulations against Hia and Hib

In the context of ongoing efforts to develop an anti-Hia vaccine candidate, it is important to provide information on the effective vaccine formulation that maximizes the population-wide benefits of vaccination. Our goal here is to provide this information using a modelling framework to evaluate the effect of bivalent vaccine formulations against Hia and Hib infections.

Based on the experience with Hib vaccination, producing a conjugate vaccine through covalent linkage to protein molecules (carrier proteins) is important for long lasting effects of adaptive immunity through stimulation of T-cell responses. Given the chemical similarities between Hia and Hib capsular polysaccharides, it has been suggested that a bivalent Hib-Hia glycoconjugate vaccine formulation with a similar carrier protein (CP) previously used for Hib vaccine could be utilized to induce effective immune protection against both

Hia and Hib infections [2, 3]. Considering that Hib and Hia have been circulating in several regions of the world [3, 30], and the Hib conjugate vaccine has been included in the universal infant immunization programs in a number of countries since the late 1980s [30], the pre-existing immunity elicited by prior vaccination or natural infection of Hib may interfere with the generation and boosting of the anti-Hia antibodies. In this context, evidence is accumulating that the glycoconjugate vaccines may elicit low titres of protective antibody against bacterial polysaccharides [99–101]. There have been a number of mechanisms proposed to explain the suboptimal immune responses to this type of vaccine, including the 'carrier-induced epitopic suppression' (CIES) [99]. In CIES, polysaccharide antigens conjugated with CP will be rapidly depleted by binding to pre-existing anti-CP antibodies and forming the immune complexes, which eventually undergo phagocytosis by phagocytes, such as macrophages or dendritic cells. Concurrently, CP-specific memory B cells quickly bind and internalize CP-linked polysaccharide antigens [99, 100]. These processes will in turn impede the polysaccharide-naïve B cell stimulations, and therefore interfere with survival and proliferations during clonal expansion as a result of rapid depletion of free antigens [99]. Therefore, we hypothesize that the production of Hia-specific antibodies using a bivalent Hia-Hib vaccine is diminished in the presence of pre-existing immune responses against CP or Hib.

At present, no bivalent vaccines against *H. influenzae* serotypes 'a' and 'b' have been developed, and experimental evaluations of pathogen-specific immune responses to analyze immune interferences induced by pre-existing immunity are infeasible. We therefore developed a stochastic simulation model of humoral immune response to encapsulate the biolog-

ical processes underlying T cell-dependent B cell activation and the antibody production. We considered two different vaccine formulations: a bivalent combined (Hib-CP/Hia-CP) glycoconjugate vaccine and a bivalent unimolecular (Hib-CP-Hia) glycoconjugate vaccine [102]. Using our model, we aim to evaluate the potential level of immune responses conferred by these vaccine formulations in the presence of pre-existing immunity to serotype 'b' of *H. influenzae* and CP.

7.1 Modelling framework

To simulate the immune response and antibody production, we developed a stochastic simulation model based on immunological mechanisms of T cell-dependent B cell proliferation. The system presented here includes compartments describing B cells, including naïve B cells (B_n), stimulated B cells (B_s), activated B cells (B_a), and proliferated B cells ($B_1, \cdots, B_8$). The system also includes Hia antigen (A_g^A), Hib antigen (A_g^B); carrier protein (CP); antibodies (A_b); and immune-complexes (I_c). To formulate our model, we first derive differential equations for each compartment of the system based on well-established biological mechanisms.

The humoral immune response is initiated upon the recognition of antigens by antigen-presenting cells (APCs), which activate naïve T cells in the form of T helper cells. These helper cells activate stimulated B cells that have already presented the same antigens on the cell surface via major histocompatibility complex class II (MHC II). Activated B cells subsequently proliferate and differentiate into plasma cells (that secrete antibodies) or long-

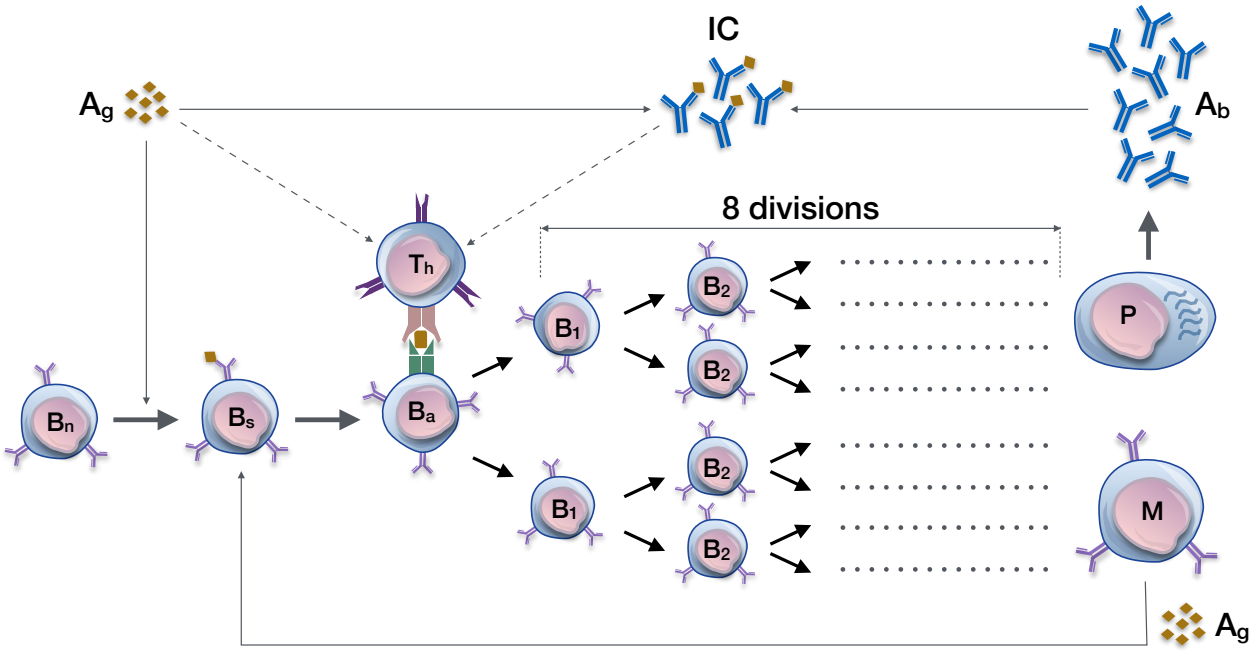

Figure 7.1: The biological model of humoral immune response. The model includes antigen (A_g), antibody (A_b); naïve B cells (B_n), stimulated B cells (B_s), activated B cells (B_a), proliferating B cells (B_1–B_8); immune complex (I_C); memory B cells (M); plasma cells (P); and T helper cells (T_h). Arrows show the transitions between biological states. The dashed-line arrows show multistep processes involved in the biological mechanisms.

lived memory B cells (for the secondary responses to the same antigenic challenge). In the presence of antigens, memory cells can further be stimulated and enter the cycle of clonal expansion and antibody production providing a faster and stronger antibody response. Following secretion, antibodies can bind to antigens to form immune complexes, which can be recognized and cleared by phagocytes (Figure 7.1).

In a bivalent unimolecular vaccine, the two antigens are covalently linked to the same molecule of carrier protein. The conjugation onto the carrier protein of two carbohydrate antigens is a strategy to co-deliver simultaneously the antigens to APCs. In this way by coupling both surface carbohydrates targeting both strains of Hia and Hib into the same CP, a unimolecular construct is obtained. Therefore we include a single compartment of antigen (A_g) in our model. This antigen peptide can activate B cells that present A_g^A, A_g^B, or CP on their cell surface.

Naïve B cell stimulation

The presence of antigen peptides causes activation of naïve B cells, leading to clonal expansion and differentiation into plasma cells that secrete antibodies. In this process, free antigen binds to the B cell surface receptors, and stimulates proliferation. We assume that the rate (γ_n) at which B cells are stimulated is proportional to the total concentration of free antigen (A_g). In the absence of stimulation, naïve B cells decay at a natural death rate δ_n. Assuming that naïve B cells are produced at a rate ρ, the equation for B cell activation is given by:

$$B_n' = \rho - \gamma_n A_g B_n - \delta_n B_n \tag{7.1}$$

Activation of stimulated B cell

While the dynamics of T-helper cells in the process of B cell clonal expansion is not directly modelled here, we include their effect through a specific compartment (C) in our model. This step incorporates all the necessary mechanisms involved in activation of B-cells, in-

cluding stimulation from T-helper cells when they encounter and recognize an antigen on APCs at the rate γ. The antibody complexes (I_C) are generated at a rate δ_c and the stimulated cells (B_s) decay at a rate δ_a. The dynamics of B cell stimulation are governed by the following equations

$$C' = \gamma A_g + \delta_c I_c \tag{7.2}$$

$$B_s' = \gamma_n A_g B_n - \gamma_1 C B_s - \delta_a B_s \tag{7.3}$$

B cell proliferation

The activated B cells proliferate through division cycles at a constant rate γ_2, and we considered 8 division cycles. Memory cells (M) can become activated through binding with free antigen peptides and initiate the process of proliferation in the same way as stimulated naïve B cells. The memory cells (M) have a relatively prolonged life span compared to naïve or plasma cells, and can be activated by a lower antigen concentration. They also have higher proliferation rates, and exhibit high avidity surface receptors due to maturation processes that occur during the primary response. We consider a rate γ_m for memory cell stimulation. Activated cells decay at a rate δ_a as described in the following equation

$$B_a' = \gamma_m C M_s + \gamma_1 C B_s - \gamma_2 B_a - \delta_a B_a \tag{7.4}$$

Antigen induced cell death (AICD) can occur when activated B cells encounter free antigen peptides during their proliferation cycles, which could eliminate proliferated cells

from becoming effectors in the form of plasma or memory [103]. This mechanism could have a number of implications for a repeated antigenic challenge during primary response. On one hand, larger antigen doses stimulate a greater fraction of naïve cells, but not necessarily the degree to which the individual cells are stimulated [103]. On the other hand, a higher fraction of proliferated cells experiences AICD, and therefore a lower number of effector cells may develop. The last division cycle in proliferation will lead to generation of memory cells, and plasma cells that secret antibody molecules. With the decay rate of δ_a for proliferated B cells, the dynamics of clonal expansion is described by

$$B_i' = 2\gamma_2 B_{i-1} - \gamma_2 B_i - d_0 \frac{A_g}{A_{g0}} B_i - \delta_a B_i \qquad i = 2, \cdots, 8 \tag{7.5}$$

Plasma cells, memory cells and antibody molecules

Plasma cells (B_p) and memory cells (M) are generated through proliferation of activated B cells. Plasma cells decay at a rate δ_p in the following equation

$$B_p' = \gamma_2 B_8 - \delta_p B_p \tag{7.6}$$

In the presence of free antigen, memory cells can go through the process of activation and proliferation. Memory cells decay at a rate δ_M, with the dynamics described by

$$M' = \gamma_2 B_8^A - \gamma_3 A_g M - \delta_M M \tag{7.7}$$

$$M_s' = \gamma_3 A_g M - \gamma_m C M_s - \delta_M M_s \tag{7.8}$$

We consider a total amount of antibodies (A_b), mainly consisting of two major antibody molecules secreted by plasma cells, IgG and IgM. The concentration of antibody molecules is increased at the rate α (i.e., production rate from plasma cells), and reduced by a removal rate of δ_b. The concentration of antibody molecules is reduced by the formation of immune complexes through binding with free antigen peptides at the constant rate β, which incorporates the average avidity of circulating antibody molecules. The dynamics of antibody molecules are governed by the following equation

$$A_b' = \alpha B_p - \beta A_g A_b - \delta_b A_b \tag{7.9}$$

Antigen and antibody complexes

The initial antigen concentration is reduced by rates that are proportional to the concentration of the antigen bound to antibody molecules and activation-induced cell death during proliferation of B cells. With a removal rate of d_g for antigen peptides, the dynamics of antigen concentration (A_g) is given by

$$A_g' = -\beta A_g A_b - \gamma_1 A_g B_n - \gamma_3 A_g M - \gamma A_g - d_0 \frac{A_g}{A_{g_0}}(B_1 + \cdots + B_8) - d_g A_g \tag{7.10}$$

The concentration of antibody complexes (I_C) increases as a result of antigen binding with antibodies, and reduces at a rate δ_c, which is governed by the equation

$$I_C' = \beta A_g A_b - \delta_c I_C \tag{7.11}$$

Summarizing the above, the dynamics of humoral immune response in the presence of a bivalent unimolecular (Hib-CP-Hia) glycoconjugate vaccine can be described by the following sub-models (7.12)–(7.16):

$$\begin{aligned} B_n' &= \rho - \gamma_n A_g B_n - \delta_n B_n \\ C' &= \gamma A_g + \delta_c I_c \end{aligned} \tag{7.12}$$

Dynamics of immune response against serotype 'a':

$$\begin{aligned} B_s'^A &= \frac{1}{3}\gamma_n A_g B_n - \gamma_1 C B_s^A - \delta_a B_s^A \\ B_a'^A &= \gamma_m C M_s^A + \gamma_1 C B_s^A - \gamma_2 B_a^A - \delta_a B_a^A \\ B_1'^A &= 2\gamma_2 B_a^A - \gamma_2 B_1^A - \delta_0 B_1^A \\ B_i'^A &= 2\gamma_2 B_{i-1}^A - \gamma_2 B_i^A - \delta_0 B_i^A - d_0 \frac{A_g}{A_{g_0}} B_i^A \qquad i = 2, \cdots, 8 \\ B_p'^A &= \gamma_2 B_8^A - \delta_p B_p^A \\ M'^A &= \gamma_2 B_8^A - \gamma_3 A_g M^A - \delta_M M^A \\ M_s'^A &= \gamma_3 A_g M^A - \gamma_m C M_s^A - \delta_M M_s^A \\ A_b'^A &= \alpha B_p^A - \beta A_g^A A_b^A - \delta_b A_b^A \end{aligned} \tag{7.13}$$

Dynamics of immune response against serotype 'b':

$$\begin{aligned} B_s'^B &= \frac{1}{3}\gamma_n A_g B_n - \gamma_1 C B_s^B - \delta_a B_s^B \\ B_a'^B &= \gamma_m C M_s^B + \gamma_1 C B_s^B - \gamma_2 B_a^B - \delta_a B_a^B \\ B_1'^B &= 2\gamma_2 B_a^B - \gamma_2 B_1^B - \delta_0 B_1^B \end{aligned}$$

$$
\begin{aligned}
B_i'^B &= 2\gamma_2 B_{i-1}^B - \gamma_2 B_i^B - \delta_0 B_i^B - d_0 \frac{A_g}{A_{g_0}} B_i^B \qquad i = 2, \cdots, 8 \\
B_p'^B &= \gamma_2 B_8^B - \delta_p B_p^B \\
M'^B &= \gamma_2 B_8^B - \gamma_3 A_g M^B - \delta_M M^B \\
M_s'^B &= \gamma_3 A_g M^B - \gamma_m C M_s^B - \delta_M M_s^B \\
A_b'^B &= \alpha B_p^B - \beta A_g A_b^B - \delta_b A_b^B
\end{aligned}
\tag{7.14}
$$

Dynamics of immune response for carrier protein 'C':

$$
\begin{aligned}
B_s'^C &= \frac{1}{3}\gamma_n A_g B_n - \gamma_1 C B_s^C - \delta_a B_s^C \\
B_a'^C &= \gamma_m C M_s^C + \gamma_1 C B_s^C - \gamma_2 B_a^C - \delta_a B_a^C \\
B_1'^C &= 2\gamma_2 B_a^C - \gamma_2 B_1^C - \delta_0 B_1^C \\
B_i'^C &= 2\gamma_2 B_{i-1}^C - \gamma_2 B_i^C - \delta_0 B_i^C - d_0 \frac{A_g}{A_{g_0}} B_i^C \qquad i = 2, ..., 8 \\
B_p'^C &= \gamma_2 B_8^C - \delta_p B_p^C \\
M'^C &= \gamma_2 B_8^C - \gamma_3 A_g M^C - \delta_M M^C \\
M_s'^C &= \gamma_3 A g M^C - \gamma_m C M_s^C - \delta_M M_s^C \\
A_b'^C &= \alpha B_p^C - \beta A_g A_b^C - \delta_b A_b^C
\end{aligned}
\tag{7.15}
$$

Dynamics of antigen and immune complexes:

$$
\begin{aligned}
A_g' &= -\beta A_g A_b^A - \beta A_g A_b^B - \beta A_g A_b^C - \gamma_n A_g B_n \\
&\quad - \gamma_3 A_g (M^A + M^B + M^C) - \gamma A_g - dg A_g - d_0 \frac{A_g}{A_{g_0}} (B_i^A + B_i^B + B_i^C) \\
I_C' &= \beta A_g A_b^A + \beta A_g A_b^B + \beta A_g A_b^C - \delta_c I_C
\end{aligned}
\tag{7.16}
$$

7.1.1 Bivalent combined Hib-CP/Hia-CP vaccine

In the case of a bivalent combined vaccine, antigens are covalently linked to carrier proteins separately. We therefore consider these two different antigen peptides in two distinct compartments in our model, denoted by A_g^A and A_g^B. The dynamics of B cell clonal expansion and antibody production for a bivalent combined (Hib-CP/Hia-CP) glycoconjugate vaccine are therefore described by the following sub-models (7.17)–(7.21):

$$C' = \gamma A_g^A + \gamma A_g^B + \delta_c I_c \tag{7.17}$$

Dynamics of immune response against serotype 'a':

$$\begin{aligned}
B_n'^A &= \rho - \gamma_n A_g^A B_n^A - \delta_n B_n^A \\
B_s'^A &= \gamma_n A_g^A B_n^A - \gamma_n C B_s^A - \delta_a B_s^A \\
B_a'^A &= \gamma_m C M_s^A + \gamma_n C B_s^A - \gamma_2 B_a^A - \delta_a B_a^A \\
B_1'^A &= 2\gamma_2 B_a^A - \gamma_2 B_1^A - \delta_0 B_1^A \\
B_i'^A &= 2\gamma_2 B_{i-1}^A - \gamma_2 B_i^A - \delta_0 B_i^A - d_0 \frac{A_g^A}{A_{g0}^A} B_i^A \qquad i = 2, \cdots, 8 \\
B_p'^A &= \gamma_2 B_8^A - \delta_p B_p^A \\
M'^A &= \gamma_2 B_8^A - \gamma_3 A_g^A M^A - \delta_M M^A \\
M_s'^A &= \gamma_3 A_g^A M^A - \gamma_m C M_s^A - \delta_M M_s^A \\
A_b'^A &= \alpha B_p^A - \beta A_g^A A_b^A - \delta_b A_b^A
\end{aligned} \tag{7.18}$$

Dynamics of immune response against serotype 'b':

$$
\begin{aligned}
B_n'^B &= \rho - \gamma_n A_g^B B_n^B - \delta_n B_n^B \\
B_s'^B &= \gamma_n A_g^B B_n^B - \gamma_n C B_s^B - \delta_a B_s^B \\
B_a'^B &= \gamma_m C M_s^B + \gamma_n C B_s^B - \gamma_2 B_a^B - \delta_a B_a^B \\
B_1'^B &= 2\gamma_2 B_a^B - \gamma_2 B_1^B - \delta_0 B_1^B \\
B_i'^B &= 2\gamma_2 B_{i-1}^B - \gamma_2 B_i^B - \delta_0 B_i^B - d_0 \frac{A_g^B}{A_{g_0}^B} B_i^B \qquad i = 2, \cdots, 8 \\
B_p'^B &= \gamma_2 B_8^B - \delta_p B_p^B \\
M'^B &= \gamma_2 B_8^B - \gamma_3 A_g^B M^B - \delta_M M^B \\
M_s'^B &= \gamma_3 A_g^B M^B - \gamma_m C M_s^B - \delta_M M_s^B \\
A_b'^B &= \alpha B_p^B - \beta A_g^B A_b^B - \delta_b A_b^B
\end{aligned}
\tag{7.19}
$$

Dynamics of immune response for carrier protein 'C':

$$
\begin{aligned}
B_n'^C &= \rho - \gamma_n A_g^A B_n^C - \gamma_1 A_g^B B_n^C - \delta_n B_n^C \\
B_s'^C &= \gamma_n A_g^A B_n^C + \gamma_1 A_g^B B_n^C - \gamma_n C B_s^C - \delta_a B_s^C \\
B_a'^C &= \gamma_m C M_s^C + \gamma_n C B_s^C - \gamma_2 B_a^C - \delta_a B_a^C \\
B_1'^C &= 2\gamma_2 B_a^C - \gamma_2 B_1^C - \delta_0 B_1^C \\
B_i'^C &= 2\gamma_2 B_{i-1}^C - \gamma_2 B_i^C - \delta_0 B_i^C - d_0 \frac{A_g^A}{A_{g_0}^A} B_i^C - d_0 \frac{A_g^B}{A_{g_0}^B} B_i^C \qquad i = 2, ..., 8 \\
B_p'^C &= \gamma_2 B_8^C - \delta_p B_p^C \\
M'^C &= \gamma_2 B_8^C - \gamma_3 A_g^A M^C - \gamma_3 A_g^B M^C - \delta_M M^C
\end{aligned}
\tag{7.20}
$$

$$M_s'^C = \gamma_3 Ag^A M^C + \gamma_3 Ag^B M^C - \gamma_m C M_s^C - \delta_M M_s^C$$

$$A_b'^C = \alpha B_p^C - \beta A_g^A A_b^C - \beta A_g^B A_b^C - \delta_b A_b^C$$

Dynamics of antigens and immune complexes:

$$\begin{aligned}
A_g'^A &= -\beta A_g^A A_b^A - \gamma_1 A_g^A B_n^A - \gamma_3 A_g^A M^A - \gamma A_g^A - dg A_g^A - d_0 \frac{A_g^A}{A_{g0}^A} B_i^A - d_0 \frac{A_g^A}{A_{g0}^A} B_i^C \\
A_g'^B &= -\beta A_g^B A_b^B - \gamma_1 A_g^B B_n^B - \gamma_3 A_g^B M^B - \gamma A_g^B - dg A_g^B - d_0 \frac{A_g^B}{A_{g0}^B} B_i^B - d_0 \frac{A_g^B}{A_{g0}^B} B_i^C \\
I_C' &= \beta A_g^A A_b^A + \beta A_g^B A_b^B - \delta_c I_C
\end{aligned} \tag{7.21}$$

7.1.2 Stochastic simulation model

We implemented the stochastic Markov-Chain simulation model, in which events occur randomly based on the rates of immunological mechanisms. The state of the model is defined by the number of cells, antigens, antibodies, and immune complexes, and is changed discretely whenever an event occurs. In our simulations, rates of immunological mechanisms are converted to probabilities of the corresponding event by considering

$$P(\text{event } i) = \frac{a_i}{\sum_i a_i}, \tag{7.22}$$

where a_i is the transition rate of the event i. In this formulation, the time to the next event (τ) is exponentially distributed with the parameter equal to the sum of the rates for all possible events. The probability density function is given by

$$f(\tau) = \big(\sum_i a_i\big) \exp\big(-\tau \sum_i a_i\big) \tag{7.23}$$

Using inverse transform sampling [104], we estimated the time to the next event: for a given random variate r drawn from the uniform distribution on the unit interval $(0, 1)$, τ was estimated as $-\ln r / \sum_i a_i$. To determine the nature of the next event, we ordered the events as an increasing fraction of the sum of all events and compared with another uniform deviate generated in the unit interval. Simulations were run for a large number of samples ($n = 500$) to calculate the average of sample realizations of the stochastic process in each scenario.

7.1.3 Parameterization

The model was parameterized using available estimates from the previous literature summarized in Table 6.1. Since the specific interactions between T cells and macrophages have been measured in a short (5 to 15 minutes) time period [105], we used an average value of 10 minutes to calculate the MHC II antigen presentation rate, giving a rate of 6 h^{-1} (per hour). Naïve B cells are stimulated and activated at a much slower rate compared to memory B cells [106, 107]. We used rates of 5.26×10^{-2} and 0.5 h^{-1} for naïve and memory B cells stimulation, respectively. Each division during proliferation cycle of immune cells takes about 8 hours [108], and we used a rate of 0.125 h^{-1}. Upon the completion of each division cycle, plasma B cells are generated, which secrete antibodies at an estimated rate of around 2000 molecules per second [109]. This gives the rate of 7.2×10^6 antibody molecules

Table 7.1: Model parameters and their values used for simulations.

Parameter	Description	Value	Reference
γ_n	Stimulation rate of B cells	5.88×10^{-2} (MHC II)$^{-1}$ h^{-1}	[106]
γ_1	Activation rate of naïve B cells	0.5 (antigen)$^{-1}$ h^{-1}	[107]
γ_2	Proliferation rate of B cells	0.125 h^{-1}	[109]
γ_m	Stimulation rate of memory B cells	1 (antigen)$^{-1}$ h^{-1}	Estimated
γ_3	Activation rate of memory B cells	1 (MHC II)$^{-1}$ h^{-1}	Estimated
γ	Rate of production of MHC II by APCs	6 h^{-1}	[105]
β	Binding rate of antibody with antigen	60 (antigen molecule)$^{-1}$ h^{-1}	[110]
δ_n	Death rate of naïve B cell	4.16×10^{-3} h^{-1}	[111]
δ_M	Death rate of memory B cells	2.1×10^{-4} h^{-1}	Estimated
d_0	Activation-induced cell death (AICD) rate in the absence of antigen	6.67×10^{-2} h^{-1}	[111]
δ_0	Natural death rate of B cells	7.5×10^{-3} h^{-1}	[111–113]
δ_p	Death rate of plasma B cells	8.33×10^{-3} h^{-1}	[111–113]
δ_b	Antibody removal rate	8.33×10^{-3} h^{-1}	[111]
δ_c	Immuno complex removal rate	4.63×10^{-4} h^{-1}	[113]
d_g	Antigen removal rate	8.33×10^{-3} h^{-1}	Estimated
ρ	Production rate of naïve B cells	10 day^{-1}	[114]
α	Rate of antibody production	7.2×10^{6}	[109]

per cell per hour. The binding rate of antibody-antigen is taken from the previous literature considering the affinity and the number of binding sites of the antibodies [110]. High avidity antibodies will react rapidly while low avidity species may continue to form complexes

for several hours after the initiation of reaction with the antigen. Since the peak rate of immune complex formation occurs within 1 minute after mixing antibodies and antigens [110], we used an antigen-antibody binding rate of 60 h^{-1} per antigen. We used an average life span of short- and long-lived plasma cells [111–113], with a rate of 8.33×10^{-3} h^{-1} within the reported ranges. For the purpose of simulations, an initial number of 4×10^4 antigens was used in four different scenarios: (i) naïve immune system; (ii) pre-existing antibodies ($Ab = 10^6$ molecules) against only one antigen; (iii) pre-existing memory B cell ($M = 400$ cells) specific to only one antigen; and (iv) pre-existing antibodies and memory B cells ($A_b = 4 \times 10^4$ molecules and $M = 200$ cells) specific to only one antigen.

7.2 Results

Simulation results for the number of antibody using the bivalent combined and unimolecular glycoconjugate vaccines are illustrated in Figures 7.2–7.4. In a naïve condition (Figures 7.2a and 7.3a), both Hib-CP-Hia and Hib-CP/Hia-CP can elicit comparable levels of anti-Hia, anti-Hib, and CP-specific antibodies. In the presence of pre-existing Hib specific immune responses, such as antibodies and/or memory B cells, the production of anti-Hia and CP antibodies by a unimolecular Hib-CP-Hia vaccine is significantly reduced (Figures 7.2b-7.2d), compared to the scenario of the naïve condition. Furthermore, pre-existing Hib antibodies may impede the boosting of Hib-specific antibodies following vaccination with both Hib-CP-Hia and Hib-CP/Hia-CP formulations (Figures 7.2b and 7.3b). In contrast, the pre-existing Hib-specific immune responses have no effect on the production of anti-Hia

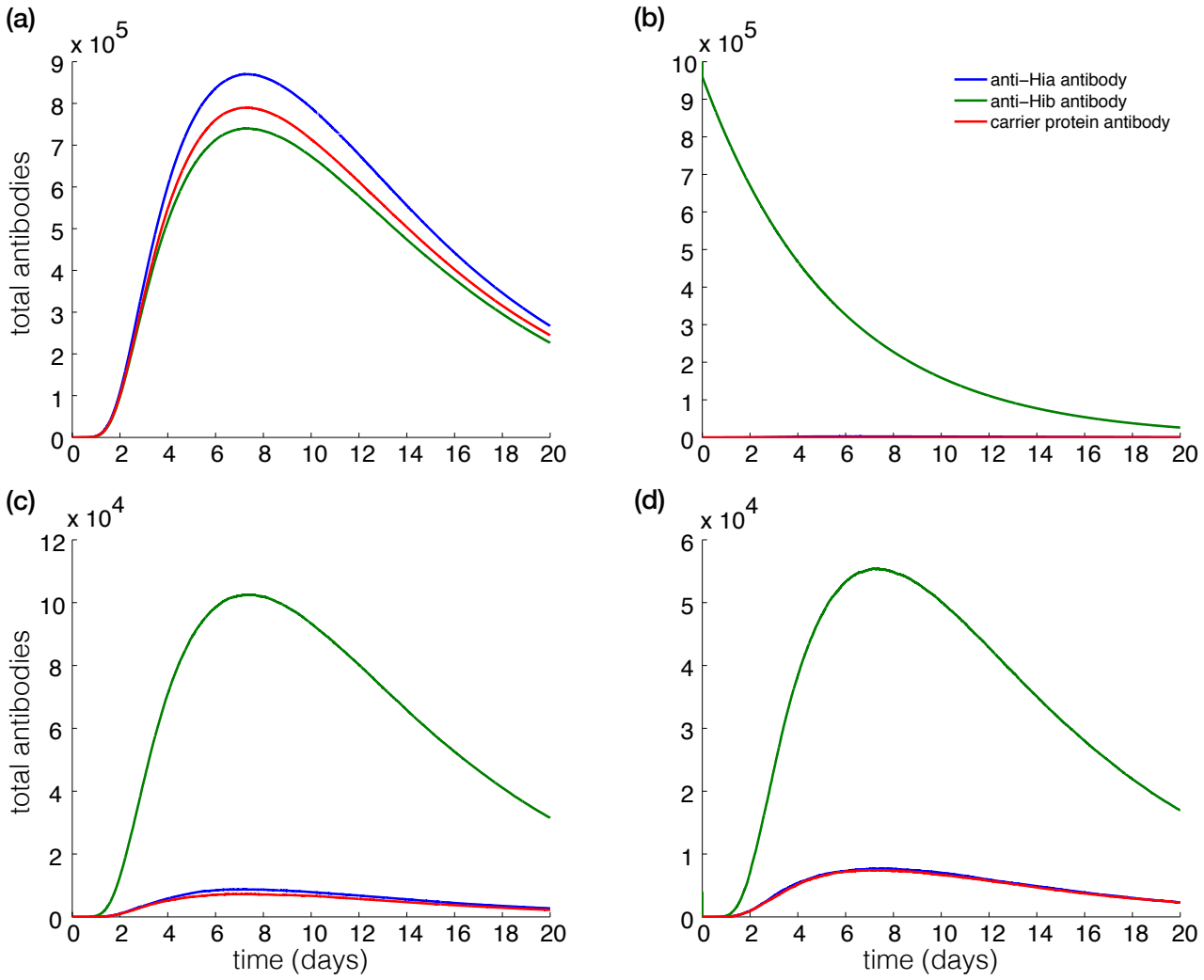

Figure 7.2: The effects of pre-existing Hib immune responses on the production of antibodies using a bivalent unimolecular Hib-CP-Hia vaccine. An initial $4x10^4$ amount of antigen was assumed for simulations in (a) the naïve condition (pre-existing $A_b = 0$ and $M = 0$); (b) the presence of pre-existing anti-Hib antibodies only (pre-existing $A_b^B = 10^6$); (c) the presence of pre-existing Hib-specific memory B cells only ($M^B = 400$); and (d) the presence of both anti-Hib antibodies and Hib-specific memory B cells ($A_b^B = 4 \times 10^4$ and $M^B = 200$)

antibodies using a combined Hib-CP/Hia-CP vaccine (Figure 7.3, b–d). However, when immune responses of CP and Hib-specific (antibodies or memory cells) exist, the generation of Hia-specific antibody is largely inhibited (Figures 7.4a–7.4b). These simulations suggest

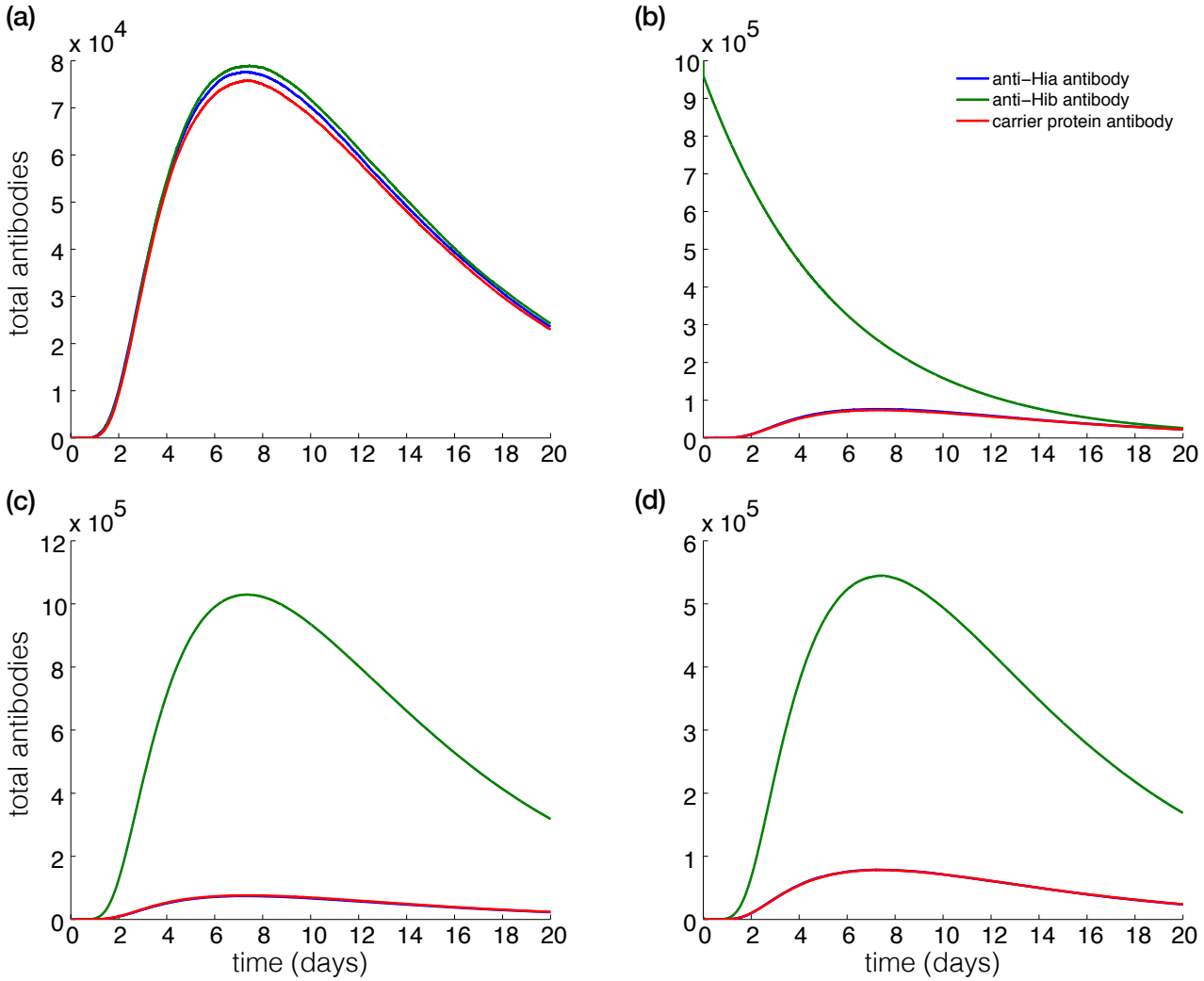

Figure 7.3: The effects of pre-existing Hib immune responses on the production of antibodies using a bivalent combined Hib-CP/Hia-CP vaccine. An initial 4×10^4 amount of antigen was assumed for simulations in (a) the naïve condition (pre-existing $A_b = 0$ and $M = 0$); (b) the presence of pre-existing anti-Hib antibodies only (pre-existing $A_b^B = 10^6$); (c) the presence of pre-existing Hib-specific memory B cells only ($M^B = 400$); and (d) the presence of both anti-Hib antibodies and Hib-specific memory B cells ($A_b^B = 4 \times 10^4$ and $M^B = 200$)

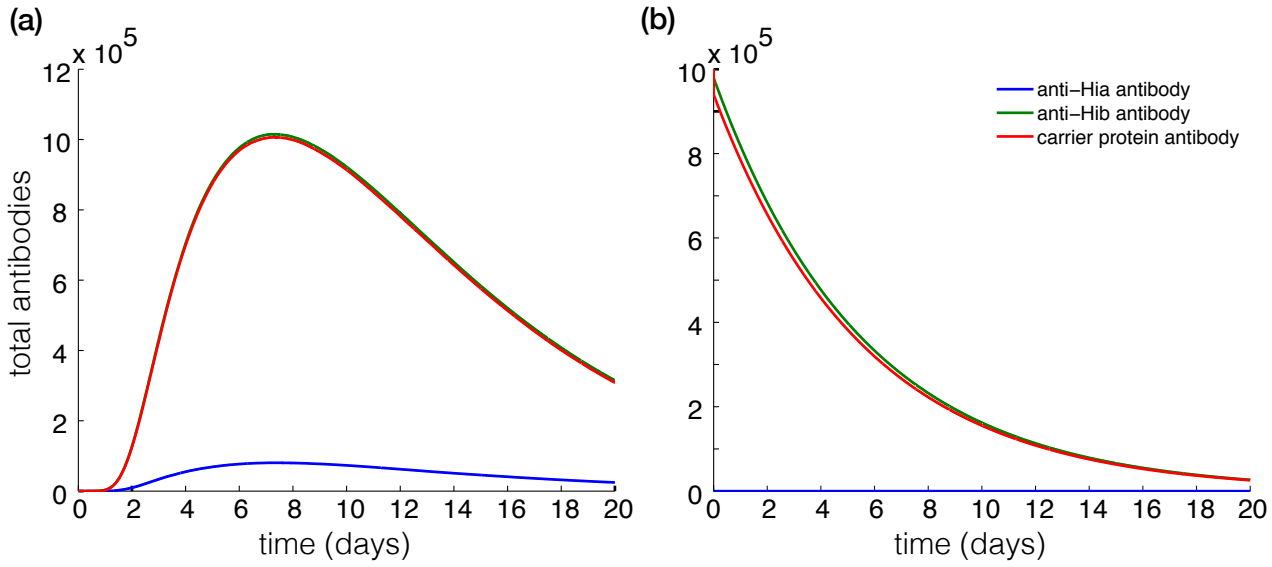

Figure 7.4: The effects of pre-existing CP and Hib immune responses on the production of antibodies using a bivalent combined Hib-CP/Hia-CP vaccine. An initial 4×10^4 amount of antigen was assumed for simulations in (a) the presence of pre-existing CP-specific and Hib-specific memory B cells only ($M^B = 400$ and $M^C = 400$); (b) the presence of pre-existing anti-Hib and CP antibodies only ($A_b^B = 10^6$ and $A_b^C = 10^6$).

that the pre-existing CP-specific immune responses may significantly impede the production of both anti-Hia and anti-Hib antibodies when a bivalent vaccine contains the same CP. However, the pre-existing Hib-specific antibodies or memory cells may interfere with, and impede the development of anti-Hia immune responses only in a bivalent unimolecular vaccine.

7.3 Sensitivity Analyses

While the relative importance of the parameters in the model may not have a significant biological implication, the results may be quantitatively sensitive to their values. In order to evaluate this sensitivity, we considered the effect of variation in the parameters used in

the in-host model. Due to the lack of specific ranges for these parameters in the literature, we perturbed each parameter around the values provided in Table 7.1, and carried out a sensitivity analysis using the Latin Hypercube Sampling (LHS) technique. We calculated Partial Rank Correlation Coefficients (PRCCs), and defined the response variable as the ratio of the maximum antibody concentrations against Hib and Hia over a period of 30 days following antigen presentation in the system. Specifically, assuming that there is no correlation between the input parameters, we considered

$$\text{Response} = \frac{\max\{A_b^B\}}{\max\{A_b^A\}}. \tag{7.24}$$

The goal of LHS/PRCC analysis is to identify key parameters whose uncertainties contribute to prediction imprecision, and to rank these parameters by their importance in contributing to this imprecision. We performed this analysis for the case where there is pre-existing immunity in the form of antibodies ($A_b^B(0) = 4 \times 10^4$) and memory cells ($M^B(0) = 200$), which are present as a result of prior exposure to the pathogen and/or vaccination against Hib infection. To allow for the simultaneous variations of these parameters, samples of size 1000 were generated in which each parameter was treated as a random variable and assigned a probability function. This analysis identified seven parameters of the model to have significant effect on the response variable (with the corresponding p-values

smaller than 0.05). These parameters include

$$\gamma \in [3,9], \qquad \gamma_n \in [0.0294, 17.0294], \qquad \gamma_1 \in [0.25, 0.75], \qquad \gamma_3 \in [0.5, 1.5],$$

$$\delta_0 \in [3.75 \times 10^{-3}, 1.125 \times 10^{-2}], \qquad \delta_M \in [1.05 \times 10^{-4}, 3.15 \times 10^{-4}],$$

$$dg \in [0.0042, 0.0125].$$

Since the range of each parameter was relatively small, the parameters were uniformly sampled (without the need to sample on a log-scale) [86]. The parameters with large PRCC values (close to 1 or -1) and their corresponding p-values smaller than the significance level (0.05) have the largest influence on the model outcomes [87]. The PRCC values and their associated t-statistics $p-$values are presented in Table 7.2. We examined scatter plots to verify the existence of monotonic relationships between the parameters used in LHS sampling and the response variable. Figure 7.5 shows the scatter plots of partial residual of parameters that were found to be significant in the analysis.

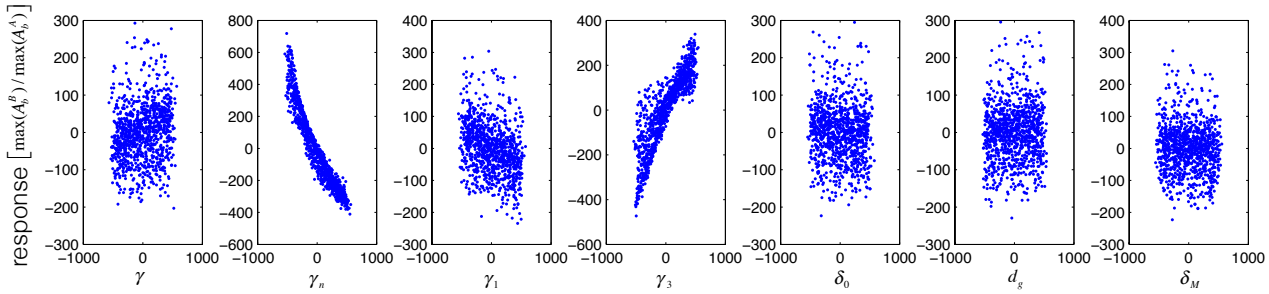

Figure 7.5: PRCC scatter plots of parameters: $\gamma, \gamma_n, \gamma_1, \gamma_3, \delta_0, dg, \delta_M$. The abscissa represents the residuals of the linear regression between the rank-transformed values of the parameter under investigation versus the rank-transformed values of all the other parameters. The ordinate represents the residuals of the linear regression between the rank-transformed values of the response versus the rank-transformed values of all the parameters under investigation.

Table 7.2: Partial rank correlation coefficients and their associated p-values.

Parameter	PRCC	p-value
γ	0.1840	< 0.001
γ_n	-0.9524	< 0.001
γ_1	-0.3472	< 0.001
γ_3	0.8833	< 0.001
δ_0	-0.0676	0.0340
dg	0.0631	0.0477
δ_M	-0.0767	0.0161

Our analysis reveals that the stimulation rate of B-cells (γ_n) is the most important parameter which has a negative effect on the response, as increasing γ_n decreases the inhibition of anti-Hia antibody production. The second most important parameter that strongly affects the response is the activation rate of memory B cells (γ_3).

7.4 Discussion

With the prospect of a vaccine candidate against Hia infection, we developed a model to evaluate bivalent unimolecular and combined formulations. Using a stochastic simulation model, we simulated the potential effect of immunization with such vaccines on the elicitation of immune responses. Our simulations suggest that, in either type of bivalent

combined or unimolecular vaccine, the pre-existing immunity to one antigen at the individual level may interfere with the production of antibodies against both antigens. In particular, the pre-existing CP or Hib-specific antibodies or memory B cells, respond faster to the same antigen (CP or Hib) than naïve B cells, which leads to rapid depletion of free antigen peptides through interaction with memory B cells or formation of immune complexes. This will in turn impede the generation of anti-Hia immune responses (Figures 7.2c-7.2d, 7.3c-7.3d, 7.4a-7.4b), or even reduce the total number of pre-existing Hib antibodies (Figures 7.2b, 7.3b, 7.4b). However, in a naïve individual with no prior exposure or vaccination, a bivalent vaccine can trigger comparable immune responses against both Hia and Hib (Figures 7.2a and 7.3a).

These findings have important implications for current efforts towards vaccine development against Hia, as well as vaccination policies. Given the fact that Hib and Hia have been circulating in several regions of the world [3, 30], and the Hib conjugate vaccine has been included in the universal infant immunization programs in a number of countries since the late 1980s [30], our results indicate that the use of a bivalent Hia-Hib vaccine in these population settings (where individuals may have varying degrees of pre-existing immunity due to natural infection or vaccination) may not be effective in raising antibody numbers to levels required for Hia prevention. While such a vaccine may be recommended for immunization of infants (as naïve individuals) to prevent the spread of both Hia and Hib, the duration of vaccine-induced protection remains undetermined, and therefore booster doses may be required [5]. Our results in Chapter 5 demonstrate that, when a monovalent Hia vaccine becomes available, achieving and maintaining a sufficiently high level of herd

immunity for curtailing Hia requires vaccination of a fraction of susceptible individuals in addition to high primary and booster vaccine coverage of infants.

Given the previous clinical and laboratory investigation of carrier-induced epitopic suppression, a new bivalent vaccine formulation may be optimized to enhance Hia-specific immune responses and antibody production via various approaches, such as the utilization of a different carrier protein from the one previously used for the Hib conjugate vaccine, or the inclusion of high-density Hia polysaccharide antigens [100, 115]. The use of a different CP from the one previously used can eliminate the potential effects of pre-existing CP immune responses on the production of anti-Hia antibodies elicited by a bivalent combined vaccine. However, in a bivalent unimolecular vaccine, a high density of Hia antigens may increase the probability of recognition by Hia-specific naïve B cells. Our findings here suggest that for the development of a bivalent combined glycoconjugate vaccine, the utilization of new carrier proteins not previously used for Hib vaccine can help to develop effective vaccine-induced protections against both Hib and Hia infections.

It should be mentioned that, for simulations presented here, we relied on parameter estimates reported in the previous literature, which may be subject to variations, and we therefore emphasize the qualitative aspects of the results. The pre-existing immunity in our model was included as the initial condition for antibodies or memory B cells at the time of vaccination without considering any prior specific mechanism for their generation. However, we note that antigens from several organisms other than Hia and Hib can induce cross-reactive antibodies to *H. influenzae* capsular polysaccharide [73]. Nevertheless, we have provided the first simulation model for evaluation of the bivalent vaccine-induced im-

munity, which can be extended with further immunological mechanisms and recalibrated as data become available through further immunological experiments.

In conclusion, we draw attention to the importance of pre-existing immune responses to Hib and CP (due to natural infection or vaccination) for the composition of a new bivalent vaccine against Hia and Hib. In this context, ongoing efforts should include experimental investigation of the immune responses elicited by bivalent vaccines in the presence of pre-existing immunity.

Chapter 8

Discussion and Future Work

Rates of Hia infections have increased in several geographic regions in Canada, including Northwestern Ontario. The burden of disease falls mainly on Aboriginal populations, but elderly and immunocompromised individuals are also at risk of infection [2, 3]. The existing mono and multivalent vaccines against Hib are specific to serotype 'b' and does not provide any protection against Hia. There is currently no vaccine available to prevent Hia infection. Considering the increasing rates of Hia and successful Hib immunizations programs, an anti-Hia vaccine may be an effective measure to curtail the incidence of Hia and possibly eliminate the pathogen from affected populations.

In this thesis, we aimed to address a number of important questions on vaccination and prevention of Hia at the individual and population levels, considering the duration and strength of immunity acquired naturally or through vaccination. We developed and analyzed mathematical models, and employed computational and statistical methodologies to evaluate the outcomes of various scenarios for long-lasting protection in the population,

and identify the most effective vaccine strategies and formulations to prevent Hia infections. Our methodology included the analysis of data collected for Hia, which were used to parameterize and simulate in-host and between-host models of immune dynamics and disease transmission, and perform simulations with sensitivity analysis of the outcomes as a result of variation in the parameter space. We developed a model of boosting immunity, and used data on anti-Hia antibody levels in a population of Northwestern Ontario to determine the timelines and frequency of exposure to Hia in this population. We then developed the stochastic models of Hia transmission and control dynamics, and extended to an age-structure model to evaluate vaccination strategies. Since the results depend on the choice of parameters, largely extracted from the published literature on Hib, we performed sensitivity analysis using the Latin Hypercube sampling technique and ranked the importance of parameters on model outcomes. In this way, we determined key parameters that critically affect the vaccination strategies in the long-term.

In the absence of vaccination, the immunity against Hia infection, in the form of anti-capsular polysaccharide antibodies, is acquired naturally as a result of exposure to Hia and other cross-reactive bacteria. Raising herd immunity through vaccination may interrupt pathogen circulation in the population, which reduces the chance of recurrent exposure and boosting of immunity. In the absence of such boosting, however, the adaptive immunity of individuals decays gradually, causing a decline in the herd immunity. The loss of immunity in the absence of boosting can have a significant impact of the long-term outcomes of vaccination programs. We therefore used the antibody boosting model to determine the timelines required for boosting protective antibodies against invasive Hia disease.

Using estimates obtained from this model, we parameterize the vaccination models at the population level to simulate various scenarios with different vaccine coverages for infants and other susceptible individuals.

8.1 Research Outcomes

The research presented in this thesis provides important information regarding vaccination strategies that can offer long-lasting protection against Hia infection. Since vaccination influences the rates of carriage in the population, we used antibody-boosting model to estimate the frequency of exposure to the pathogen and timelines for boosting protective antibodies. Our results are based on the data collected in a pre-dominantly Aboriginal population in Northwestern Ontario. In our analysis, we considered ethnicity, health state, and age of participants. Data suggest that adult serum antibody concentrations are above the threshold required for prevention of Hia disease in this population. We showed that frequent boosting of natural immunity may be required to maintain the level of protective antibodies above the threshold. Since the circulation of bacteria is high among Aboriginal people and individuals with CRF condition, they may be at higher risk of developing Hia disease, which highlights the need to develop preventive measures for curtailing Hia infection in vulnerable populations.

For the use of a vaccine, the stochastic model of disease transmission and control suggests that primary and booster vaccination programs will need to go beyond infant immunization programs. While recent studies emphasize the importance of maintaining control

of the disease and, most probably carriage, in children, they provide evidence for the lack of seroprotection against Hib in adults, suggesting that long-term routine boosting of pre-school children or adolescents may be required [116–118]. Given the estimates for the duration of vaccine-induced protection, the model simulations indicate that a sizeable portion of susceptible individuals needs to be vaccinated to maintain the decline trend of carriage over time. However, estimates of vaccine coverage for susceptible individuals (children older than 2 years of age or adults) may be affected by several factors, including vaccine protection efficacy, population demographics, and other health statuses of the individuals. It is therefore essential to monitor vaccination outcomes and rates of Hia infection over time when a vaccine becomes available and implemented.

We further extended the vaccination model to include age-structure and consider a contact matrix for interactions between different age groups in the population. While reproducing similar results to the original model for vaccination of only infants, this model also demonstrates age-specific rates of carriage. Our simulations show that the highest incidence of carriage occurs amongst children between 1 and 2 years of age. As shown by the model results, the incidence of carriage in children affects the long-term incidence of carriage in other age groups, highlighting the effect of population contact matrix on disease outcomes.

Formulation and efficacy of vaccines remain key determinants in the effectiveness of vaccination strategies. In the context of pre-existing immunity, vaccine formulation may influence the generation and boosting of immunity. Since multivalent vaccines are increasingly used for prevention of different pathogens (e.g., DTaP-HB-IPV-Hib) or different

serotypes of a pathogen (e.g., PCV10 and PCV13), a bivalent Hia-Hib vaccine may become a vaccine candidate to protect against both serotypes 'a' and 'b' of *H. influenzae*. Considering the pre-existing immunity to Hib bacteria acquired naturally or through pediatric immunization programs, the competitive interference between serotypes using a bivalent vaccine is an important factor to be considered. We developed an in-host immune-dynamics model, based on well-established biological mechanisms of T-cell dependent B-cell proliferations, to simulate the effect of a bivalent glycoconjugate Hia-Hib vaccine formulation (unimolecular and combined). Our simulations suggest that pre-existing immunity to one antigen may interfere with the production of antibodies against both antigens. We concluded that a bivalent vaccine formulation with a different carrier protein from the one previously used in anti-Hib vaccines may be more effective to generate optimal immune responses in the context of pre-existing immunity against Hia or Hib.

The outcomes of this research provide important information for optimizing vaccination policies when an anti-Hia vaccine becomes available. While Hia is currently mainly affecting Aboriginal populations, the risk of its spread to the general population cannot be discounted, especially amongst the elderly and immunocompromised individuals. Therefore, our results may be considered in a broader population scope than only Aboriginal communities. Optimizing vaccination strategies can lead to substantial healthcare and economic benefits by reducing the rates of hospitalization and severe outcomes associated with Hia infection, as well as the costs of healthcare resource utilization.

8.2 Limitations

Our study has several limitations that merit further investigation in future research. In the absence of parameter estimates specific to Hia epidemiology, natural history of infection, and immune dynamics, we parameterized our models using available estimates in the literature for Hib infection. However, to estimate Hia-specific decay rates of antibody concentrations in the absence of vaccination, subsequent measurements of serum samples should be collected for several years. Such data and information are currently not available. Furthermore, epidemiological data on Hia incidence published in the literature do not provide sufficient information on the transmission rates of Hia in different population or age groups. We therefore calculated the transmission rates using the expression for the basic reproduction number, while fixing other parameters in this expression. The basic reproduction number is also currently unknown for Hia, and we considered the estimates for Hib disease and other bacterial diseases with similar outcomes. Vaccination models were also parameterized using estimates for Hib vaccination and vaccine-induced protection periods. In the in-host antibody boosting model, the levels of IgG and IgM were considered as indicators of protection against Hia disease. However, we note that clinical protection does not necessarily fully correlate with the immunological data. Clinical protection could be affected by antibody avidity and isotype subclass distribution, considering that certain isotypes may be more important than others in protecting against infections.

To develop the antibody-boosting model we used data collected for anti-Hia antibodies in serum samples of healthy and immunocompromised adults in a population of North-

western Ontario, Canada. But since the majority of invasive Hia disease cases occur among young children, the demographics of our study group, comprised of adults older than 18 years of age, do not fully reflect the immunoepidemiology of this infection. Future studies on the level of naturally acquired immunity in pediatric populations could help refine estimates for the timelines of boosting and frequency of exposure to Hia.

We also note that antigens from several organisms other than Hia can induce cross-reactive antibodies to Hia capsular polysaccharide, and may therefore increase the antibody concentrations. In this context, measurements of the serum Hia antibody concentration may not reliably correspond to the occurrence of Hia infection. Since the relative importance of cross-reactive bacteria in the immune dynamics of Hia is unknown, it is important to further investigate the role of cross-reactive bacterial organisms in the maintenance of immunity at the individual level.

Despite these limitations, the findings of this study suggest that high rates of primary and booster vaccination are required for curtailing Hia infection when a new vaccine becomes available. Enhanced surveillance of the incidence and monitoring of the population level of immunity could help determine these rates specific to the population at risk. The findings presented in this thesis have important implications for current efforts towards vaccine development, as well as vaccination policies in the fight against Hia.

8.3 Future Work

The research presented here provides a solid foundation for further studies in modelling, epidemiology, and clinical aspects of Hia disease. Extension of the age-structured vaccination model could help determine optimal strategies for primary and booster vaccination. Previous studies on Hib vaccination raise the question of optimal timing for booster vaccination following primary series offered to infants between the age of 2 and 6 months [116, 118, 119]. Given that the immune protection induced by vaccine may wane over time, timing of booster dose may be a key factor in the long-term disease outcomes [117]. In our vaccination models, we assumed that the level of vaccine-induced protection for infants and susceptible individuals is the same as that acquired by natural infections. Lifting this assumption by further investigating the differences between the average protection periods resulting from vaccination or natural infections may reveal outcomes that could be used in optimizing age-specific vaccination schedules. In this context, it is important to note that polysaccharide protein conjugate vaccines result in the generation of immune memory in addition to antibodies, and can therefore lead to a longer protection period.

In understanding the timelines of immune protection, our model suggests a difference in the frequency of boosting required to generate protective antibodies against Hia infection among Aboriginal and non-Aboriginal populations. In developing our antibody-boosting model, we assumed the same thresholds for protecting against invasive disease and carriage in all population groups. However, we understand that these protection thresholds may be different, especially in the context of increased vulnerability and risk factors due to

underlying health conditions. The true reasons for higher vulnerability of Aboriginal people to Hia infection compared to non-Aboriginal populations are still unknown, and remain a subject of future work. However, explicators may include socio-economic and environmental factors, and prevalence of co-morbid conditions, particularly in Canadian northern communities. These factors could affect the incidence of carriage and disease, and warrant further investigation to better understand the mechanisms responsible for high rates of Hia circulation in vulnerable populations.

This research also highlights the importance of epidemiological and clinical studies to inform models and provide estimates of parameters specific to Hia infection. For example, subsequent measurements of antibody concentrations in serum samples over several years can be used to determine the rates of Hia-specific antibody decay in the absence of vaccination. Furthermore, improved epidemiological data on Hia disease in specific populations can help refine transmission rates, and will allow models to inform vaccination strategies that fit the demographics the populations at risk.

Finally, when an anti-Hia vaccine becomes available, modelling studies with the use of enhanced surveillance and clinical data are needed to tailor vaccination and booster strategies. These studies, considering the characteristics of different communities, could contribute to the possible elimination of Hia from affected populations.

Bibliography

[1] Ryan KJ, Ray CG, 2004. Sherris Medical Microbiology 4th ed. McGraw Hill. 396-401. ISBN 0-8385-8529-9.

[2] Ulanova M, 2013. Global epidemiology of invasive *Haemophilus influenzae* type a disease: do we need a new vaccine? J Vaccines; Article ID 941461, 14 pages.

[3] Ulanova M, Tsang RSW, 2014. *Haemophilus influenzae* serotype a as a cause of serious invasive infections. Lancet Infect Dis; 14:70–82.

[4] Galil K, Singleton R, Levine OS, Fitzgerald MA, Bulkow L, Getty M, Perkins BA, Parkinson A, 1999. Reemergence of invasive *Haemophilus influenzae* type b disease in a well-vaccinated population in remote Alaska. J Infect Dis; 179:101–106.

[5] Jackson ML, Rose CE, Cohn A, Coronado F, Clark TA, Wenger JD, Bulkow L, Bruce MG, Messonnier NE, Hennessy TW, 2012. Modeling insights into *Haemophilus influenzae* type b disease, transmission, and vaccine programs. Emerg Infect Dis; 18:13–20.

[6] Oh SY, Griffiths D, John T, Lee YC, Yu LM, McCarthy N, 2008. School-aged children:

a reservoir for continued circulation of *Haemophilus influenzae* type b in the United Kingdom. J Infect Dis; 197:1275–1281.

[7] Leino T, Auranen K, Mäkelä PH, Käyhty H, Takala AK, 2000. Dynamics of natural immunity caused by subclinical infections, case study on *Haemophilus influenzae* type b (Hib). Epidemiol Infect; 125:583–591.

[8] McVernon J, Ramsay ME, McLean AR, 2008. Understanding the impact of Hib conjugate vaccine on transmission, immunity and disease in the United Kingdom. Epidemiol Infect; 136:800–812.

[9] Ramsay, ME, McVernon J, Andrews NJ, Heath PT, Slack MP, 2003. Estimating *Haemophilus influenzae* type b vaccine effectiveness in England and Wales by use of the screening method. J Infect Dis; 188:481–485.

[10] Trotter CL, McVernon J, Ramsay ME, Whitney CG, Mulholland EK, Goldblatt D, Hombach J, Kieny MP, SAGE subgroup, 2008. Optimising the use of conjugate vaccines to prevent disease caused by *Haemophilus influenzae* type b, *Neisseria meningitidis* and *Streptococcus pneumonia*. Vaccine; 26:4434–4445.

[11] Murphy TF, 2001. In: Harrisons Principles of Internal Medicine 15th ed. McGraw Hill, New York. *Haemophilus* infections; 939-942.

[12] Ladhani SN, Ramsay M, Slack MPE, 2011. The impact of *Haemophilus influenzae* serotype B resurgence on the epidemiology of childhood invasive *Haemophilus influenzae* disease in England and Wales. Pediat Infect Dis J; 30:893–895.

[13] Bachiller LP, Eiros Bouza JM, Blanco QA, 2000. Clinical manifestations, diagnosis and treatment of *Haemophilus influenzae* infection. An Med Interna; 17(4):204–212.

[14] Centers for Disease Control and Prevention, 2012. *Haemophilus influenzae* type b. In: Epidemiology and Prevention of Vaccine-Preventable Diseases – The Pink Book 12th Edition; 87–100.

[15] Murray PR, Rosenthal KS, Pfaller MA, 2005. Medical microbiology 5th ed. Elsevier Mosby, Pennsylvania; 367–376.

[16] Waksman G, Caparon M, Hultgren S, 2005. Structural biology of bacterial pathogenesis. ASM Press. Washington, DC.

[17] Coen PG, Heath PT, Barbour ML, Garnett GP, 1998. Mathematical models of *Haemophilus influenzae* type b. Epidemiol Infect; 120:281–295.

[18] Faden H, Duffy L, Williams A, Krystofik DA, Wolf J, 1995. Epidemiology of nasopharyngeal colonization with nontypeable *Haemophilus influenzae* in the first 2 years of life. J Infect Dis; 172(1):132-135.

[19] Gilsdorf JR, 1998. Antigenic diversity and gene polymorphisms in *Haemophilus influenzae*. Infect Immun; 66(11):5053-5059.

[20] Lin X, Koopman JS, Chick SE, 2007. Mathematical model comparisons of potential non-typeable *Haemophilus influenzae* vaccine effects. J Theor Biol; 245(1):66-76.

[21] Zwahlen A, Kroll JS, Rubin LG, Moxon ER, 1989. The molecular basis of pathogenicity

in *Haemophilus influenzae*: comparative virulence of genetically-related capsular transformants and correlation with changes at the capsulation locus cap. Microb Pathog; 7:225–35.

[22] Ulanova M and Tsang R, 2009. Invasive *Haemophilus influenzae* disease: changing epidemiology and host-parasite interactions in the 21st century. Infect Gen Evol; 9:594–605.

[23] http://www.historyofvaccines.org/content/articles/haemophilus-influenzae-type-b-hib.

[24] Lipsitch M, 1999. Bacterial vaccines and serotype replacement: lessons from *Haemophilus influenzae* and prospects for *Streptococcus pneumoniae*. Emerg Infect Dis; 5:336-345.

[25] Rotondo JL, Sherrard L, Helferty M, Tsang R, Desai S, 2013. The epidemiology of invasive disease due to *Haemophilus influenzae* serotype a in the Canadian North from 2000 to 2010. Int J Circumpolar Health; 2013:72.

[26] Kelly L, Tsang RS, Morgan A, Jamieson FB, Ulanova M, 2011. Invasive disease caused by *Haemophilus influenzae* type a in Northern Ontario First Nations communities. J Med Microbiol; 60:384–390.

[27] Brown VM, Madden S, Kelly L, Jamieson FB, Tsang RS, Ulanova M, 2009. Invasive *Haemophilus influenzae* disease caused by non-type b strains in Northwestern Ontario, Canada, 2002-2008. Clin Infect Dis; 49:1240–1243.

[28] Leino T, Auranen K, Mäkelä PH, Käyhty H, Ramsay M, Slack M, Takala AK, 2002. *Haemophilus influenzae* type b and cross-reactive antigens in natural Hib infection dynamics; modelling in two populations. Epidemiol Infect; 129:73–83.

[29] Fontanals D, Bou R, Pons I, Sanfeliu I, Domnguez A, Pineda V, Renau J, Muoz C, Latorre C, Sanchez F, and the Working Group on Invasive Disease Caused by *Haemophilus influenzae*, 2000. Prevalence of *Haemophilus influenzae* Carriers in the Catalan Preschool Population.Eur J Clin Microbiol Infect Dis; 19:301–304.

[30] World Health Organization WHO position paper on *Haemophilus influenzae* type b conjugate vaccines, 2006. (Replaces WHO position paper on Hib vaccines previously published in the Weekly Epidemiological Record). Wkly Epidemiol Rec; 81:445–452.

[31] Mäkelä PH, Takala AK, Peltola H, Eskola J, 1992. Epidemiology of Invasive *Haemophilus influenzae* Type b Disease. J Infect Dis; 163:S2–S6.

[32] Bruce MG, Deeks SL, Zulz T, Navarro C, Palacios C, Case C, Hemsley C, Hennessy T, Corriveau A, Larke B, Sobel I, Lovgren M, DeByle C, Tsang R, Parkinson AJ, and the International Circumpolar Surveillance Hia Working Group, 2008. Epidemiology of *Haemophilus influenzae* serotype a, North American Arctic, 2000-2005. Emerg Infect Dis; 14:48–55.

[33] McConnell A, Tan B, Scheifele D, Halperin S, Vaudry, W, Law B, Embree J, 2007. Invasive infections caused by *Haemophilus influenzae* serotypes in twelve Canadian IMPACT centers, 1996-2001. Pediatr Infect Dis J; 26:1025-1031.

[34] Langereis JD, de Jonge MI, 2015. Invasive disease caused by nontypeable *Haemophilus influenzae*. Emer Inf Dis; 21(10):1711–1718.

[35] Ladhani SN,Collins S, Vickers A, Litt DJ, Crawford C, Ramsay ME, Slack MPE, 2012. Invasive *Haemophilus influenzae* Serotype e and f Disease, England and Wales. Emerg Infect Dis; 18(5):725-732.

[36] Zhigang J, Romero-Steiner S, Carlone GM, Robbins JB, Schneerson R, 2007. *Haemophilus influenzae* type a infection and its prevention. Infect Immun; 75:2650–2654.

[37] Barbour ML, 1996. Conjugate Vaccines and the Carriage of *Haemophilus influenzae* Type b. Emerg Infect Dis; 2(3):176–182.

[38] Todar K, 2011. Todar's Online Textbook of Bacteriology. Kenneth Todar University of Wisconsin-Madison Dept of Bacterology.

[39] Sukupolvi-Petty S, Grass S, St Geme III JW, 2006. The *Haemophilus influenzae* Type b hcsA and hcsB gene products facilitate transport of capsular polysaccharide across the outer membrane and are essential for virulence. J Bacteriol; 188:3870–3877.

[40] Moxon ER, Krol JS, 1990. The Role of Bacterial Polysaccharide Capsules as Virulence Factors. Curr Top Microbiol Immunol; 150:65–85.

[41] Finney LJ, Ritchie A, Pollard E, Johnston SL, Mallia P, 2014. Lower airway colonization and inflammatory response in COPD: a focus on *Haemophilus influenzae*. Int J Chron Obstruct Pulmon Dis; 9:1119-1132.

[42] Janson H, Ruan M, Forsgren A, 1993. Limited diversity of the protein D gene (hpd) among encapsulated and nonencapsulated *Haemophilus influenzae* strains. Infect Immun; 61(11):45464552.

[43] Forsgren J, Samuelson A, Ahlin A, Jonasson J, Rynnel-Dag B, Lindberg A, 1994. *Haemophilus influenzae* resides and multiplies intracellularly in human adenoid tissue as demonstrated by in situ hybridization and bacterial viability assay. Infect Immun; 62(2):673-679.

[44] Turk DC, 1975. An investigation of the family background of acute *Haemophilus* infections of children. J Hyg; 75:315–332.

[45] Green M, Li KI, Wald ER, Guerra N, Byers C, 1992. Duration of rifampin chemoprophylaxis for contacts of patients infected with *Haemophilus influenzae* type B. Antimicrob Agents Chemother; 36(3):545–547.

[46] Goetghebuer T, West TE, Wermenbol V, Cadbury AL, Milligan P, Lloyd-Evans N, Adegbola RA, Mulholland EK, Greenwood, BM, Weber MW, 2000. Outcome of meningitis caused by *Streptococcus pneumoniae* and *Haemophilus influenzae* type b in children in The Gambia. Trop Med Int Health; 5:207–213.

[47] Limcangco MR, Salole EG, Armour CL, 2000. Epidemiology of *Haemophilus influenzae* type b meningitis in Manila, Philippines, 1994 to 1996. Pediat Infect Dis J; 19:7–11.

[48] Molyneux EM, Walsh AL, Forsyth H, Tembo M, Mwenechanya J, Kayira K, Bwanaisa

L, Njobvu A, Rogerson S, Malenga G, 2002. Dexamethasone treatment in childhood bacterial meningitis in Malawi: a randomised controlled trial. Lancet; 360:211–218.

[49] Auranen K, Eichner M, Leino T, Takala AK, Mäkelä PH, Takala K, 2004. Modelling transmission, immunity and disease of *Haemophilus influenzae* type b in a structured population. Epidemiol Infect; 132(5):947–957.

[50] Samuelson A, Freijd A, Jonasson J, Lindberg AA, 1995. Turnover of nonencapsulated *Haemophilus influenzae* in the nasopharynges of otitis-prone children. J Clin Microbiol; 33:2027-2031.

[51] Michaels RH, Norden CW, 1977. Pharyngeal colonization with *Haemophilus influenzae* type b: a longitudinal study of families with a child with meningitis or epiglottitis due to emphH. influenzae type b. J Infect Dis; 136:222–228.

[52] http://www.phac-aspc.gc.ca/lab-bio/res/psds-ftss/haemophilus-influenzae-eng.php

[53] Santosham M, Rivin B, Wolff M, Reid R, Newcomer W, Letson GW, Almeido-Hill J, Thompson C, Siber GR, 1992. Prevention of *Haemophilus influenzae* type b infections in Apache and Navajo children. J Infect Dis; 165 Suppl 1:S144–151.

[54] Singleton R, Hammitt L, Hennessy T, Bulkow L, DeByle C, Parkinson A, Cottle TE, Peters H, Butler JC, 2006. The Alaska *Haemophilus influenzae* type b experience: lessons in controlling a vaccine-preventable disease. Pediatrics; 118:e421–429.

[55] Adderson EE, Johnston JM, Shackerford PG, Carroll WL, 1992. Development of the human antibody repertoire. Pediatr Res; 32:257.

[56] Käyhty H, Peltola H, Karanko V, Makela PH. 1983. The protective level of serum antibodies to the capsular polysaccharide of *Haemophilus influenzae* type b. J Infect Dis; 147:1100.

[57] Hall DB, Lum MK, Knutson LR, Heyward WL, Ward JI, 1987. Pharyngeal carriage and acquisition of anticapsular antibody to *Haemophilus influenzae* type b in a high-risk population in southwestern Alaska. Am J Epidemiol; 126:1190-1197.

[58] Anderson P, 1984. The protective level of serum antibodies to the capsularpolysaccharide of *Haemophilus influenzae* type b. J. Infect Dis; 149:1034–1035.

[59] Peltola H, Käyhty H, Virtanen M, Makela PH, 1984. Prevention of Hemophilus influenzae type b bacteremic infections with the capsular polysaccharide vaccine. N Engl J Med; 310:1561–1566.

[60] Concepcion N, Frasch CE, 1998. Evaluation of previously assigned antibody concentrations in pneumococcal polysaccharide reference serum 89SF by the method of cross-standardization. Clin Diagn Lab Immunol; 5:199–204.

[61] Hawdon N, Nix EB, Tsang RS, Ferroni G, McCready WG, Ulanova M, 2012. Immune response to *Haemophilus influenzae* type b vaccination in patients with chronic renal failure. Clin Vaccine Immunol; 19:967–969.

[62] Leino T, Takala T, Auranen K, Mäkelä PH, Takala AK, 2004. Indirect protection obtained by *Haemophilus influenzae* type b vaccination: analysis in a structured population model. Epidemiol Infect; 132:959–966.

[63] Auranen K, Ranta J, Takala AKT, Arjas E, 1996. A statistical model of transmission of Hib bacteria in a family. Stat Med; 15:2235–2252.

[64] Keeling MJ, Danon L, 2009. Mathematical modelling of infectious diseases. Oxford J; 92(1):33–42.

[65] Allen LJ, Burgin AM, 2000. Comparison of deterministic and stochastic SIS and SIR models in discrete time. Math Biosci; 163:1-33.

[66] Branefors-Helander P, 1977. The structure of the capsular antigen from *Haemophilus influenzae* type A. Carbohydr Res; 56:117–122.

[67] Crisel RM, Baker RS, Dorman DE, 1975. Capsular polymer of *Haemophilus influenzae*, type b. I. Structural characterization of the capsular polymer of strain Eagan. J Biol Chem; 250:4926-4930.

[68] Nix EB, Williams K, Cox AD, Michael F St., Romero-Steiner S, Schmidt DS, McCready WG, Ulanova M, 2015. Naturally acquired antibodies against *Haemophilus influenzae* type a in Aboriginal adults, Canada. Emerg Infect Dis; 21(2):273–279.

[69] Auranen K, Eichner M, K ayhty H, Takala AK, Arjas E, 1999. A hierarchical Bayesian model to predict the duration of immunity to haemophilus Influenzas type B. Biometrics; 55(4): 1306–1313.

[70] Fowler AC, 1981. Approximate solution of a model of biological immune responses incorporating delay. J Math Biology; 13:23–45.

[71] Eskola J, Käyhty H, Peltola H, Karanko V, Mäkelä PH, Samuelson J, Gordon LK, 1985. Antibody levels achieved in infants by course of *Haemophilus influenzae* type B polysaccharide/diphtheria toxoid conjugate vaccine. Lancet; 1:1184–1186.

[72] Betjes MG, 2013. Immune cell dysfunction and inflammation in end-stage renal disease, Nat Rev Nephrol; 9:255–265.

[73] Lagergard T, Branefors P, 1983. Nature of cross-reactivity between *Haemophilus influenzae* types a and b and *Streptococcus pneumoniae* types 6A and 6B. Acta Pathologica, Microbiologica, et Immunologica Scandinavica Section C. Immunology; 91:371–376.

[74] Fekete A, Hoogerhout P, Zomer G, Kubler-Kielb J, Schneerson R, Robbins JB, Pozsgay V, 2006. Synthesis of octa- and dodecamers of D-ribitol-1-phosphate and their protein conjugates. Carbohyd Res; 341:2037–2048.

[75] Moghadas SM, 2004. Modelling the effect of imperfect vaccines on disease epidemiology. Discrete Contin Dyn Syst Ser B; 4:999–1012.

[76] Alexander ME, Moghadas SM, Rohani P, Summers AR, 2006. Modelling the effect of a booster vaccination on disease epidemiology. J Math Biol; 52:290-306.

[77] Moghadas SM, Alexander ME, Sahai BM, 2008. Waning herd immunity: A challenge for eradication of measles. Rocky Mt J Math; 38,5:1587–1607.

[78] Diekmann O, Heesterbeek JAP, Robert MG, 2010. The construction of next-generation matrices for compartmental epidemic models. J R Soc Interface; 7:873-885.

[79] van den Driessche P, Watmough J, 2002. Reproduction numbers and sub- threshold endemic equilibria for compartmental models of disease transmission. Math Biosci; 180:29-48.

[80] Brauer F, Xiao Y, Moghadas SM, 2015. Drug resistance in an age-of-infection model. Math Popul Stud, in press.

[81] Xiao Y, Brauer F, Moghadas SM, 2015. Can treatment increase the epidemic size? J Math Biol; 72:343–361.

[82] Farrington CP, Kanaan MN, Gay NJ, 2001. Estimation of the basic reproduction number for infectious diseases from age-stratified serological survey data. Appl Stat; 50:251-292.

[83] Stephens DS, 2011. Protecting the herd: the remarkable effectiveness of the bacterial meningitis polysaccharideprotein conjugate vaccines in altering transmission dynamics. Trans Am Clin Climatol Assoc; 122:115-123.

[84] Heymann DL, 2004. Hemophilus meningitis. Control of Communicable Diseases Manual 18th ed. American Public Health Association, Washington. 366-368.

[85] Allen LJS, 2003. An Introduction to Stochastic Processes with Applications to Biology. Prentice-Hall, Upper Saddle River, NJ.

[86] Marino S, Hogue IB, Ray CJ, Kirschner DE, 2008. A methodology for performing global uncertainty and sensitivity analysis in systems biology. J Theor Biol; 254:178-196.

[87] Taylor R, 1990. Interpretation of the correlation coefficient: a basic review. J Diagn Med Sonogr; 6(1):35-39.

[88] Millar, EV, O'Brien, KL, Watt JP, Lingappa J, Pallipamu R, Rosenstein N, 2005. Epidemiology of invasive *Haemophilus influenzae* type A disease among Navajo and White Mountain Apache children, 1988-2003. Clin Infect Dis; 40:823-830.

[89] Hammitt LL, Hennessy TW, Romero-Steiner S, Butler JC, 2006. Assessment of carriage of *Haemophilus influenzae* type a after a case of invasive disease. Clin Infect Dis; 43:386-387.

[90] Baker M, Das D, Venugopal K, Howden-Chapman P, 2008. Tuberculosis associated with household crowding in a developed country. J Epidemiol Commun Health; 62:715–721.

[91] Clark M, Riben P, Nowgesic E, 2002. The association of housing density, isolation and tuberculosis in Canadian First Nations communities. Int J Epidemiol; 31:940–945.

[92] Laskowski M, Mostaco-Guidolin LC, Greer AL, Wu J, Moghadas SM, 2011. The impact of demographic variables on disease spread: influenza in remote communities. Sci Rep 1; 105:1–7.

[93] Mostaco-Guidolin LC, Towers SMJ, Buckeridge DL, Moghadas SM, 2009. Age distri-

bution of infection and hospitalization among Canadian First Nations during the 2009 H1N1 pandemic. Am J Public Health 103:e39–e44.

[94] Mostaco-Guidolin LC, Bowman CS, Greer AL, Fisman DN, Moghadas SM, 2009. Transmissibility of the 2009 H1N1 pandemic in remote and isolated Canadian communities: a modelling study. Brit Med J - Open; 2:e001614.

[95] Schmidt DS, Bieging KT, Gomez-de-Leon P, Villasenor-Sierra A, Inostroza J, Robbins JB, 2012. Measurement of *Haemophilus influenzae* type a capsular polysaccharide antibodies in cord blood sera. Pediatr Infect Dis J; 31(8):876–878.

[96] Eames KTD, Tilston NL, Brooks-Pollock E, Edmunds WJ, 2012. Measured Dynamic Social Contact Patterns Explain the Spread of H1N1v Influenza. Salath M, ed. PLoS Comput Biol; 8(3):e1002425. doi:10.1371/journal.pcbi.1002425.

[97] Konini A, Nix E, Ulanova M, Moghadas SM, 2016. Dynamics of naturally acquired antibody against *Haemophilus influenzae* type a capsular polysaccharide in a Canadian Aboriginal population. Prev Med Rep; 3:145–150.

[98] Konini A, Moghadas S, 2015. Modelling the impact of vaccination on curtailing *Haemophilus influenzae* serotype a. J Theor Biol; 387:101-110.

[99] Dagan R, Poolman J, Siegrist CA, 2010. Glycoconjugate vaccines and immune interference: A review. Vaccine; 28:5513–5523.

[100] Insel RA, 1995. Potential alterations in immunogenicity by combining or simultaneously administering vaccine components. Ann New York Acad Sci; 754:35–47.

[101] Knuf M, Kowalzik F, Kieninger D, 2011. Comparative effects of carrier proteins on vaccine-induced immune response. Vaccine; 29:4881–4890.

[102] Adamo R, Nilo A, Harfouche C, Brogioni B, Pecetta S, Brogioni G, Balducci E, Pinto V, Filippini S, Mori E, Tontini M, Romano MR, Costantino P, Berti F, 2014. Investigating the immunodominance of carbohydrate antigens in a bivalent unimolecular glycoconjugate vaccine against serogroup A and C meningococcal disease. Glycoconj J; 31:637–647.

[103] Kaech SM, Ahmed R, 2001. Memory CD8+ T cell differentiation: initial antigen encounter triggers a developmental program in naive cells. Nat Immunol; 2(5):415–422.

[104] Rubinstein RY, Kroese DP, 2008. Simulation and the Monte Carlo method, Wiley Series in Probability and Statistics 2nd ed. John Wiley and Sons, Hoboken, NJ, USA.

[105] Ziegler K, Unanue ER, 1981. Identification of a macrophage antigen-processing event required for I-region-restricted antigen presentation to T lymphocytes. J Immunol; 127:1869–1875.

[106] Perelson AS, Goldstein B, Rocklin S, 1980. Optimal strategies in immunology III. The IgM-IgG switch. J Math Biol; 10:209–256.

[107] Perelson AS, Weisbuch G, 1997. Immunology for physicists. Rev Mod Phys; 69:1219–1267.

[108] Janeway C, 2001. Immunobiology: the immune system in health and disease 5th ed. Garland Pub, London, New York, NY, US.

[109] Alberts B, Johnson A, Lewis J, 2002. B Cells and Antibodies. Molecular Biology of the Cell 4th ed.

[110] Butt WR, 1984. Practical immunoassay: the state of the art. M. Dekker, New York.

[111] Na D, Kim D, Lee D, 2006. Mathematical modeling of humoral immune response suppression by passively administered antibodies in mice. J Theor Biol; 241:830–851.

[112] Ochsenbein AF, Pinschewer DD, Sierro S, Horvath E, Hengartner H, Zinkernagel RM, 2000. Protective long-term antibody memory by antigen-driven and T help-dependent differentiation of long-lived memory B cells to short-lived plasma cells independent of secondary lymphoid organs. Proc Natl Acad Sci USA; 97:13263–13268.

[113] Rundell A, DeCarlo R, HogenEsch H, Doerschuk P, 1998. The humoral immune response to *Haemophilus influenzae* type b: a mathematical model based on T-zone and germinal center B-cell dynamics. J Theor Biol; 194:341–381.

[114] Casrouge A, Beaudoing E, Dalle S, Pannetier C, Kanellopoulos J, Kourilsky P, 2000. Size estimate of the alpha beta TCR repertoire of naive mouse splenocytes. J Immunol; 164:5782–5787.

[115] Jegerlehner A, Wiesel M, Dietmeier K, Zabel F, Gatto D, Saudan P, Bachmann MF, 2010. Carrier induced epitopic suppression of antibody responses induced by virus-like particles is a dynamic phenomenon caused by carrier-specific antibodies. Vaccine; 28:5503–5512.

[116] Heath PT1, Booy R, Azzopardi HJ, Slack MP, Bowen-Morris J, Griffiths H, Ramsay ME, Deeks JJ, Moxon ER, 2000. Antibody concentration and clinical protection after Hib conjugate vaccination in the United Kingdom. JAMA; 284(18):2334–2340.

[117] Ladhani SN, Ramsay ME, Flood JS, Campbell H, Slack MP, Pebody R, Findlow J, Newton E, Wilding M, Warrington R, Crawford H, Min SY, Gray K, Martin S, Frankland S, Bokuvha N, Laher G, Borrow R, 2012. *Haemophilus influenzae* serotype B (Hib) seroprevalence in England and Wales in 2009. Euro Surveill; 17(46):pii=20313

[118] Low N, Redmond SM, Rutjes AW, Martnez-Gonzlez NA, Egger M, di Nisio M, Scott P, 2013. Comparing *Haemophilus influenzae* type b conjugate vaccine schedules: a systematic review and meta-analysis of vaccine trials. Pediatr Infect Dis J; 32(11):1245–1256.

[119] Jackson C, Mann A, Mangtani P, Fine P, 2013. Effectiveness of *Haemophilus influenzae* type b vaccines administered according to various schedules: systematic review and meta-analysis of observational data. Pediatr Infect Dis J; 32(11):1261–1269.

[120] Cox AD, St Michael F, Neelamegan D, Lacelle S, Cairns C, Richards JC, 2010. Investigating the candidacy of LPS-based glycoconjugates to prevent invasive meningococcal disease: chemical strategies to prepare glycoconjugates with good carbohydrate loading. Glycoconj J; 27:401–17.

Appendix A: Details of Computational Methods

Mathematical models presented in this thesis are complex and non-linear, and therefore cannot be solved analytically. In order to show the results and their sensitivity to input parameters, we used computational methods to implement these models. We developed computational algorithms to implement the models stochastically and considered the range of parameter values obtained from our analysis of serum sample data for Hia, or from previously published literature on Hib.

Computational algorithms for stochastic simulations were developed and ran in Matlab©. To consider the stochastic nature of events, we ran a large number of independent realizations (i.e., 500 realizations) in the prescribed scenarios, and calculated the average. In these simulations, the time to the next event (i.e., step-size) was exponentially distributed, estimated for a given random variate drawn from the uniform distribution on the unit interval, and used to determine the nature of the next event. Variables of the system were then updated according to the occurrence of the events in each time-step. Since the step-size in simulations were adaptive, often very small to capture the impending event, the simulations were computationally intensive and time-consuming. The amount of time in computations varied depending on the scenario, and ranged from 2 to 8 hours per 100 realizations. Simulations were run using a Shared-Memory Multiprocessor computer with 64 AMD Opteron 2.1GHz processors, 264GB of Memory and 20TB of storage.

Here we provide the algorithm used to simulate the stochastic model of vaccination presented in Chapter 5. Similar structures were developed to simulate models presented

in Chapters 6 and 7.

Part 1: variables, parameters, initial values, and simulation time

```
function [t,S,Vn,Vp,Vb,L,Lv,C,A,I,Vbp,Sv,Sp,Sn] = simul(p,mu,beta,
    delta,sigmap,sigma,gamma1,gamma2,theta,alpha,q,eta,p1,xi,p2,S0,
    Vn0,Vp0,Vb0,L0,Lv0,C0,A0,I0,Vbp0,Sv0,Sp0,Sn0,tmax)
% The main iteration
[t, pop] = Stoch_Iteration([0 tmax],[S0,Vn0,Vp0,Vb0,L0,Lv0,C0,A0,I0
    ,Vbp0,Sv0,Sp0,Sn0],[p,mu,beta,delta,sigmap,sigma,gamma1,gamma2,
    theta,alpha,q,eta,p1,xi,p2]);
S=pop(:,1); Vn=pop(:,2); Vp=pop(:,3); Vb=pop(:,4); L=pop(:,5);
Lv=pop(:,6); C=pop(:,7); A=pop(:,8); I=pop(:,9); Vbp=pop(:,10); Sv=
    pop(:,11);  Sp=pop(:,12); Sn=pop(:,13);
```

Part 2: initialize the system, estimate step-size, and vary specific parameters at specific time of simulations

```
function [T,P]=Stoch_Iteration(Time,Initial,Parameters)
S=Initial(1); Vn=Initial(2); Vp=Initial(3); Vb=Initial(4); L=
    Initial(5); Lv=Initial(6); C=Initial(7); A=Initial(8); I=Initial
    (9); Vbp=Initial(10); Sv=Initial(11); Sp=Initial(12); Sn=Initial
    (13);
```

```
3  T=0; P(1,:)=[S Vn Vp Vb L Lv C A I Vbp Sv Sp Sn];
4  old=[S Vn Vp Vb L Lv C A I Vbp Sv Sp Sn];
5  loop=1;
6  t_new1=0;
7  while (T(loop)<Time(2))
8      [step,new]=Iterate(old,Parameters);
9      t_new1=t_new1+step;
10     if (t_new1<10*365)
11         Parameters(1)=0;
12         Parameters(13)=0;
13     else
14         Parameters(1)=0.0;
15         Parameters(14)=0.0;
16     end
17     p=Parameters(1);
18     xi=Parameters(14);
19     loop=loop+1;
20     T(loop)=T(loop-1)+step;
21     P(loop,:)=old;
22     loop=loop+1;
23     T(loop)=T(loop-1);
```

```
24        P(loop,:)=new; old=new;
25        if loop>=length(T)
26            T(loop*2)=0;
27            P(loop*2,:)=0;
28        end
29    end
30    T=T(1:loop); P=P(1:loop,:);
```

Part 3: running simulations with given parameter and initial values

```
1  % Parameters values, initial values, simulation time, and averaging
2  % Parameter values
3  p=0.0;
4  p1=0.0;
5  p2=0;
6  xi=0;
7  RRR0=1.3;
8  delta=0.5;
9  mu=1/(70*365);
10 gamma1=1/50;
11 gamma2=1/2;
12 eta=0.5;
```

```
13 alpha=1;
14 q=0.6;
15 theta=1/2;
16 % Simulation time
17 tmax = 10*365;
18 tau=2;
19 ttime=0:tau:tmax;
20 % Initial values
21 S0=100000-10-1;
22 Vn0=0;
23 Vp0=0;
24 Vb0=0;
25 L0=0;
26 Lv0=0;
27 C0=10;
28 A0=0;
29 I0=1;
30 Vbp0=0;
31 Sv0=0;
32 Sp0=0;
33 Sn0=0;
```

```
% Estimating beta from the reproduction number
beta=RRR0/(delta*q*theta/((mu+gamma1)*(mu+theta)) + delta*(1-q)*
    theta/((mu+theta)*(mu+alpha)) + (1-q)*theta*alpha/((mu+theta)*(
    mu+gamma2)*(mu+alpha)));
% Start of simulations
nsims=500; % Number of simulations to run
for i=1:nsims
    KK1 = 2*rand(1,1) + 2;
    KK2 = 4*rand(1,1) + 6;
    sigma = 1/(KK1*365);
    sigmap = 1/(KK2*365);
    [t,S,Vn,Vp,Vb,L,Lv,C,A,I,Vbp,Sv,Sp,Sn] = simul(p,mu,beta,delta,
        sigmap,sigma,gamma1,gamma2,theta,alpha,q,eta,p1,xi,p2,S0,Vn0
        ,Vp0,Vb0,L0,Lv0,C0,A0,I0,Vbp0,Sv0,Sp0,Sn0,tmax);
    SS(i,1)=S(1);
    VVn(i,1)=Vn(1);
    VVp(i,1)=Vp(1);
    VVb(i,1)=Vb(1);
    LL(i,1)=L(1);
    LLv(i,1)=Lv(1);
    CC(i,1)=C(1);
```

```
51      AA(i,1)=A(1);
52      II(i,1)=I(1);
53      VVbp(i,1)=Vbp(1);
54      SSv(i,1)=Sv(1);
55      SSp(i,1)=Sp(1);
56      SSn(i,1)=Sn(1);
57      k=2;
58      for j=1:length(t)
59          for bb=k:length(ttime)
60              if ttime(bb)<=t(j)
61                  SS(i,bb)=S(j-1);
62                  VVn(i,bb)=Vn(j-1);
63                  VVp(i,bb)=Vp(j-1);
64                  VVb(i,bb)=Vb(j-1);
65                  LL(i,bb)=L(j-1);
66                  LLv(i,bb)=Lv(j-1);
67                  CC(i,bb)=C(j-1);
68                  AA(i,bb)=A(j-1);
69                  II(i,bb)=I(j-1);
70                  VVbp(i,bb)=Vbp(j-1);
71                  SSv(i,bb)=Sv(j-1);
```

```
72                          SSp(i,bb)=Sp(j-1);
73                          SSn(i,bb)=Sn(j-1);
74                  else
75                      break
76                  end
77              end
78              k=bb;
79          end
80  end
81  % Averaging independent realizations
82  AveS=sum(SS,1)/size(SS,1);
83  AveVn=sum(VVn,1)/size(VVn,1);
84  AveVp=sum(VVp,1)/size(VVp,1);
85  AveVb=sum(VVb,1)/size(VVb,1);
86  AveL=sum(LL,1)/size(LL,1);
87  AveLv=sum(LLv,1)/size(LLv,1);
88  AveC=sum(CC,1)/size(CC,1);
89  AveA=sum(AA,1)/size(AA,1);
90  AveI=sum(II,1)/size(II,1);
91  AveVbp=sum(VVbp,1)/size(VVbp,1);
92  AveSv=sum(SSv,1)/size(SSv,1);
```

```
93 AveSp=sum(SSp,1)/size(SSp,1);
94 AveSn=sum(SSn,1)/size(SSn,1);
```

Part 4: updating system variables

```
1  function[step, new_value]=Iterate(old, Parameters)
2  % Parameters
3  p=Parameters(1); mu=Parameters(2); beta=Parameters(3); delta=
       Parameters(4); sigmap=Parameters(5); sigma=Parameters(6); gamma1
       =Parameters(7); gamma2=Parameters(8); theta=Parameters(9); alpha
       =Parameters(10); q=Parameters(11); eta=Parameters(12); p1=
       Parameters(13); xi=Parameters(14); p2=Parameters(15);
4  % Variables
5  S=old(1); Vn=old(2); Vp=old(3); Vb=old(4); L=old(5); Lv=old(6); C=
       old(7); A=old(8); I=old(9); Vbp=old(10); Sv=old(11);
6  Sp=old(12); Sn=old(13);
7  % Updating variables based on the events
8  Change=zeros(35,13);
9  Rate(1) = (1-p)*mu*(S+Vn+Vp+Vb+L+Lv+C+A+I+Vbp+Sv+Sp+Sn);
10 Change(1,:)= [+1   0   0   0   0   0   0   0   0   0   0   0   0];
11
12 Rate(2) = p*mu*(S+Vn+Vp+Vb+L+Lv+C+A+I+Vbp+Sv+Sp+Sn);
```

```
13 Change(2,:)= [0   +1   0   0   0   0   0   0   0   0   0   0   0];
14
15 Rate(3) = beta*S*(I+delta*(C+A))/(S+Vn+Vp+Vb+L+Lv+C+A+I+Vbp+Sv+Sp+
       Sn);
16 Change(3,:)= [-1   0   0   0   +1   0   0   0   0   0   0   0   0]*sign(S);
17
18 Rate(4) = (1-p1)*sigmap*Vp;
19 Change(4,:)= [0   0   -1   0   0   0   0   0   0   0   0   0   +1]*sign(Vp);
20
21 Rate(5) = p1*sigmap*Vp;
22 Change(5,:)= [0   0   -1   +1   0   0   0   0   0   0   0   0   0]*sign(Vp);
23
24 Rate(6) = mu*S;
25 Change(6,:)= [-1   0   0   0   0   0   0   0   0   0   0   0   0]*sign(S);
26
27 Rate(7) = eta*beta*Vp*(I+delta*(C+A))/(S+Vn+Vp+Vb+L+Lv+C+A+I+Vbp+Sv
       +Sp+Sn);
28 Change(7,:)=[0   0   -1   0   0   +1   0   0   0   0   0   0   0]*sign(Vp);
29
30 Rate(8) = mu*Vp;
31 Change(8,:)=[0   0   -1   0   0   0   0   0   0   0   0   0   0]*sign(Vp);
```

```
32
33 Rate(9) = sigma*Vn;
34 Change(9,:)= [0 -1 +1 0 0 0 0 0 0 0 0 0 0]*sign(Vn);
35
36 Rate(10) = mu*Vn;
37 Change(10,:)=[0 -1 0 0 0 0 0 0 0 0 0 0 0]*sign(Vn);
38
39 Rate(11) = mu*Vb;
40 Change(11,:)=[0 0 0 -1 0 0 0 0 0 0 0 0 0]*sign(Vb);
41
42 Rate(12) = sigmap*Vb;
43 Change(12,:)= [0 0 0 -1 0 0 0 0 0 +1 0 0 0]*sign(Vb);
44
45 Rate(13) = eta*beta*Vbp*(I+delta*(C+A))/(S+Vn+Vp+Vb+L+Lv+C+A+I+Vbp+
    Sv+Sp+Sn);
46 Change(13,:)=[0 0 0 0 0 +1 0 0 0 -1 0 0 0]*sign(Vbp);
47
48 Rate(14) = mu*Vbp;
49 Change(14,:)= [0 0 0 0 0 0 0 0 0 -1 0 0 0]*sign(Vbp);
50
51 Rate(15) = sigmap*Vbp;
```

```
52 Change(15,:)= [0  0  0  0  0  0  0  0  0  -1  0  0  +1]*sign(Vbp);
53
54 Rate(16) = gamma2*I;
55 Change(16,:)= [0  0  0  +1  0  0  0  0  -1  0  0  0  0]*sign(I);
56
57 Rate(17) = gamma1*C;
58 Change(17,:)= [0  0  0  +1  0  0  -1  0  0  0  0  0  0]*sign(C);
59
60 Rate(18) = q*theta*L;
61 Change(18,:)=[0  0  0  0  -1  0  +1  0  0  0  0  0  0]*sign(L);
62
63 Rate(19) = (1-q)*theta*L;
64 Change(19,:)=[0  0  0  0  -1  0  0  +1  0  0  0  0  0]*sign(L);
65
66 Rate(20) = mu*L;
67 Change(20,:)=[0  0  0  0  -1  0  0  0  0  0  0  0  0]*sign(L);
68
69 Rate(21) = theta*Lv;
70 Change(21,:)=[0  0  0  0  0  -1  +1  0  0  0  0  0  0]*sign(Lv);
71
72 Rate(22) = mu*Lv;
```

```
Change(22,:)=[0  0  0  0  0  -1  0  0  0  0  0  0  0]*sign(Lv);

Rate(23) = mu*C;
Change(23,:)=[0  0  0  0  0  0  -1  0  0  0  0  0  0]*sign(C);

Rate(24) = alpha*A;
Change(24,:)=[0  0  0  0  0  0  0  -1  +1  0  0  0  0]*sign(A);

Rate(25) = mu*A;
Change(25,:)=[0  0  0  0  0  0  0  -1  0  0  0  0  0]*sign(A);

Rate(26) = mu*I;
Change(26,:)=[0  0  0  0  0  0  0  0  -1  0  0  0  0]*sign(I);

Rate(27) = xi*S;
Change(27,:)=[-1  0  0  0  0  0  0  0  0  0  +1  0  0]*sign(S);

Rate(28) = mu*Sv;
Change(28,:)=[0  0  0  0  0  0  0  0  0  0  -1  0  0]*sign(Sv);

Rate(29) = sigma*Sv;
```

```
94 Change(29,:)=[0  0  0  0  0  0  0  0  0  0  -1  +1  0]*sign(Sv);
95
96 Rate(30) = mu*Sp;
97 Change(30,:)=[0  0  0  0  0  0  0  0  0  0  0  -1  0]*sign(Sp);
98
99 Rate(31) = eta*beta*Sp*(I+delta*(C+A))/(S+Vn+Vp+Vb+L+Lv+C+A+I+Vbp+
       Sv+Sp+Sn);
100 Change(31,:)=[0  0  0  0  0  +1  0  0  0  0  0  -1  0]*sign(Sp);
101
102 Rate(32) = p2*sigmap*Sp;
103 Change(32,:)=[0  0  0  +1  0  0  0  0  0  0  0  -1  0]*sign(Sp);
104
105 Rate(33) = (1-p2)*sigmap*Sp;
106 Change(33,:)=[0  0  0  0  0  0  0  0  0  0  0  -1  +1]*sign(Sp);
107
108 Rate(34) = mu*Sn;
109 Change(34,:)=[0  0  0  0  0  0  0  0  0  0  0  0  -1]*sign(Sn);
110
111 Rate(35) = beta*Sn*(I+delta*(C+A))/(S+Vn+Vp+Vb+L+Lv+C+A+I+Vbp+Sv+Sp
       +Sn);
112 Change(35,:)= [0  0  0  0  +1  0  0  0  0  0  0  0  -1]*sign(Sn);
```

```
113 % Determining the nature of events
114 R1=rand(1,1);
115 R2=rand(1,1);
116 if(sum(Rate) > 0)
117     step = -log(R2)/(sum(Rate));
118 else
119     step=0.001;
120     new_value=old;
121     return
122 end
123 % Find which event occurs and update the corresponding variable
124 m=min(find(cumsum(Rate)>=R1*sum(Rate)));
125 new_value=old+Change(m,:);
```

Appendix B: Serum Assays

Serum samples were obtained from the participants (after informed consent was given) and stored at -80°C prior to use.

Anti-Hia capsular polysaccharide IgG ELISA

The assay was developed by Dr. Nix based on published methodology with some modifications [95]. The Hia capsular polysaccharide was isolated according to the method of Anderson and Smith. Based on a developed methodology, the isolated polysaccharide was then oxidized and conjugated to human serum albumin, and the resulting conjugate was purified and characterized [120]. Hia polysaccharide conjugated to human serum albumin was dissolved in coating buffer (0.01M PBS) and 100 μl added to each well of a 96-well ELISA plate (Cedarlane, Burlington, Canada) at a concentration of 1 μg/ml, covered with plate sealer (Fisher Scientific, Ottawa, Canada) and incubated at 37°C for 1.5 hours. The standard and samples were serially diluted in dilution buffer (0.01M PBS, 0.3% Tween 20) 1:400 to 1:25,600 and 1:200 to 1:1,600, respectively and run in duplicate. Plates were washed five times with 250 μl wash buffer (0.01M PBS, 1.2% Tween 20), the first addition of wash solution was left on the plate for 1 minute. Next, 100 l of diluted serum was added to each well and left at room temperature for 90 minutes then washed as previously described. Horseradish peroxidase conjugated mouse anti-human IgG antibody (Hybridoma Reagent Laboratory, Baltimore, MD) was diluted 1:4,000 in antibody buffer (0.01M PBS, 0.05% Tween 20), 100 μl added to each well and incubated for 2 hours at room temper-

ature. Then 100 μl of Sure Blue TMB peroxidase substrate (Mandel Scientific, Guelph, Canada) was added to each well and incubated at room temperature for 30 minutes followed by the addition of 100 μl of 1N HCl. The colorimetric substrate was detected using a microplate reader (BioTek Powerwave XS; Winooski,VT) at 450 nm with 630 nm reference. Quantification of antibody was performed using a previously described methodology [95]. The concentration of anti-Hia polysaccharide IgG (4.1 μg/ml) in the standard was determined by cross-standardization to the Hib (FDA 1983) reference serum. The quantification range was 0.10-4 μg/ml. Samples above the upper limit of quantification were diluted an additional 5 times and re-assayed effectively increasing the upper limit of quantification to 20 μg/ml.

Anti-Hia capsular polysaccharide IgM ELISA

To quantify anti-Hia capsular polysaccharide IgM, the anti-Hia PS IgG protocol was used by Dr. Nix with the following modifications. Following coating, the plates were blocked for 2 hours at room temperature with antibody dilution buffer containing 1% fish gelatin (Sigma-Aldrich, Oakville, Canada) and washed as described. Serum IgG was depleted using IgG/RF stripper. As a standard, we selected the serum of a volunteer (NOSM 97/13) from our collection that exhibited high bactericidal activity against Hia. Following a two-fold serial dilution scheme (1:100 to 1:6,400) serum samples were incubated with coated plates for 60 minutes. As a secondary antibody, horseradish peroxidase conjugated goat anti-human IgM (Southern Biotech, Birmingham, AL) diluted 1:5,000 in antibody dilution buffer was used and incubated in the wells for 1 hour at room temperature. The

concentration of anti-Hia PS IgM (3.84 μg/ml) in the standard was determined by cross-standardization [60] to the Hib (FDA 1983) standard. The estimated range of quantification was 0.01–18 μg/ml, for statistical purposes samples below the lower limit of quantification were assigned a value one half the lower quantification limit. Samples above the upper limit of quantification were diluted an additional 5 times and re-assayed increasing the upper limit of quantification to 90 μg/ml.